

**REPORT
59**



GEOLOGY AND MINERALIZATION OF THE PALAEOPROTEROZOIC BRYAH AND PADBURY BASINS WESTERN AUSTRALIA

by F. Pirajno, S. A. Occhipinti, and C. P. Swager



**GEOLOGICAL SURVEY OF WESTERN AUSTRALIA
DEPARTMENT OF MINERALS AND ENERGY**



GEOLOGICAL SURVEY OF WESTERN AUSTRALIA

REPORT 59

GEOLOGY AND MINERALIZATION OF THE PALAEOPROTEROZOIC BRYAH AND PADBURY BASINS WESTERN AUSTRALIA

by

F. Pirajno, S. A. Occhipinti, and C. P. Swager

Perth 2000

MINISTER FOR MINES
The Hon. Norman Moore, MLC

DIRECTOR GENERAL
L. C. Ranford

DIRECTOR, GEOLOGICAL SURVEY OF WESTERN AUSTRALIA
David Blight

Copy editor: D. P. Reddy

REFERENCE

The recommended reference for this publication is:

PIRAJNO, F., OCCHIPINTI, S. A., and SWAGER, C. P., 2000, Geology and mineralization of the Palaeoproterozoic Bryah and Padbury Basins, Western Australia: Western Australia Geological Survey, Report 59, 52p.

National Library of Australia
Cataloguing-in-publication entry

Pirajno, Franco, 1939–.

Geology and mineralization of the Palaeoproterozoic Bryah and Padbury Basins, Western Australia.

Bibliography.

ISBN 0 7309 6653 4.

1. Geology, Structural — Western Australia — Bryah Basin.
2. Geology, Structural — Western Australia — Padbury Basin.
3. Mines and mineral resources — Western Australia — Bryah Basin.
4. Mines and mineral resources — Western Australia — Padbury Basin.
5. Bryah Region (W.A.).
6. Padbury Region (W.A.)
 - I. Swager, C. P.
 - II. Occhipinti, S. A., (Sandra Anne)
 - III. Geological Survey of Western Australia.
 - IV. Title. (Series: Report (Geological Survey of Western Australia); 59).

553.1099413

ISSN 0508-4741

Grid references in this publication refer to the Australian Geodetic Datum (AGD84)

Printed by Optima Press, Perth, Western Australia

Copies available from:
Information Centre
Department of Minerals and Energy
100 Plain Street
EAST PERTH, WESTERN AUSTRALIA 6004
Telephone: (08) 9222 3459 Facsimile: (08) 9222 3444
www.dme.wa.gov.au

Cover photograph:
Ferruginous shale of the Millidie Creek Formation with a well-developed pencil cleavage; 2.5 km northwest of Fraser Well (BRYAH, AMG 651660).

Contents

Abstract	1
Introduction	1
Regional tectonic setting	3
Geology, stratigraphy, and geochronology	4
Peak Hill Schist and Marymia Inlier	5
Bryah Group	6
Karalundi Formation	6
Narracoota Formation	7
Peridotitic and high-Mg basalt association	7
Intrusive rocks and layered intrusions	7
Mafic and ultramafic schist	8
Metabasaltic hyaloclastite	9
Felsic schist	9
Volcaniclastic rocks	10
Carbonated and silicified metavolcanic rocks	11
Jasperoidal chert	11
Geochemistry of the Narracoota Formation	11
Ravelstone Formation	16
Horseshoe Formation	16
Padbury Group	17
Labouchere Formation	18
Wilthorpe Formation	19
Beatty Park and Heines Members	19
Robinson Range Formation	20
Millidie Creek Formation	20
Unassigned units of the Padbury Group	21
Structure	21
D ₁ structures	23
D ₂ structures	23
D ₃ structures and their relationship to D ₂ structures	25
D ₄ structures	25
Metamorphism	25
Structural synthesis	27
Mineralization	32
Gold deposits	33
Peak Hill, Jubilee, and Mount Pleasant deposits	39
Harmony deposit	41
Labouchere, Nathans, and Fortnum deposits	41
Wembley deposit	42
Wilgeena deposit	43
Durack, St Crispin, and Heines Find prospects	43
Ruby Well group	43
Mikhaburra deposit	43
Wilthorpe deposit	43
Cashman deposit	44
Volcanogenic copper–gold deposits	44
Supergene manganese deposits	44
Iron ore	45
Talc	45
Discussion	45
Tectonic model and conclusions	46
Acknowledgements	48
References	49

Appendix

Gazetteer of localities	52
-------------------------------	----

Plate

Interpreted geology of the Palaeoproterozoic Bryah and Padbury Basins

Figures

1. Stratigraphy of the former 'Glengarry Basin'	2
2. Simplified geology of the Bryah, Padbury, and Yerrida Basins	4
3. Rotated orthoclase porphyroblast, Peak Hill Schist	5
4. Partially recrystallized mylonite, Peak Hill Schist	5
5. Peak Hill Schist mylonite from the Hangingwall Sequence	5
6. Outcrop of quartz mylonite, Peak Hill Schist	6
7. Peak Hill Schist (Crispin Mylonite), illustrating a typical mylonitic fabric	6
8. Mafic-ultramafic volcanic rocks of the Narracoota Formation (Dimble Belt)	8
9. Basaltic hyaloclastite, Narracoota Formation	9
10. Mafic volcanoclastic rock, Narracoota Formation	10
11. Volcanic breccia intersected in diamond drillhole BD1	10
12. Total alkali versus silica diagram for rocks the Narracoota Formation	13
13. Total alkali versus silica diagram defining limits of alkaline and subalkaline basalts of the Narracoota Formation	14
14. Geochemical characteristics of the Narracoota Formation rocks	14
15. Geochemical discriminant plots for Narracoota Formation	15
16. TiO ₂ versus FeO/MgO plot for mafic-ultramafic rocks of the Narracoota Formation	16
17. Schematic stratigraphy of the Horseshoe Formation	17
18. Major regional structures in the Bryah and Padbury Groups	22
19. Simplified geological map of the Bryah and Padbury Groups	24
20. Selected hypothetical cross sections through the Bryah and Padbury Groups	27
21. Model of the structural development of the Bryah-Padbury Group succession	29
22. New model of the structural development of the Bryah-Padbury Group succession	31
23. New model for the structural development of the Bryah-Padbury Group succession and the Peak Hill Schist	32
24. Schematic north-northwest to south-southeast cross section from the Bangemall Basin, into the Yarlalweelor gneiss complex, and then into the Bryah and Padbury Basins	33
25. Distribution of mineral deposits and occurrences in the Bryah-Padbury and Yerrida Basins	36
26. Distribution of mineral deposits and occurrences in the Bryah Group, within the BRYAH 1:100 000 map sheet	38
27. Albite porphyroblasts in mylonitic schist at Mount Pleasant	39
28. The Mine Sequence schist	40
29. Schematic geological map of the Fiveways, Main, and Mini opencuts, Peak Hill deposit	40
30. Peak Hill Mini opencut, showing the ore-bearing mylonitic schist, graphitic schist and Marker quartzite unit	40
31. Diagrammatic cross section of the Harmony ore zones	41
32. The west wall opencut, showing the contact between biotite-sericite-quartz schist and deformed Despair Granite	44
33. Sketch illustrating a conceptual model for the origin of precious and base metal deposits in the Bryah-Padbury and Yerrida Basins	45
34. Schematic illustration showing the preferred model of the tectonic evolution of the Bryah and Padbury Basins, within the context of the Capricorn Orogen	46

Tables

1. Stratigraphy of the Bryah and Padbury Groups	3
2. Representative chemical analyses of the Narracoota Formation	12
3. Magnesium numbers for the Narracoota and Killara Formations	13
4. Selected geochemical parameters for the Narracoota Formation	13
5. Sequence of deformation events in the Bryah and Padbury Basins	23
6. Mineral paragenesis of the Bryah Group and relationships between diagnostic metamorphic minerals of the Bryah Group and deformation fabrics	28
7. Gold production and remaining resources in the Bryah and Padbury Groups	34
8. Mineral production and remaining resources in the Bryah and Padbury Groups	35
9. Mineral deposits and occurrences in the Bryah and Padbury Basins	36

Digital dataset (in pocket)



Whole-rock geochemical analyses of Narracoota Formation rocks (narracoota.csv)

Geology and mineralization of the Palaeoproterozoic Bryah and Padbury Basins, Western Australia

by

F. Pirajno, S. A. Occhipinti, and C. P. Swager

Abstract

The Palaeoproterozoic Bryah and Padbury Basins are part of the Capricorn Orogen, a collision zone between the Archaean Pilbara and Yilgarn Cratons. The Bryah Basin contains a succession of mafic and ultramafic rocks of mid-oceanic ridge basalt to oceanic plateau affinity, overlain by clastic and chemical sedimentary rocks. The Bryah Basin was formed during back-arc sea-floor spreading and rifting on the northern margin of the Yilgarn Craton. The Padbury Basin contains a succession of clastic and chemical sedimentary rocks, and was formed on top of the Bryah Basin as a foreland structure resulting from either the c. 1800 Ma oblique collision of the Pilbara and Yilgarn Cratons (Capricorn Orogeny) or the c. 2000 Ma collision of the Glenburgh terrane and the Yilgarn Craton (Glenburgh Orogeny).

Important mineral deposits are contained in both basins and include mesothermal orogenic gold, copper–gold volcanogenic massive sulfides, manganese, and iron ore. The origin of the gold mineralization is related to metamorphism and deformation linked to the Capricorn Orogeny at c. 1.8 Ga. The formation of other deposits is related to pre-orogenic syngenetic processes.

KEYWORDS: Bryah Basin, Padbury Basin, Palaeoproterozoic, stratigraphy, geochemistry, mafic rocks, ultramafic rocks, mineralization, mesothermal deposits, gold.

Introduction

In early 1994 the Geological Survey of Western Australia (GSWA) commenced fieldwork to reassess the geology and mineralization of the Palaeoproterozoic Glengarry Basin, as part of a program of new mapping initiatives. The Glengarry Basin, as defined by Gee and Grey (1993), constitutes the western part of the greater Palaeoproterozoic Nabberu Province, which in the east includes the Earraheedy Basin (Bunting et al., 1977; Hall and Goode, 1978; Gee, 1990).

The new mapping initiative resulted in the reappraisal of the geology, tectonic evolution, and mineralization of the Glengarry Basin, which is now recognized to consist of three main geotectonic units: the Bryah, Padbury, and Yerrida Basins. As a result, the volcano-sedimentary rocks of the former ‘Glengarry Group’ are now divided into the Bryah and Yerrida Groups (Fig. 1 and Table 1), characterized not only by different lithologies, but also by different regional structures, metamorphism, and mineral deposit types. Some formations previously assigned to the ‘Glengarry Group’ have been reassigned

to the Padbury Group (Martin, 1992). In addition, there is evidence to suggest that the economically important ‘Peak Hill Metamorphic Suite’, previously considered to be part of the ‘Glengarry Group’ (Gee, 1987), constitutes a separate unit, the Peak Hill Schist, derived from a protolith of probable Archaean age. Consequently, the previous nomenclature (‘Glengarry Group’ and ‘Glengarry Basin’) is no longer used. Details of the old and new stratigraphy are presented in Figure 1 and Table 1 and discussed in later sections. The revised stratigraphy of the former ‘Glengarry Basin’ is presented in Occhipinti et al. (1997). Details of the stratigraphy and structure of the lower Padbury Group are presented in Martin (1998).

The Bryah and Padbury Basins lie within the ROBINSON RANGE* and PEAK HILL 1:250 000 sheets (MacLeod, 1970; Elias and Williams, 1980; Gee, 1987), and the north-western and northeastern corners of the BELELE and GLENGARRY 1:250 000 sheets (Elias, 1982; Elias et al.,

* Capitalized names refer to standard 1:100 000 map sheets, unless otherwise specified.

Gee (1987)		Gee and Grey (1993)		Occhipinti et al. (1997); Pirajno et al. (1998b; this study)		
PADBURY BASIN/GROUP	Millidie Creek Formation Robinson Range Formation Wilthorpe Formation			TECTONIC CONTACT		
Unconformity						
GLENGARRY BASIN/GROUP	Labouchere Formation Horseshoe Formation Thaduna Greywacke Narracoota Volcanics Karatundi Formation Doolgunna Formation Johnson Cairn Shale Juderina Formation Crispin Conglomerate Maraloou Formation Finlayson Sandstone			Unconformity		

NOTE: *New or redefined units (Occhipinti et al., 1997)

FMP409a

17.01.00

Figure 1. Stratigraphy of the former 'Glengarry Basin'

1982). The Bryah and Padbury Groups (Fig. 2) make up the western part of the former 'Glengarry Basin', and are now interpreted to have developed in rift and foreland basins respectively (Martin, 1994; Pirajno, 1996; Pirajno et al., 1996; Pirajno et al., 1998b). The Yerrida Group (Fig. 2) makes up the eastern part of the former 'Glengarry Basin' and includes two subgroups, the Windplain and Mooloogool Subgroups (Fig. 2, Table 1), which developed in sag and rift basins respectively (Pirajno et al., 1995a,b; 1996). The geology and mineralization of the Yerrida Basin are described in a separate Report (Pirajno and Adamides, 2000). The Bryah Group is in faulted contact with the Yarlalweelor gneiss complex, the Marymia Inlier of the Archaean Yilgarn Craton, and the Palaeoproterozoic Yerrida Group. The contact between the Bryah and the Yerrida Groups is along a northeasterly trending high-angle reverse fault (the Goodin Fault).

Based on structural and metamorphic criteria, the area occupied by the Bryah and Padbury Groups and the Peak Hill Schist can be regarded as a single domain. In this Report, where appropriate, this domain is referred

to as the Bryah–Padbury Basin. The geology, new stratigraphy, geochronological constraints, structure, and metamorphism of the Bryah and Padbury Groups are discussed. The geochemistry of the volcanic component of the Bryah Group and mineral deposits of the Bryah and Padbury Basins are also summarized. A tectonic overview and proposed model for the geodynamic evolution of the Bryah and Padbury Basins, within the framework of the Capricorn Orogen, conclude the report.

Work in the Bryah–Padbury area involved 1:25 000-scale mapping to produce 1:100 000-scale geological maps. Geological mapping was carried out using 1:25 000-scale colour aerial photography (available from the Western Australian Department of Land Administration), aeromagnetic images (400 m line-spaced, collected by GSWA in 1994), and Landsat TM images. Results of geological mapping were integrated with petrographic, geochemical, and geochronology studies. During this work a total of 1450 rock samples were collected, of which 776 were thin-sectioned and 136 geochemically analysed. In addition, logging of diamond

Table 1. Stratigraphy of the Bryah and Padbury Groups

<i>Group</i>	<i>Age (Ma)</i>	<i>Formation</i>	<i>Rock type</i>
Padbury Group (peripheral foreland basin)	<c. 2000	Millidie Creek	sericitic siltstone, chloritic siltstone, banded iron-formation, dolomitic arenite
		Robinson Range	ferruginous shale, banded iron-formation
		Wiltorpe (Beatty Park and Heines Members)	quartz-pebble conglomerate (siltstone–wacke and polymictic conglomerate respectively)
		Labouchere	turbidite sequence (quartz wacke, siltstone)
..... <i>unconformable contact — tectonized in many places</i>			
Bryah Group (rift basin)	<c. 2000	Horseshoe	banded iron-formation, wacke, shale
		Ravelstone	quartz–lithic wacke
		Narracoota	mafic–ultramafic volcanic rocks and intercalated sedimentary rocks
		Karalundi	conglomerate, quartz wacke
..... <i>faulted contact</i>			
Yerrida Group (sag and rift basin)	c. 2174		

SOURCE: Modified after Pirajno et al. (1996)

drillcore (1100 m) and several visits to prospects and operating mines considerably enhanced our knowledge of the geology of the area. Most of the mapped areas were also included in a regional regolith geochemical sampling program covering the PEAK HILL, ROBINSON RANGE, and GLENGARRY 1:250 000 sheets (Subramanya et al., 1995; Bradley et al., 1997; Crawford et al., 1996).

Interim accounts of the structural and stratigraphic relations of the Bryah–Padbury and Yerrida Basins have been reported by Pirajno et al. (1995a,b, 1996) and Occhipinti et al. (1997). Pirajno (1996) and Pirajno et al. (1995a, 1998b) discussed possible models for the tectonic evolution of the Bryah–Padbury and Yerrida Basins. The structure and metamorphism of the Bryah–Padbury Basin have been described by Occhipinti et al. (1998a,b,c), whereas details of mineral potential, production, and ore deposit geology can be found in Pirajno and Occhipinti (1995) and Pirajno and Preston (1998). Published 1:100 000 geological maps and accompanying Explanatory Notes that wholly or partly cover the Bryah–Padbury Basin comprise: BRYAH (Pirajno and Occhipinti, 1998), GLENGARRY (Pirajno et al., 1998a), MILGUN (Swager and Myers, 1999), PADBURY (Occhipinti et al., 1998a), DOOLGUNNA (Adamides, 1998), and MARYMIA (Bagas, 1998). The southern portion of the JAMINDI 1:100 000 map sheet, containing rocks of the Bryah Group, was also mapped. The layout of these map sheets in relation to the Bryah–Padbury Basin and adjacent tectonic units is shown in Figure 2. The geology of the Bryah and Padbury Basins is presented in Plate 1.

Regional tectonic setting

The Bryah and Padbury Basins are situated along the northern margin of the Archaean Yilgarn Craton and are part of the Capricorn Orogen (Fig. 2; inset of Plate 1). The Capricorn Orogen also includes the Ashburton Basin

and the Gascoyne Complex, and can be traced for more than 1000 km with northwesterly to westerly trends, forming a broad belt of deformed, low-grade volcano-sedimentary, high-grade metamorphic, and granitoid rocks.

The Capricorn Orogeny resulted from the collision between the Pilbara and Yilgarn Cratons at c. 1800 Ma, and involved the closure of an intervening ocean, formation of a back-arc basin, and the possible accretion of microcontinental fragments (Myers, 1993; Myers et al., 1996; Tyler et al., 1998). Prior to the Capricorn Orogeny, the c. 2000 Ma Glenburgh Orogeny (Occhipinti et al., 1999) resulted in the accretion of the Glenburgh terrane onto the Yilgarn Craton. The convergence between the Pilbara and Yilgarn Cratons was essentially oblique and resulted in the development of easterly trending strike-slip movements, which included regional sinistral faults. The Capricorn Orogeny also affected other tectonic units, such as the Archaean Narryer Terrane, Marymia Inlier, Sylvania Inlier, and parts of the Hamersley Basin (Tyler and Thorne, 1990; Myers et al., 1996; Tyler et al., 1998).

The Palaeoproterozoic volcano-sedimentary and sedimentary successions of the Bryah and Padbury Basins are unconformable on the northern margin of the Yilgarn Craton, whereas to the north they are either unconformably overlain by, or in faulted contact with, rocks of the Bangemall Basin and the Archaean granitic rocks of the Marymia Inlier. The Marymia Inlier is economically important because it hosts a number of gold deposits, including the Peak Hill deposit (AMG 672190E, 7163150N*) on the southwestern tip of the inlier (see **Mineralization**).

* Localities are specified by the Australian Map Grid (AMG) system. AMG coordinates (eastings and northings) of localities discussed in the text are listed in Appendix 1.

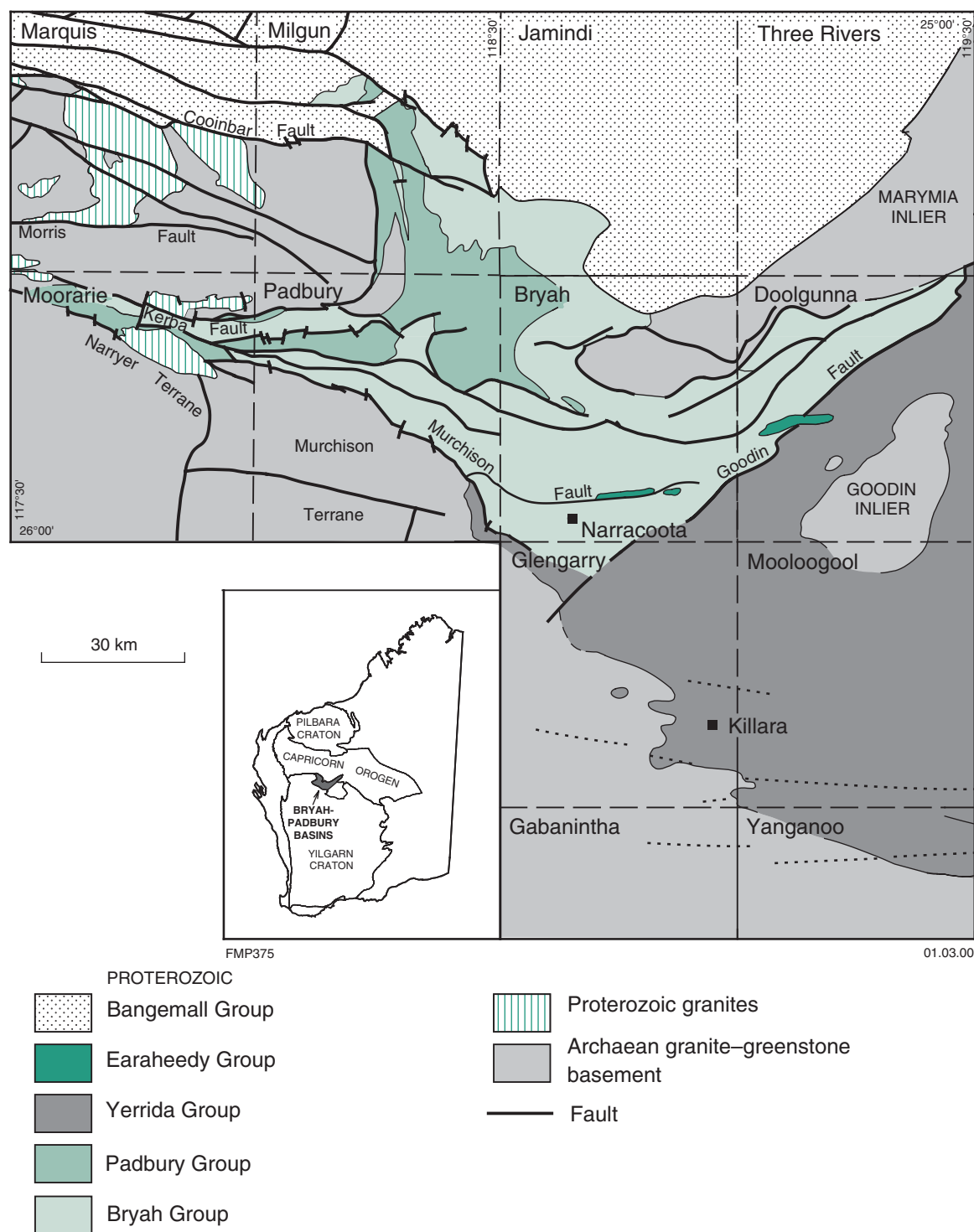


Figure 2. Simplified geology of the Bryah, Padbury, and Yerrida Basins, showing 1:100 000 map sheet boundaries. Inset shows the position of the basins in relation to the Capricorn Orogen

Geology, stratigraphy, and geochronology

The Bryah–Padbury Basin contains the Bryah and Padbury Groups and the Peak Hill Schist. The stratigraphy for the Bryah and Padbury Groups is summarized in

Figure 1 and Table 1, where a comparison with previous GSWA work is also provided. The Peak Hill Schist is a separate tectono-stratigraphic unit that is discussed here with the Marymia Inlier as basement to the Bryah Group. Detailed descriptions of the various formations and their contact relationships are presented in Occhipinti et al. (1997), Martin (1998), Adamides (1998), Pirajno and

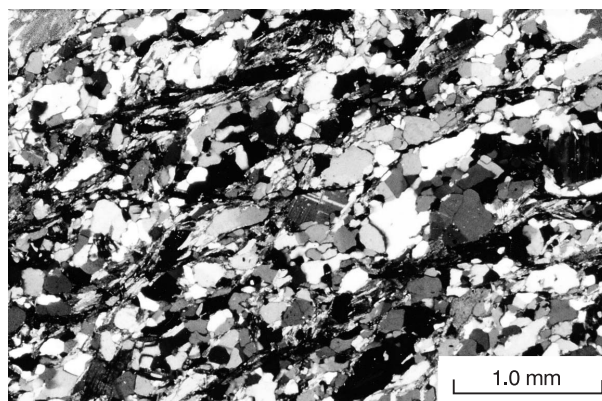
Occhipinti (1998), Pirajno et al. (1998b), Occhipinti et al. (1998c), and Swager and Myers (1999).

In this section the geology, field relations, stratigraphy, and geochronological constraints of the Peak Hill Schist, Marymia Inlier, and the formations that make up the Bryah and Padbury Groups are discussed.

Peak Hill Schist and Marymia Inlier

The Peak Hill Schist (formerly called the 'Peak Hill Metamorphic Suite'; Gee, 1987) is exposed in the 'Peak Hill Dome' or anticline, and constitutes a tectonic unit representing the southwestern tip of the Marymia Inlier (Fig. 2; Thornett, 1995). The Peak Hill Schist is continuous with the Marymia Inlier, and Thornett (1995) suggested that the 'Peak Hill Dome' represents the deformed southwestern end of the Marymia Inlier. Field observations, and petrographic and aeromagnetic data support this view. The boundary between the Peak Hill Schist and granitic rocks of the Marymia Inlier is a zone of intense deformation and metamorphism characterized by tectonic interleaving and duplexing. Towards the northeast the intensity of the Capricorn Orogeny deformation in the Marymia Inlier granites decreases to areas where they are undeformed. The contacts between the Peak Hill Schist and rocks of the Bryah Group are faulted (probably thrust), and tectonically interleaved in places.

Rocks of the Peak Hill Schist include phyllonite, quartz–muscovite schist, calc-silicate schist, sericite(–quartz) schist, and quartz–muscovite–biotite–chlorite schist, locally with rotated alkali feldspar porphyroblasts (Fig. 3), and minor metabasite. These units have been variously deformed and contain a range of mylonitic textures. The mylonitic fabric of these rocks is revealed by S–C surfaces and lines of 'mica fish' (Lister and Snoke, 1984) in a dominantly and variably recrystallized quartz-rich matrix (Figs 4 and 5). A few discrete mylonitic units

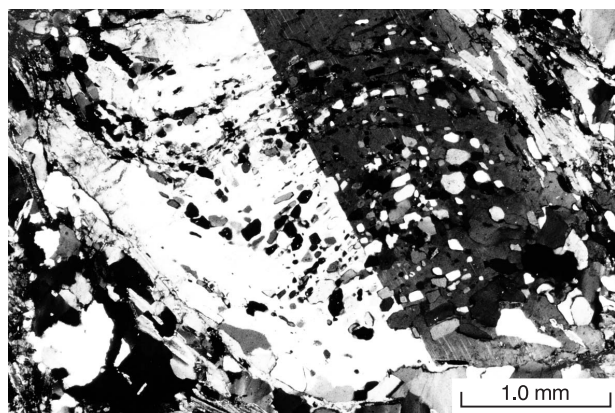


FMP 412

18.10.99

Figure 4. Partially recrystallized mylonite (Crispin Mylonite) from the Peak Hill Schist. This sample is from a mylonitic quartz–biotite–albite schist from the Mine Sequence, in which the biotite defines C planes. The S planes were obliterated by recrystallization to a blastomylonite; crossed polars

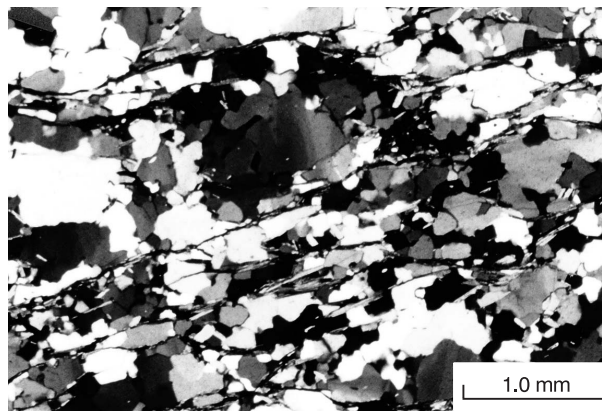
form arcuate zones, interpreted as early, possibly thrust, fault zones (see **Structure**). One of these units is the Peak Hill Mylonite (Pirajno and Occhipinti, 1998), which is a refolded quartz blastomylonite and quartz mylonite lens within quartz–muscovite schist. The Peak Hill Mylonite (Figs 6 and 7) is an important unit because it is spatially associated with gold mineralization (Peak Hill and Mount Pleasant deposits). Other, less conspicuous, quartz mylonite lenses are common within the Peak Hill Schist, and were previously mapped as cherts or banded cherts (Windh, 1992). Another important unit is the Crispin Mylonite (Pirajno and Occhipinti, 1998), which lies in the southern part of the Peak Hill Schist between sericite schist and quartz–muscovite schist. The Crispin Mylonite, referred to by Gee (1987) as the 'Crispin Conglomerate', is characterized by square to rounded quartz arenite clasts, up to 60 cm long, in a sericite-rich matrix. On the basis of field and petrographic observations, it is concluded



FMP 170

18.10.99

Figure 3. Orthoclase porphyroblast with curved inclusion trails in quartz–muscovite schist of the Peak Hill Schist; crossed polars



FMP 172

20.10.99

Figure 5. Peak Hill Schist mylonite. The C surfaces have survived recrystallization and now form thin mica trails; crossed polars



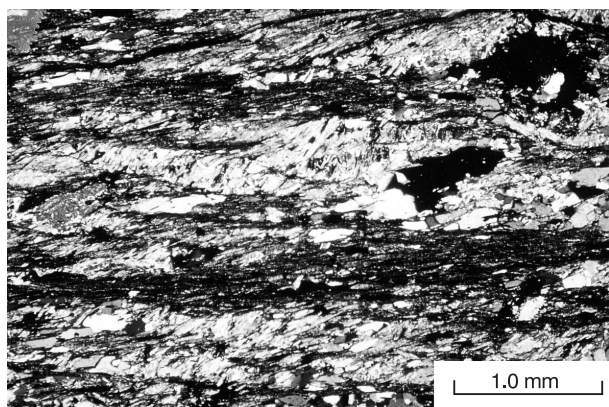
FMP 410

18.10.99

Figure 6. Outcrop of quartz mylonite, Peak Hill Schist. Note the flaggy nature of this rock and its steep dip

here that this unit is not a conglomerate, but a mylonite (Pirajno and Occhipinti, 1998). Mylonites that resemble conglomerates (pseudo- or tectonic conglomerates) have been reported by Peters (1993) and Raymond (1984a,b).

The Marymia Inlier (Windh, 1992; ‘Marymia Dome’ of Gee, 1987) represents a fragment of northeasterly trending, Archaean granite–greenstone basement. Rocks of the Marymia Inlier are mainly granitic, but also include small enclaves of calc-silicate rock, orthoamphibolite, and minor metamorphosed banded iron-formation (BIF). The Peak Hill Schist is also tentatively placed within the Marymia Inlier. The granitic rocks are locally strongly foliated to gneiss or display strong cataclastic fabrics. Granitic rocks include both fine-grained (aplitic) and coarse-grained porphyritic phases. Some outcrops previously mapped as granite by Gee (1987) have been included in the Peak Hill Schist. The granitic rocks of the Marymia Inlier are monzogranite in the east, and show increasing cataclastic deformation towards the southwest (Pirajno and Occhipinti, 1998; Bagas, 1998).



FMP 171

18.10.99

Figure 7. Peak Hill Schist (Crispin Mylonite), illustrating a typical mylonitic fabric and S–C planes (C planes are horizontal, S planes trend from upper right to lower left between the C planes); crossed polars

Bryah Group

The Bryah Group is divided into four formations: the Karalundi, Narracoota, Ravelstone, and Horseshoe Formations (Figs 1 and 2, Table 1). The basal unit of the Bryah Group is the Karalundi Formation, which is in faulted contact with the Doolgunna Formation of the Yerrida Group, along the Goodin Fault. The Karalundi Formation predominantly consists of quartz conglomerate, quartz arenite, lithic wacke, and shale. The Narracoota Formation (parts of which were previously known as ‘Narracoota Volcanics’; Gee and Grey, 1993) is the dominant lithology in the Bryah Basin and consists of tholeiitic extrusive and intrusive rocks and subordinate ultramafic units, intercalated with minor jasperoidal chert units and clastic sedimentary rocks. The Narracoota Formation is disconformably overlain by, and locally interfingers with, the Ravelstone Formation. The Ravelstone Formation comprises a succession of lithic and quartz wacke, shale, and siltstone that was deposited by turbidity currents. This formation is in turn conformably overlain by the Horseshoe Formation, comprising quartz wacke, manganeseiferous shale, and banded iron-formation.

The age of the Bryah Group is poorly constrained between c. 2000 and 1800 Ma. Detrital zircons of uncertain provenance in the Ravelstone Formation (upper Bryah Group) provide a maximum age of 2014 ± 22 Ma (Nelson, 1997). The Bryah Group must be older than the unconformably overlying Mount Leake Formation (outlier of the Earraheedy Group), which has a U–Pb (detrital zircon) maximum age of 1785 ± 11 Ma (Nelson, 1997). The Pb–Pb isochron ages obtained from pyrite from the mesothermal Mikhaburra gold deposit (1.74 Ga; Pirajno and Occhipinti, 1998) and from inferred syngenetic pyrite from the Narracoota Formation (1920 ± 35 Ma; Windh, 1992) probably represent mineralizing events in the Bryah Basin, rather than the depositional age of the Bryah Group.

Karalundi Formation

The Karalundi Formation forms the base of the Bryah Group, outcropping in a northeasterly trending belt along the southeastern margin of the Bryah Basin (Plate 1). Rocks of the Karalundi Formation are estimated to reach a thickness of approximately 2500 m. In the southeast, along the Great Northern Highway, Karalundi Formation rocks are in faulted contact with the Doolgunna Formation (Yerrida Group). On the southeastern side of the Peak Hill Schist and in faulted contact with it, the Karalundi Formation outcrops 3.5 km east of the Wilgeena mine. In the south, the Karalundi Formation is intercalated with mafic volcanoclastic rocks of the Narracoota Formation.

The Karalundi Formation is characterized by immature clastic (mainly quartz–lithic wacke and conglomerate) units containing angular quartz and lithic fragments set in a sericite–clay-rich matrix. Other rock types include siltstone, calcareous siltstone, cross-bedded arenite, ferruginous arenite, litharenite, minor dolomite, and purple, green, and black shale. The Karalundi Formation also contains pods of hematitic jasperoidal chert (see

below), which were interpreted by Gee (1979, 1987) as fumarolic pipes.

On DOOLGUNNA, quartz arenite and conglomerate units are present within a dominantly hematitic shaly succession that was interpreted by Adamides (1998) as a deep-water lateral facies of the Bryah rift succession. This succession also contains olistoliths (exotic blocks), whose origin is not clear. Adamides (1998) suggested that they might have been derived from units of the Juderina Formation, as a result of inversion of the adjacent Yerrida Basin and uplift of the Goodin Inlier.

Narracoota Formation

Rocks of the Narracoota Formation constitute a major lithotype of the Bryah Group. They form the bulk of the group with a thickness estimated at about 6 km (Pirajno and Occhipinti, 1998), and extend for more than 180 km, east to west, across the Bryah Basin. The Narracoota Formation conformably overlies and locally interfingers with the Karalundi Formation, and also interfingers with, and is in disconformable contact with, the base of the overlying Ravelstone Formation. Contacts between the Narracoota Formation and Padbury Group are tectonic. In the north, regional structural relationships suggest that the Narracoota Formation is also in tectonic contact with the Horseshoe Formation. Gravity modelling indicates that the Narracoota Formation forms the floor of the central parts of the Bryah Basin (Pirajno and Occhipinti, 1998).

Rocks of the Narracoota Formation are affected by sea-floor metasomatism and regional prograde and retrograde metamorphism (see **Structure**). On the basis of field observations, texture, geochemistry, and petrology, rocks of the Narracoota Formation can be subdivided into metamorphosed peridotitic and high-Mg metabasalt, basaltic hyaloclastite, pyroclastic rocks, intrusive rocks, and mafic and ultramafic schist. Collectively, these subdivisions are referred to as metabasites. Mafic and ultramafic schists are characterized by a pervasive schistosity, but the distinction between mafic and ultramafic is subtle and most clearly demonstrated using geochemistry. In the area 2 km northeast of the Ravelstone manganese opencuts, a texture described by Hynes and Gee (1986) as polygonal jointing has been observed in the metabasalt and appears to be a well-developed pencil cleavage. High-Mg basalts are associated with peridotitic units. Intrusive rocks cover a range of types from pyroxenite to gabbroic rocks and dykes. Metabasaltic hyaloclastites are lava flows that interacted with seawater and have a distinct spilitic character. Volcaniclastic rocks, including vent breccias, are commonly present in both basaltic hyaloclastite and mafic schist.

Typically, the metabasite rocks of the Narracoota Formation contain no, or very few, feldspar phenocrysts. Other authors have suggested that the presence of medium-grained embayed quartz crystals indicates the proximity of felsic volcanic rocks (Hill and Cranney, 1990; Windh, 1992). Felsic volcanic rocks are associated with the upper part of the Narracoota Formation at and around the Horseshoe Lights copper–gold mine on JAMINDI, 29 km east of the Fortnum mine on MILGUN.

Fine-grained, grey to black, metamorphosed shale and slate are present in places as lenses of interflow sedimentary rocks within the volcanic succession. Where more deformed and metamorphosed, these slates are finely laminated biotite–chlorite schists. South of the Robinson Range, small lenses of sedimentary rock (lithic wacke and shale) are intercalated with the volcanic rocks of the Narracoota Formation. In places, pods and lenses of jasperoidal chert are associated with the volcanic rocks.

Peridotitic and high-Mg basalt association

Massive, layered, high-Mg basaltic rocks (possibly lava flows; shown on Plate 1 as *EAnu*) are preserved in prominent hills between Top Dimble Well and Despair Bore on MILGUN. Hynes and Gee (1986) described this sequence as komatiitic basalt with up to 20% MgO. Unequivocal pillow structures, as mentioned by Hynes and Gee (1986), were not observed. The rocks are metamorphosed, but their protoliths include olivine cumulate (peridotite), high-Mg basalt with plumose and harrisitic textures, and medium-grained basalt. Layering is mainly defined by massive olivine cumulate layers, up to 20 m thick, and plumose-textured basalt layers, up to 5 m thick. Locally, large sheaves of skeletal amphibole (after pyroxene) are arranged at approximately right angles to the layering and resemble harrisitic textures (Fig. 8a). The high-Mg basalt units are characterized by well-developed ‘spinfex’-like textures with acicular tremolite–actinolite after pyroxene and up to 30% interstitial plagioclase (replaced by epidote or zoisite). The high-Mg basalt is interlayered with medium-grained basalt of similar mineralogy and composition, with 8–9% MgO. The whole-rock geochemistry of these rocks is discussed in **Geochemistry of the Narracoota Formation**.

Peridotite units commonly consist of 70–80% fine- to medium-grained olivine replaced by tremolite(–talc), skeletal amphiboles after pyroxene, and 20–30% fine-grained matrix of plumose-textured amphibole. High-Mg basalt contains up to 30% locally glomeroporphyritic olivine (now tremolite), lesser amounts of acicular pyroxene in a 60–70% amphibole plumose-textured matrix, and 15% MgO. One particular example contains 35% olivine (only partly altered to talc), skeletal (‘swallow-tail’) fresh orthopyroxene, and lesser amounts of acicular, skeletal amphibole prisms, possibly after clinopyroxene (Fig. 8b).

Intrusive rocks and layered intrusions

A metadolerite sheeted dyke complex (shown as *EAnd* on Plate 1) outcrops north of the Robinson Syncline. These rocks are associated with deformed pillow metabasalt and tend to be internally undeformed, but commonly form elongate bodies subparallel to the S_2 foliation. They contain diopside, amphibole, epidote, and minor olivine.

Lenses of cumulate-textured units, represented by pyroxenite or peridotite, and gabbroic rocks are locally intercalated with the mafic and ultramafic schist. A lensoidal outcrop of metapyroxenite is present near Durack Well. Gabbroic rocks are common between Trillbar Homestead and Friday Pool on MOORARIE

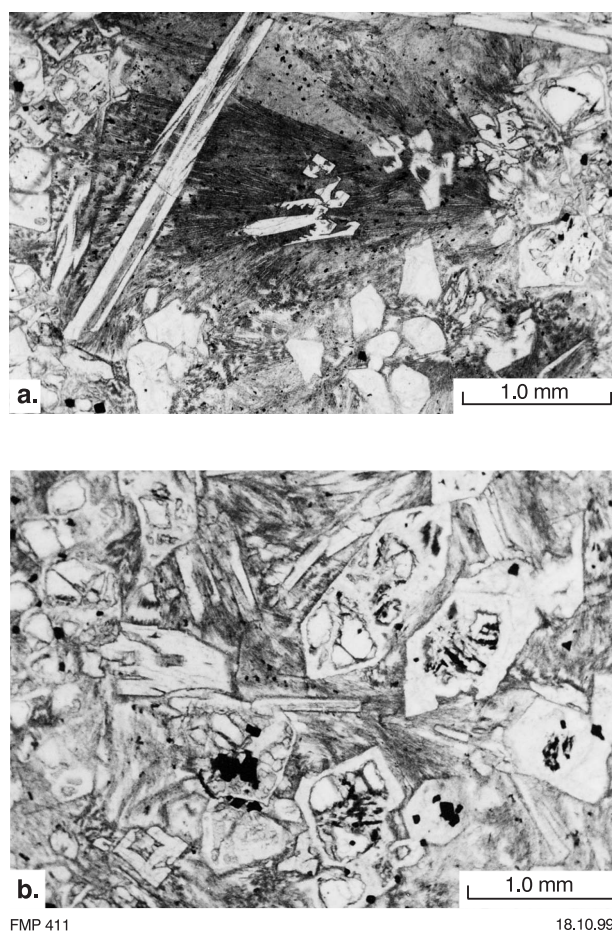


Figure 8. Mafic–ultramafic volcanic rocks of the Narracoota Formation (Dimble Belt): a) Komatiitic pyroxenite with skeletal amphibole prisms after a quench-textured pyroxene matrix; b) Peridotite with olivine, partly altered to talc around the edges, and pyroxene in a fine-grained tremolite matrix; both in plane polarized light

(Occhipinti and Myers, 1999). These rocks have been metamorphosed and folded, but are largely undeformed internally. The gabbroic rocks are surrounded by higher strain zones consisting of tremolite–actinolite schist.

The Trillbar Complex (shown as *EAnt* on Plate 1) is a 30 km long by 2.5 km wide, layered mafic–ultramafic intrusion in the westernmost part of the Bryah Basin. The complex consists of rhythmically layered mafic and ultramafic rocks, with the layering oriented at a low angle to the regional foliation (Occhipinti and Myers, 1999). Rock types include rhythmically layered gabbro, melanogabbro, leucogabbro, pyroxenite, and peridotite. These rocks are metamorphosed to greenschist facies, but the original igneous textures are locally well preserved. The Trillbar Complex rocks contain assemblages of serpentine–tremolite–talc, tremolite–talc–magnetite, tremolite–actinolite, and actinolite–feldspar. Cumulate rocks include olivine–pyroxene pseudomorphed by tremolite and sphene. West of the Trillbar Homestead are layers of metamorphosed pyroxenite and peridotite in which the original mineral phases are totally replaced by

tremolite, talc, magnetite, and chlorite. The Trillbar Complex is interpreted here as representing a remnant of Layer 3 (layered gabbroic rocks) of an oceanic crust succession (Burke et al., 1981). If this is correct, then progressively lower levels of the Narracoota Formation are exposed from east to west, and this is supported by the widespread occurrence of volcanoclastic units in the central and eastern parts of the Bryah Basin.

Mafic and ultramafic schist

Mafic–ultramafic schist consists of actinolite(–chlorite–clinozoisite) schist and chlorite schist (shown as *EAnu* and *EAn* on Plate 1). In the south-central part of BRYAH, schist outcrops form an arcuate band (possibly an antiform structure; Gee, 1987) south of, and following the trends of, the Robinson Syncline and the southern limbs of the Fraser Synclinorium (see **Structure**). North of these structures, sparse outcrops of mafic schist are present just south and north of the Peak Hill Schist. Within the schist are pods of less deformed or internally undeformed metabasites in which pillow structures are locally well preserved. Overall, this large band forms a major anastomosing sheared domain (Pirajno et al., 1995b). The dominant schistosity strikes approximately easterly or west-northwesterly, and dips steeply to the north and south. A number of quartz veins within this shear domain also strike easterly. Mafic–ultramafic schist was formed as a result of deformation and metasomatism of metabasite rocks along D_2 shear zones (see **Structure**). In most cases all original volcanic textures are obliterated, although, in places, round or elongate chlorite aggregates are interpreted as original amygdalae or fine pyroclasts.

To the northwest on MILGUN, the mafic volcanic schist occurrences are in faulted or sheared contact with rocks of the Labouchere, Wilthorpe, and Robinson Range Formations. Hill and Cranney (1990) documented a sequence of ultramafic to mafic schists, with or without jasperoidal chert lenses, overlain by fragmental volcanoclastic rocks, fine-grained siltstone, and felsic (intermediate and dacitic) crystal tuffs. These are in turn overlain by the Ravelstone and Horseshoe Formations.

Mineral constituents of the mafic schist are actinolite, chlorite, and clinozoisite with minor calcite, pumpellyite, sericite, titanite, quartz, and relict albite. Ultramafic schist has a simpler and commonly almost monomineralic mineralogy, consisting of actinolite–tremolite with retrogressed patches of pale-green chlorite. In zones of more intense deformation, chlorite- or epidote-dominated assemblages are present (chlorite schist and epidote schist respectively). These minerals developed due to strong magnesium and calcium metasomatism, probably during circulation of H_2O – CO_2 fluids (Pirajno et al., 1995b). Fluid infiltration caused the breakdown of tremolite and clinozoisite to produce chlorite, calcite, and silica. The silica thus liberated was then channelled through shear zones resulting in silicification and quartz veins (Pirajno et al., 1995b). An example of this can be seen in a breakaway 1.3 km east of the Wembley gold mine, where mafic schist and deformed pillow lavas display chlorite alteration and pervasive silicification near and along a west-northwesterly trending shear zone. In high-strain

zones a new fabric is defined by the alignment of amphibole prisms, elongate epidote, and quartz. These schists are commonly characterized by well-developed 'pencil cleavage' as a result of two intersecting planar fabrics.

Metabasite rocks commonly show relict igneous textures of prismatic plagioclase and interstitial amphibole and, more abundant unoriented prisms or acicular grains of fine- to medium-grained amphibole. Massive, sheaf-like textures of acicular amphibole are interpreted as primary igneous textures. A few plagioclase phenocrysts (3–5 mm) are preserved. The amphibole is colourless to pale-green pleochroic actinolite (or actinolite–tremolite); plagioclase is albite, and commonly pseudomorphed by clinozoisite–epidote or sericitized in zones of alteration. Minor constituents include chlorite, quartz, and sphene–leucosene, with local zones of massive epidote(–carbonate).

A schistose metabasite, 5 to 8 km northeast of the Peak Hill opencut, contains actinolite, arfvedsonite, calcite, diopside, epidote, and quartz. The alignment of actinolite and arfvedsonite defines the S_2 schistosity and, therefore, both these minerals were formed during pre–syn- D_2 (see **Structure**). The presence of the arfvedsonite (sodic amphibole) suggests either an original sodium-rich rock or later sodic metasomatism during or prior to D_2 .

Metabasaltic hyaloclastite

Metabasaltic hyaloclastites form a prominent outcrop area, partly covered by ferricrete and colluvium, south of the Murchison River. These rocks are separated from the mafic and ultramafic schist by the Murchison Fault (Plate 1), and probably represent a substantial thickness of mafic lavas and hypabyssal material. Hynes and Gee (1986) and Gee (1987) estimated a total thickness ranging from 4 to 6 km. On the northern part of the GLENGARRY 1:100 000 sheet, the metabasalts are intercalated with sedimentary rocks of the Karalundi Formation (Pirajno et al., 1998a). These metabasaltic rocks are interpreted as hyaloclastites — a term that denotes fragmentation due to quenching (Fig. 9), of lavas flowing in water or erupting under an ice sheet. This results in non-explosive fracturing and disintegration of the quenched lavas (McPhie et al., 1993; Fischer and Schmincke, 1984).

The metabasaltic hyaloclastites are undeformed, dominantly of mafic composition, and have a spilitic character. Spilites are basaltic rocks that become altered through metasomatic exchange with seawater, thereby increasing their sodium content. The hyaloclastites have normative albite from 13 to 23 wt%, and Na_2O contents of up to 6 wt%.

The metabasaltic hyaloclastites are commonly aphyric and composed mainly of acicular crystals of actinolite arranged in sheaves, together with epidote, minor carbonate, prehnite, quartz, and titanite, in a fine-grained groundmass of albite microlites, chlorite, and epidote. Coarse-grained equivalents (clinopyroxene and plagioclase laths) display ophitic to subophitic textures. North of the Mikhaburra (Holdens Find) gold deposit, a small shaft has

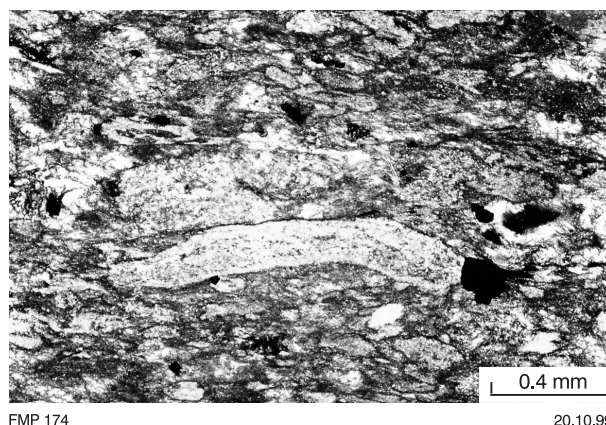


Figure 9. Basaltic hyaloclastite of the Narracoota Formation showing cuneiform devitrified shards, now replaced by silica and sericite; plane polarized light

exposed a vesicular rock containing serpentinized olivine crystals set in a very fine grained altered matrix of actinolite, probably replacing pyroxenes.

These metabasalts are commonly unfoliated and massive, with a characteristic brecciated or jigsaw-fit texture outlined by epidote, carbonate, prehnite, and quartz veining along cooling joints. In places these cooling joints may form pseudo-pillow structures, and may be mistaken for pillow lavas (Hynes and Gee, 1986). Microscale jigsaw-fit textures are also seen.

Felsic schist

Felsic schists, which host sulfide mineralization (see **Mineralization**) at the Horseshoe Lights copper–gold deposit, are present in the northern part of the Bryah Basin. Stratigraphically, the felsic schist are at the top of mafic metavolcanic rocks of the Narracoota Formation and overlain by rocks of the Ravelstone Formation (see below), which contain chert lenses and layers close to this contact. The felsic rocks are offset by a northeasterly trending fault near the mine area, and extend for about 7.5 km in a southeasterly direction, where they are offset again by a northeasterly trending fault. However, they do not reappear on the other side of the fault, where the mafic metavolcanic rocks are in contact with the clastic sedimentary rocks of the Ravelstone Formation.

Felsic schist includes quartz–sericite schist, sericite schist, and chlorite schist, all showing varying degrees of deformation and development of mylonite. Examination of drillcore from the Horseshoe Lights mine revealed structures reminiscent of felsic volcanoclastic rocks, such as collapsed pumice fragments. Quartz–sericite and sericite schist are composed of quartz and feldspar porphyroclasts, partially replaced by quartz and sericite, carbonate or chlorite, and wrapped around by granoblastic aggregates of quartz and sericite; these aggregates are traversed by anastomosing bands of sericite. Tourmaline is present in places. In one example, sericite schist contains elliptical opaque fragments, suggestive of collapsed pumice. Chlorite schist is composed of chlorite

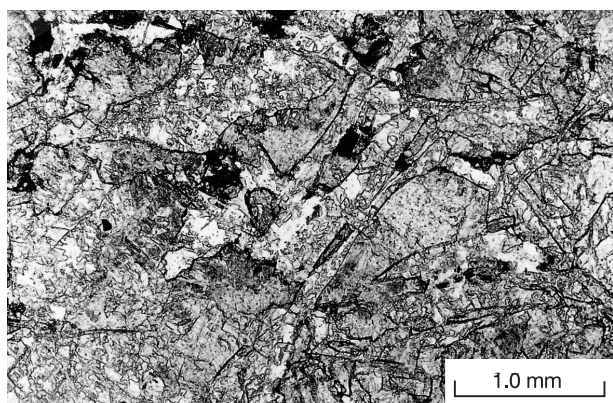


Figure 10. Mafic volcanoclastic rock of the Narracoota Formation showing relict glass shard (in centre); plane polarized light

and granular quartz, with the chlorite forming distinct monomineralic laminae. X-ray diffraction analyses of altered schist indicate the presence of quartz, kaolin, pyrite, hematite, goethite, and dioctahedral sodian muscovite or potassian paragonite.

Based on petrographic and core examinations, the felsic schist precursor rocks may have been quartz-feldspar porphyry and felsic volcanoclastic rocks.

Volcanoclastic rocks

Mafic volcanoclastic rocks have well-preserved eutaxitic or fragmental textures despite intensive foliation (Fig. 10). In the Fortnum mine area, mafic fragmental rocks and fine-grained mafic volcanoclastic rocks are spatially associated with jasperoidal chert pods. The fragmental rocks are strongly schistose, with flattened and stretched

fragments of chlorite schist, quartz–chlorite schist with plagioclase phenocrysts, quartz–feldspar–amphibole rock (metabasalt), medium-grained plagioclase grains, and, more rarely, quartz crystals in a fine-grained matrix. Finely layered mafic schists consist of an amphibole–plagioclase matrix with scattered prismatic to ovoid plagioclase phenocrysts and quartz ‘eyes’. Amphibole, accessory biotite, and sericite lenses have a strong preferred orientation, suggesting that recrystallization in these fine-grained rocks has destroyed any volcanoclastic texture.

Volcanic breccia is present in at least three localities. The most important of these is 5 km north of the old Cashman mine, in the southern part of BRYAH (see **Mineralization**). Outcrops of volcanic breccia are also present at the Cashman mine and 3 km west of the Peak Hill – Fortnum road junction. The nature of these angular, clast-supported, poorly sorted blocks of mafic volcanic material suggest that they are vent breccias. Volcanic breccia was intersected throughout 455 m of core in drillhole BD1 (BRYAH, AMG 380380), drilled by North Exploration Ltd in 1993 (McDonald, 1994). This core intersection is briefly described below.

Drillhole BD1 was drilled to a depth of 520 m at an inclination of 70° towards the south, and intersected clays and gravels to a depth of 65 m, followed by weathered mafic volcanic breccias to 96 m. Below this depth, to the end of the hole at 520 m, spectacular fresh proximal vent-facies material consisting of angular blocks and clasts of basaltic lava, tuff, and chert were intersected (Fig. 11). Crude bedding is present locally, as are thin layers of laminated or cross-laminated cherty material. The hole bottomed in cross-laminated chert, which is interpreted as pyroclastic surge and tuff deposits. The basaltic rocks include fine-grained vesicular basalt, and feldspar-phyric and augite-phyric basalts. The porphyritic varieties are characterized by a microlite-rich feldspar matrix, clinopyroxene granules, interstitial glass and chlorite, and opaque minerals (titanite or rutile). The feldspar



Figure 11. Volcanic breccia of the Narracoota Formation intersected in diamond drillhole BD1. Clasts are predominantly of basaltic rocks; the matrix exhibits albitic alteration. Width of the core trays is 0.40 m

phenocrysts are selectively altered to sericite, whereas the augite phenocrysts are fresh and exhibit distinct zoning. Vesicles are infilled (from rim to core) by albite, epidote, chlorite, and calcite. Minor sulfide specks, mainly chalcopyrite, may be present in the vesicular basalt. Tuffs, characterized by fluidization (due to degassing) and eutaxitic textures, consist of glass shards and crystal and lithic fragments set in a devitrified and variably altered glassy matrix. Alteration phases are mainly chlorite, calcite, quartz, and albite. Chalcopyrite blebs are present in places. Hydraulic fracturing and veins of calcite, prehnite, quartz, and chlorite are abundant. One section between 200 and 360 m is characterized by albitic alteration (sodium metasomatism), which imparts a pink to reddish colouration to veinlets and patches where the albite is present.

The fragmental mafic volcanic rocks in drillhole BD1 are interpreted to represent a proximal vent-facies volcanic breccia. This vent-facies material coincides with prominent magnetic and Bouguer gravity anomalies (Pirajno et al., 1995a). The magnetic anomaly, which is related to the presence of magnetite in pyroxene basalt, has a well-defined northeasterly trending elliptical shape and could conceivably indicate the remnants of a major volcanic edifice. Magnetic modelling suggests the presence of two tabular bodies, dipping 25° to the north (Bui Dung, 1999, pers. comm.). The gravity anomaly is at the centre of a large regional gravity high, which underlies most of the area occupied by the Narracoota Formation (Pirajno and Occhipinti, 1998).

Carbonated and silicified metavolcanic rocks

Carbonated and silicified mafic-ultramafic rocks, interpreted as part of the Narracoota Formation, outcrop in the Horseshoe anticlinal block (Plate 1). These rocks are compositionally heterogeneous, and both underlie and are intercalated with rocks of the Horseshoe Formation. This suggests that the interleaving is tectonic because elsewhere in the Bryah Group, the Horseshoe Formation is not observed to be in direct contact with the Narracoota Formation (Occhipinti et al., 1999).

Jasperoidal chert

Jasperoidal chert pods are present locally within the Narracoota Formation (Gee, 1987; Hill and Cranney, 1990; Pirajno and Occhipinti, 1998), but are commonly too small to be represented individually on geological maps. One of the largest pods outcrops 1.5 km due south of Ruby Duffer Well in the southern part of BRYAH. Windh (1992) investigated the chert pods in some detail, geochemically discriminated them on the basis of their Ni/Cr ratios, and distinguished jasperoidal syngenetic exhalative chert, silicified volcanic or sedimentary rocks, silicified shear zone rocks, and surface silicification. Several of these chert pods, such as those in the Narracoota Formation south of the Peak Hill Schist in northern BRYAH, are quartz mylonites — probably Windh's (1992) silicified shear zone rocks. A few may be chemical precipitates deposited by hot springs, whereas others may represent silicified fault zones.

The cherty material is reddish to grey coloured, massive to banded, and extensively veined by quartz. The chert consists of very fine grained recrystallized quartz with equant to elongate polygonal-granoblastic textures, locally with a crystallographic preferred orientation. Minute opaque minerals, locally including magnetite or pyrite, define trails parallel to the quartz foliation. In the Yarlalweelor opencut (Fortnum mine), pebbles of these cherts in overlying mafic fragmental rocks suggest that the cherts formed as exhalative horizons related to volcanism. Alternatively, the jasperoids may represent iron-rich silicification along major shear zones. In the Yarlalweelor opencut, the chert pods host epigenetic gold mineralization in and around quartz(-pyrite) vein systems (Hill and Cranney, 1990).

Geochemistry of the Narracoota Formation

Major, trace, and rare earth element (REE) whole-rock analyses of samples of metabasite rocks of the Narracoota Formation collected during this study are included in the digital dataset in the back pocket. These data were used to characterize the geochemistry of the volcanic rocks of the Narracoota Formation, in an attempt to better define the rock types and gain an insight into the nature of the parent magma(s) and tectonic setting. Representative analyses of Narracoota Formation rocks are presented in Table 2.

The Narracoota metabasite rocks are commonly of tholeiitic composition with mixed mid-ocean ridge basalt (MORB) – oceanic island and continental geochemical signatures. They span the range from high-Mg basalt to komatiite and peridotitic komatiite or peridotite (possibly subvolcanic cumulates). Common characteristics include high MgO, high Ni and Cr, moderate to low REE abundances, and nearly flat chondrite-normalized REE patterns with weak Eu anomalies, possibly reflecting depleted asthenospheric mantle sources (Pirajno and Davy, 1996; Pirajno et al., 1996; Pirajno and Occhipinti, 1998; Occhipinti et al., 1998a,c). There are subtle chemical differences between the hyaloclastites and mafic-ultramafic schists (Tables 3 and 4; see below).

Hynes and Gee (1986) and Pirajno and Davy (1996) reported on the petrochemistry and tectonic setting of the Narracoota Formation metabasite rocks. Hynes and Gee (1986) concluded that they have fairly uniform chemistry and are of MORB affinity, although the original mafic volcanic rocks may have been emplaced through the rifting of continental crust. Pirajno and Davy (1996) proposed that the Narracoota Formation metavolcanic rocks might have formed in a setting analogous to that of the present-day Gulf of California (Lonsdale and Becker, 1985). The origin of the Narracoota Formation metabasites is discussed in **Tectonic model and conclusions**.

Classification based on chemistry

The total alkali – silica (TAS) and high-Mg plot (Le Maitre, 1989) indicates that the bulk of the rocks of the Narracoota Formation range in composition from komatiite-picrite through basalt to basaltic andesite

Table 2. Representative chemical analyses of the Narracoota Formation.

Rock type	Mafic schist					Hyaloclastite			Ultramafic schist			Trillbar Complex	
Sample	132788	132789	132790	133033	133050	112643	116485	104256	132791	139138	139139	135482	143538
Percent													
SiO ₂	54.24	49.45	52.77	46.3	49.07	51.87	51.39	50.11	49.23	47.23	47.89	51.37	49.61
TiO ₂	0.28	1.13	0.31	0.19	0.26	0.73	0.63	0.53	0.19	0.16	0.17	0.37	1.41
Al ₂ O ₃	14.22	11.72	14.66	9.48	7.94	13.8	15.12	15.03	10.43	7.65	8.67	14.81	13.91
Fe ₂ O ₃	2.48	3.45	1.84	6.61	6.35	2.24	2.96	2.78	1.46	3.96	2.01	2.32	5.61
FeO	5.98	8.24	7.05	7.41	1.01	8.48	6.62	5.29	8.34	5.48	7.08	5.61	7.17
MnO	0.17	0.19	0.18	0.25	1.98	0.2	0.16	0.14	0.18	0.12	0.15	0.16	0.22
MgO	9.29	12.43	10.36	15.17	7.78	10.36	8.3	9.36	20.63	28.77	26.78	8.69	6.56
CaO	11.06	11.07	9.62	14.51	22.62	9.74	11.44	15.14	8.6	6.41	7.04	10.68	11.36
Na ₂ O	2.18	2.12	2.74	0.03	0.09	2.16	3.2	1.45	0.92	0.18	0.19	3.06	2.04
K ₂ O	0.07	0.08	0.46	0.01	2.84	0.36	0.1	0.11	0.02	0.03	0.01	0.06	0.22
P ₂ O ₅	0.03	0.13	0.02	0.03	0.07	0.07	0.06	0.05	0.01	0.01	0.01	0.03	0.11
Total	100.00	100.01	100.01	99.99	100.01	100.01	99.98	99.99	100.01	100.00	100.00	97.16	98.22
Mg#	66.87	66.15	67.95	66.92	67.36	63.77	61.42	68.16	79.2	85	84.3	–	–
Parts per million													
Ag	–	–	–	–	–	1	–	1	–	–	–	–	–
As	1.55	1.57	0.52	225.51	130.32	–	–	–	–	8.32	–	–	–
Au	–	–	–	–	–	10.4	–	–	–	–	–	–	–
Ba	55	140	79	27	2 846	341	127	92	74	37	102	39	322
Cd	–	–	–	–	–	–	–	–	–	–	–	–	–
Co	55	86	58	223	51	–	–	–	99	113	111	–	–
Cr	509	1 201	686	2 574	72	489	364	283	1 836	2 530	3 146	593	82
Cu	168	124	63	327	20	108	101	39	55	9	11	59	172
Ga	10	16	10	8	9	12	12	13	8	6	6	12	19
Hf	–	–	–	–	–	–	–	–	–	–	–	0.7	1.4
Mo	–	–	–	–	–	–	–	–	–	–	–	0.8	2.6
Nb	–	6.3	–	–	5.2	–	–	–	–	–	–	1	9
Ni	203	548	241	1 274	91	258	143	164	866	1 531	1 230	124	98
Pb	–	2	–	–	7	–	–	–	–	–	–	1	4
Pd	–	–	–	–	–	–	–	–	–	–	–	–	–
Pt	–	–	–	–	–	–	–	–	–	–	–	–	–
Rb	1	–	6	–	85	6	–	2	–	1	–	1	4
Sb	–	–	–	–	–	4.15	–	5.11	–	–	–	–	–
Sc	50	41	51	31	10	–	–	–	40	34	38	51	48
Sr	64	149	64	54	100	163	82	188	23	23	7	61	279
Ta	–	–	–	–	–	–	–	–	–	–	–	–	–
Th	–	1.04	–	–	7.17	–	–	–	–	–	–	–	–
U	–	–	–	0.64	1.3	–	–	–	–	–	–	0.8	1.4
V	196	277	202	138	78	250	249	217	144	115	143	235	362
W	–	–	–	–	–	–	–	–	–	–	–	–	–
Y	13	18	12	8	16	17	14	11	8	6	7	17	24
Zn	65	94	68	45	50	85	73	55	62	51	45	61	91
Zr	13	68	15	17	50	51	47	38	7	7	8	20	86
La	0.89	9.36	0.43	0.54	18.19	3.6	3.5	3.5	0.93	0.17	0.56	2	6
Ce	2.18	22.64	1.29	0.84	44.45	9	8.3	8.3	1.53	0.42	0.82	2	15
Pr	0.37	2.9	0.2	0.2	4.18	1.2	1.1	1.3	0.2	0.09	0.19	0	2
Nd	1.66	11.93	1.08	1.02	15.11	5.7	5.1	5.7	1.02	0.47	0.79	5	12
Sm	0.8	3.28	0.65	0.56	3.06	1.5	1.4	1.5	0.65	0.3	0.34	–	–
Eu	0.42	1.3	0.32	0.28	2.23	0.9	0.7	0.8	0.29	0.11	0.11	–	–
Gd	1.66	4.09	1.41	0.85	3.05	2.3	1.7	2	1.29	0.65	0.71	–	–
Tb	0.4	0.69	0.31	0.18	0.4	0.4	0.4	0.4	0.29	0.14	0.16	–	–
Dy	2.68	4.08	2.33	1.2	2.02	2.7	2.4	2.4	2.14	1.08	1.16	–	–
Ho	0.71	0.87	0.57	0.28	0.37	0.5	0.5	0.5	0.53	0.27	0.3	–	–
Er	2.22	2.31	1.73	0.94	1.15	1.8	1.5	1.6	1.62	0.83	0.91	–	–
Tm	0.39	0.33	0.27	0.16	0.17	0.2	0.2	0.2	0.27	0.14	0.15	–	–
Yb	2.29	1.96	1.82	1.15	1.25	1.5	1.4	1.5	1.66	0.86	0.9	–	–
Lu	–	–	–	0.19	0.2	0.2	0.2	0.2	–	0.13	0.14	–	–

Table 3. Magnesium numbers for the Narracoota and Killara Formations

<i>Rock</i>	<i>Formation</i>	<i>Range of Mg#</i>	<i>Average Mg#</i>	<i>Standard deviation of Mg#</i>
Metabasaltic hyaloclastite	Narracoota	46.77 – 68.16	57.16	5.25
Mafic schist	Narracoota	43.37 – 74.09	59.57	6.69
Ultramafic schist	Narracoota	75.16 – 85.60	81.05	2.54
Tholeiitic basalt	Killara	35.04 – 66.03	50.35	7.39

NOTE: Mg#: Magnesium number, defined as $\text{MgO}/(\text{FeO} + \text{MgO})$

(Fig. 12). A small number of samples plot in the boninite and andesite fields. All metabasites of the Narracoota Formation (ultramafic and mafic schists and basaltic hyaloclastite) are of subalkaline tholeiitic affinity (Fig. 13). They commonly have restricted silica contents ranging from 45 to 55 wt% (Fig. 12).

The metabasites are all quartz, albite, anorthite, diopside, hypersthene, and magnetite normative. The mafic schists are hypersthene normative, with lower MgO contents (<15 wt%) and magnesium numbers (Mg# — defined as $\text{MgO}/(\text{FeO} + \text{MgO})$) ranging from 43 to 74 (Table 3). Some mafic schists have no quartz and are olivine normative (5–6% and up to 20% in some mafic schists). The ultramafic schist is hypersthene and olivine normative, with MgO contents ranging from 15.3 to 22.7 wt%, and Mg# ranging from 75 to 86 (Table 3). The metabasaltic hyaloclastites are albite and clinopyroxene normative and have MgO contents of <10 wt% and Mg# of between 47 to 68 (Table 3).

Ultramafic schist, mafic schist, and metabasaltic hyaloclastite can be distinguished in terms of their Cr, Ni, and Ti abundances, FeO/MgO ratios (Tables 3 and 4; Figs 14a and 14b), and chondrite-normalized REE patterns. The hyaloclastite rocks are depleted in Cr and Ni and enriched in TiO_2 relative to the mafic–ultramafic rocks (Fig. 14c).

The Jensen (1976) cationic plot is based on the proportion of $\text{Fe}^{2+} + \text{Fe}^{3+} + \text{Ti}$ versus Al and Mg cations, recalculated to 100%, and is particularly useful for discriminating subalkaline and Mg-rich metamorphosed volcanic rocks in which the alkali content may have been modified during deformation and metamorphism (Rollinson, 1993). In the Jensen plot (Fig. 15a) the

Narracoota Formation rocks span the range of compositions from high-Mg tholeiite through to komatiite and peridotitic komatiite, in a trend of increasing MgO.

Chondrite-normalized rare-earth element diagrams, commonly regarded as the most useful of the trace element plots in the petrogenesis of igneous rocks, are used to determine the possible nature and source of the melts. Particularly important are the overall patterns from light to heavy rare earth elements (LREE to HREE), the normalized abundance of Eu, controlled by feldspar, and that of Ce, controlled by seawater or hydrothermal fluids. For the Narracoota Formation rocks, chondrite-normalized REE abundances (Figs 15b and 15c) are commonly low (<1 to <40 times chondrite). The mafic schist is characterized by a spread in LREE from depleted to enriched (Fig. 15b), with individual patterns almost identical to those of mid-ocean ridges (O’Nions et al., 1976; Schilling, 1982) and the recent basaltic lavas of Iceland (Schilling et al., 1982). More specifically, the LREE-depleted patterns (western Bryah Basin) are strikingly similar to those of the Lau Basin spreading centre in Fiji (Pearce et al., 1995), whereas slightly depleted to slightly enriched LREE patterns (eastern Bryah

Table 4. Selected geochemical parameters for the Narracoota Formation

<i>Parameters (mean values)</i>	<i>Hyaloclastite</i>	<i>Mafic schist</i>	<i>Ultramafic schist</i>
$(\text{La/Yb})_N$	1.44	1.702	0.37
TiO_2 (wt%)	0.86	0.68	0.19
Ni/Cr	0.43	0.39	0.42
$\text{Al}_2\text{O}_3/\text{TiO}_2$	16.2	20.5	46.68
MgO (wt%)	7.31	7.80	21.19

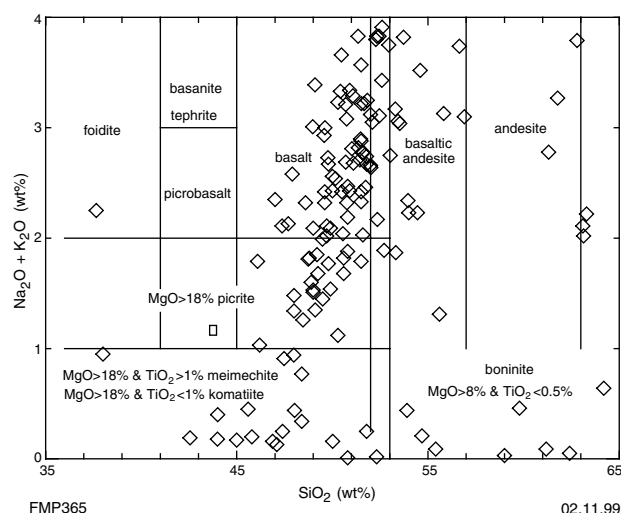


Figure 12. Total alkali versus silica diagram (Le Maitre, 1989) for rocks of the Narracoota Formation. Note that a small number of samples fall within the boninite field; this, however, may be due to hydrothermal alteration

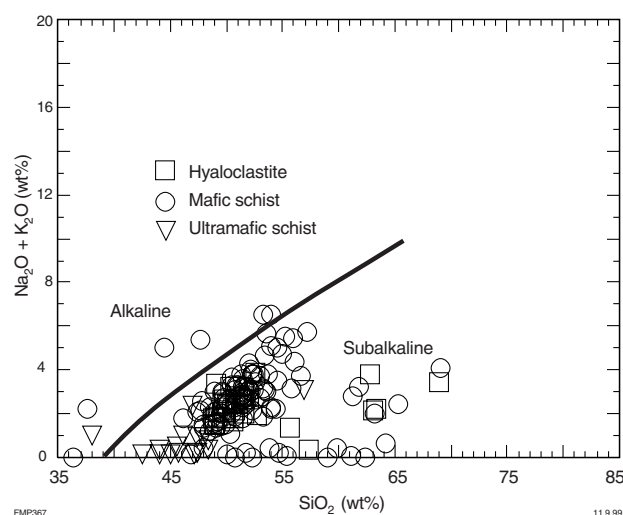


Figure 13. Total alkali versus silica diagram (Le Maitre, 1989) defining limits of alkaline and subalkaline basalts, showing the predominantly subalkaline nature of the Narracoota Formation

Basin) are comparable to those of seamounts, reflecting a more enriched source. The nearly flat patterns have negative Eu anomalies, reflecting the primitive nature of the rocks, presence of olivine, clinopyroxene, and orthopyroxene, and fractionation of feldspar from the melt. The patterns of the Iceland basalts that are nearly identical to those of the mafic schist of the Bryah Group were explained by Schilling et al. (1982) as due to advection of asthenospheric mantle at a mid-ocean ridge. Considering field relations, and petrological and geochemical data, it is conceivable that the Narracoota Formation metatholeiites may have had a similar origin. Chondrite-normalized REE abundances for the metabasaltic hyaloclastite are very low (9 to 14 times chondrite), slightly LREE-enriched, and with a distinct positive Eu anomaly (Fig. 15c), reflecting the addition of albite due to seawater metasomatism.

The overall REE abundances and patterns of mafic schist and hyaloclastite are strikingly similar to 1.92 – 1.84 Ga mafic rocks of the Flin Flon belt in the Trans-Hudson Orogen in Canada (Lucas et al., 1996). Some of the mafic rocks of the Flin Flon belt have been interpreted to belong to tectono-stratigraphic assemblages of ocean floor and ocean island affinity. Also, the Flin Flon ocean island tholeiites have REE patterns similar to

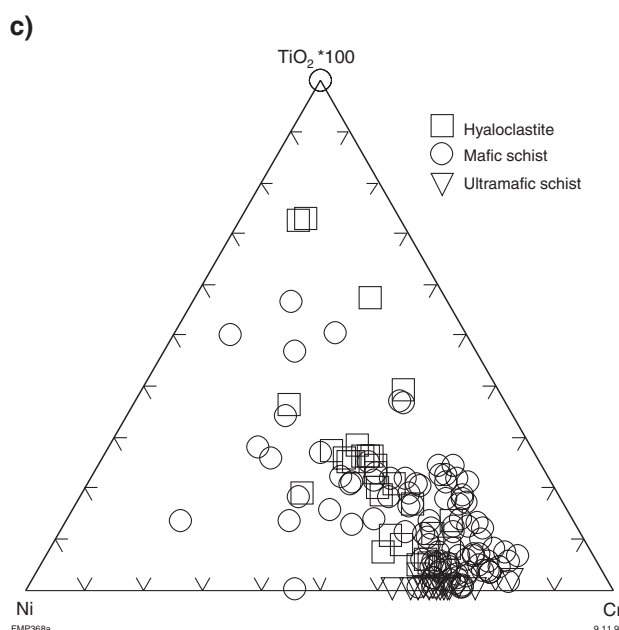
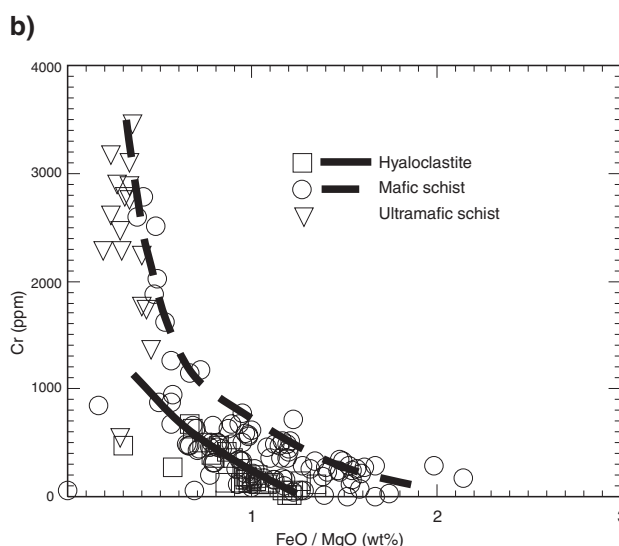
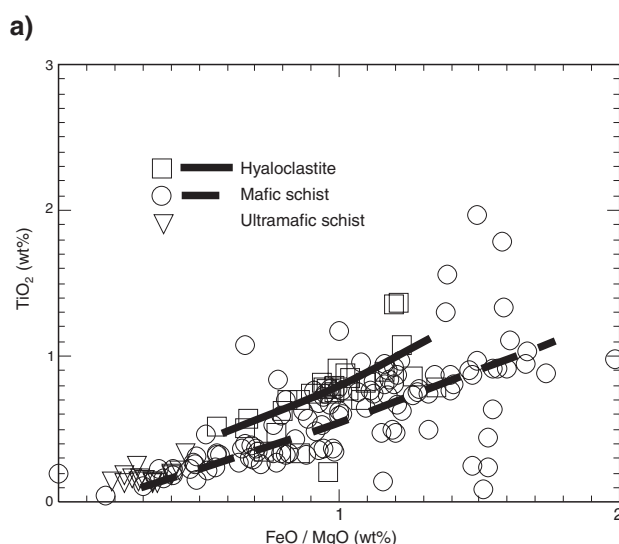


Figure 14. Geochemical characteristics of the Narracoota Formation: a) TiO_2 versus FeO/MgO ratios; note the slight TiO_2 enrichment of metabasaltic hyaloclastite compared to mafic-ultramafic schist; b) Cr versus FeO/MgO ratios; note the Cr enrichment of mafic-ultramafic schist compared to metabasaltic hyaloclastite; c) TiO_2 -Ni-Cr triangular plot, showing Ni and Cr enrichment of mafic-ultramafic schist compared to metabasaltic hyaloclastite

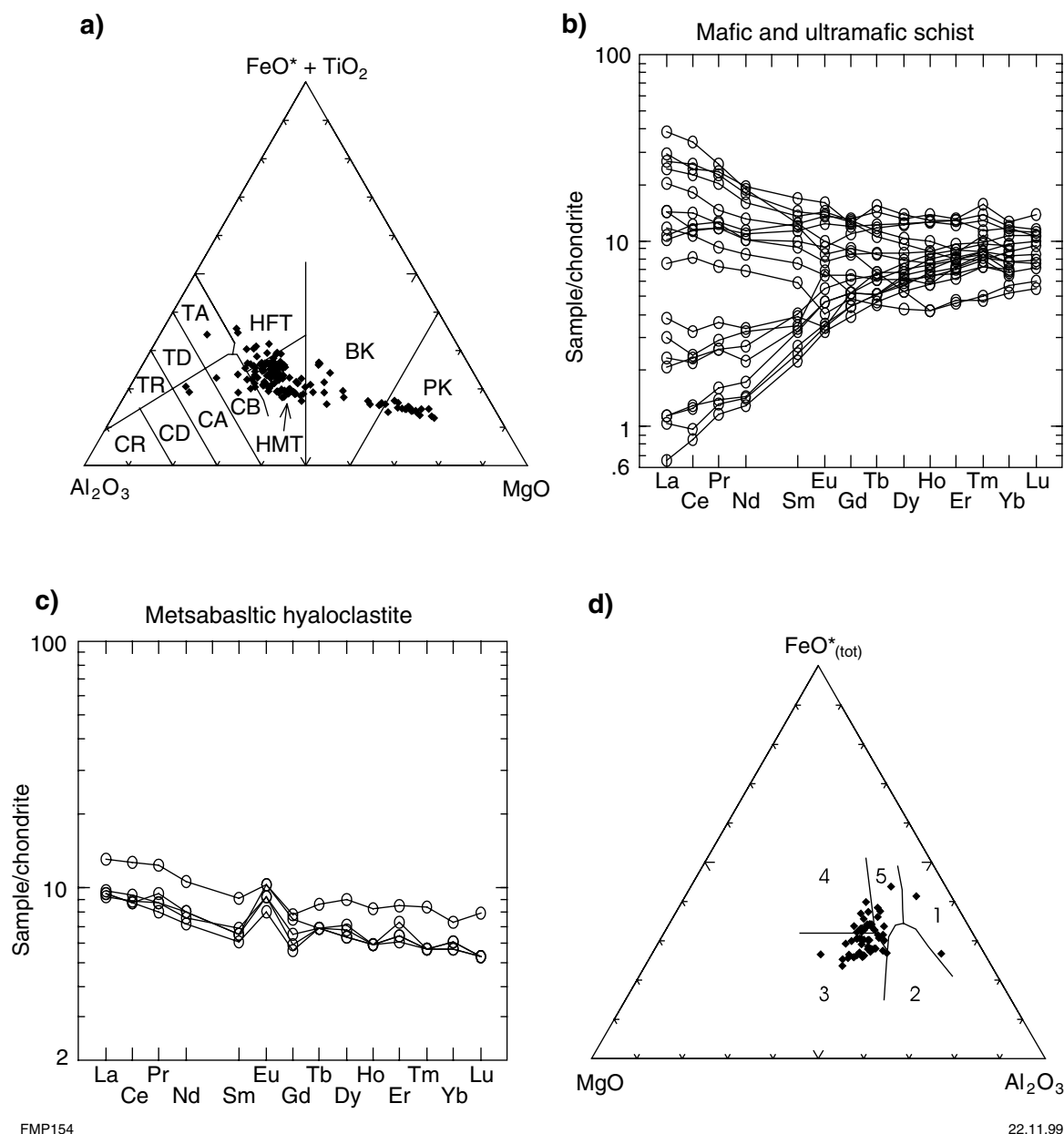


Figure 15. Geochemical discriminant plots for Narracoota Formation rocks: a) Jensen (1976) cationic plot showing range of compositions from high-Mg tholeiite (HMT), through high-Fe tholeiite (HFT), basaltic komatiite (BK), peridotitic komatiite (PK), tholeiitic andesite (TA), tholeiitic dacite (TD), calc-alkaline basalt (CB), and calc-alkaline andesite (CA); b) Chondrite-normalized rare-earth element plot of mafic (HREE-enriched) and ultramafic (HREE-depleted) schist (normalizing factors after Sun, 1982); c) Chondrite-normalized rare-earth element plot of metabasaltic hyaloclastite (normalizing factors after Sun, 1982); d) Triangular discriminant plot (Pearce et al., 1977), showing the tectonic environment of the Narracoota Formation. Tectonic fields are as follows: 1) spreading-centre island; 2) orogenic; 3) ocean ridge and floor; 4) ocean island; and 5) continental

Hawaiian tholeiites (Stern et al., 1995). The inference from these comparisons is that submarine volcanoes may have been a component of the Narracoota Formation.

Tectonic discriminant diagrams do not provide reliable information on the palaeotectonic environment within which igneous rocks were emplaced (Duncan, 1987; Wang and Glover, 1992). Nevertheless, if there is petrological evidence that the rocks have not undergone extensive crystal fractionation and the overall geological context is

taken into account, selected discriminant diagrams can be used to estimate palaeotectonic settings. With the above considerations in mind, and remembering that the rocks in question have a subalkaline chemistry, the $\text{FeO}_{(\text{tot})}$ – MgO – Al_2O_3 plot of Pearce et al. (1977) is deemed appropriate (Fig. 15d). The $\text{FeO}_{(\text{tot})}$ – MgO – Al_2O_3 plot has been used successfully in geologically well constrained areas (Breitkopf and Maiden, 1988). The $\text{FeO}_{(\text{tot})}$ – MgO – Al_2O_3 plot suggests that the Narracoota Formation volcanic rocks were formed in tectonic environments of

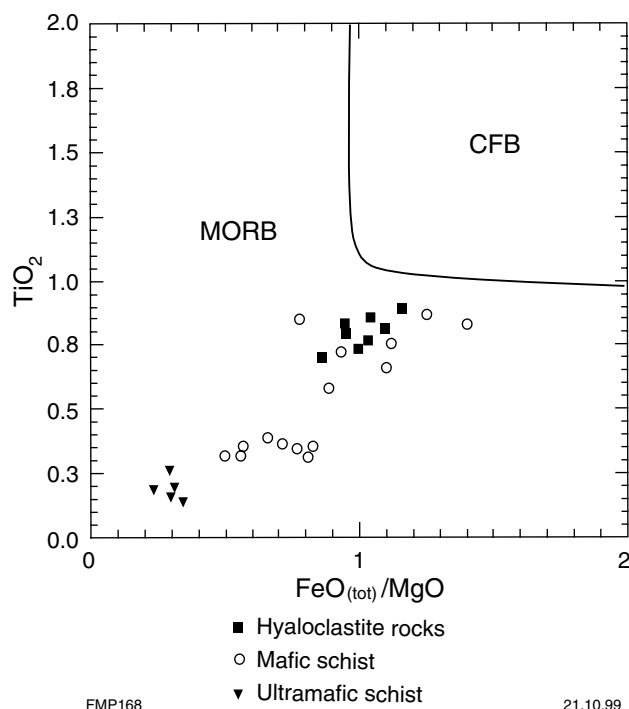


Figure 16. TiO_2 versus FeO/MgO plot (Breitkopf and Maiden, 1988) for the Narracoota Formation showing the mid-ocean ridge basalt (MORB) affinity of the mafic and ultramafic schist, and the transitional chemistry of the hyaloclastites towards continental flood basalts (CFB)

MORB – oceanic island to continental affinity (Fig. 15d). This diagram, however, has limitations if the rocks have been subjected to ocean-floor metamorphism. A more useful plot is the TiO_2 – $\text{FeO}_{(\text{tot})}$ – MgO plot, which was used by Breitkopf and Maiden (1988) in their study of the Neoproterozoic Matchless Amphibolite Belt of the Damara Orogen in Namibia. The TiO_2 – $\text{FeO}_{(\text{tot})}$ – MgO plot supports the gradation from MORB towards continental flood basalt because the hyaloclastite rocks plot closer to the continental field than do the mafic schist (Fig. 16). This feature, together with other considerations, such as Mg#, and geological and petrological constraints, indicate that the hyaloclastite was erupted on a continental rift margin. This has important implications for the tectonic evolution of the Bryah–Padbury Basin, as explained in **Tectonic model and conclusions**.

Ravelstone Formation

The Ravelstone Formation is poorly exposed in scattered low outcrops over a wide area in the northern and central parts of the Bryah Basin. Rocks of the Ravelstone Formation were previously considered by MacLeod (1970) and Gee (1979, 1987) to belong to the ‘Thaduna Greywacke’ (now Thaduna Formation of the Yerrida Group), for which the type area is about 100 km to the east-northeast on THADUNA (Pirajno and Adamides, 1998).

The Ravelstone Formation comprises a succession of lithic and quartz wacke, shale, and siltstone that was

deposited from turbidity currents. In the north, the Ravelstone Formation contains lenses of chert and is unconformably overlain by the Mesoproterozoic Bangemall Group. West of the Peak Hill open-cut, the lower contact with the Narracoota Formation is disconformable, whereas the upper contact with the Horseshoe Formation appears to be conformable. In the central and northern parts of BRYAH, the Ravelstone Formation, although metamorphosed, has no tectonite fabric. On MILGUN (around Fortnum), however, a well-developed foliation is present.

Drillcore from the Harmony gold deposit shows that the contact between the base of the Ravelstone Formation and the top of the Narracoota Formation is interfingered, possibly due to shearing. The disconformable contact between the base of the Ravelstone Formation and the top of the Narracoota Formation is exposed in a river bed about 1 km due east of the Fortnum – Peak Hill turn-off. In this area, graded layers of immature subarkosic sandstone to siltstone contain fresh plagioclase, K-feldspar, sericitized lithic fragments, and angular quartz grains in a matrix composed of sericite and biotite. In addition, the siltstone contains euhedral crystals of tourmaline. Metamorphic brown biotite and muscovite are abundant and replace feldspars, quartz, and lithic fragments. Lithic fragments include massive chlorite(–rutile) derived from mafic precursors, chert, hematite–quartz shale, as well as partly sericitized feldspar grains. Quartz grains include rounded to irregular shapes, and biotite is metamorphic in origin. Quartz, white mica, chlorite, and variable amounts of carbonate are part of the fine-grained matrix. Well-developed foliation, where present, is defined by aligned sericite, elongate quartz, and, to a lesser extent, feldspar grains, and by mica seams. New muscovite flakes have grown along and across the foliation.

In the Fortnum mine area, on MILGUN, graded bedded lithic wacke and siltstone overlie the volcanic rocks of the Narracoota Formation. The wacke contains medium to coarse-grained crystals of feldspar (plagioclase, minor K-feldspar) and quartz as well as fragments (fine metabasalt and chlorite) derived from mafic volcanic rocks. The feldspar crystals, which are strongly sericitized, dominate over quartz. The matrix consists of sericite–chlorite–quartz, with or without carbonate. The reworked rocks include fragmental layers with fine metabasalt debris and graded chloritic siltstone containing plagioclase laths. The derivation of the mafic component is easily explained, but the well-preserved feldspar crystals suggest nearby granitic or felsic ?volcanic precursors.

Horseshoe Formation

The Horseshoe Formation occupies areas west of the Peak Hill open-cut and the northern parts of BRYAH and MILGUN. This formation includes finely laminated ferruginous (hematitic) shale and siltstone, fine-grained quartz–feldspar wacke with interleaved iron formation and chert, graded quartz wacke, manganese shale, garnetiferous biotite–chlorite schist, and garnetiferous iron-formation. Relatively high manganese contents are inferred from the abundant manganese oxide staining in

weathered and lateritic rocks, and lateritic manganese ore has been mined at the Horseshoe and Mount Padbury mines. The type area of the Horseshoe Formation is the Horseshoe Range (Occhipinti et al., 1997), where a thickness of approximately 1000 m was estimated by Gee (1979). The Horseshoe Formation overlies the Narracoota Formation; however, the contact is either conformable or tectonic. Elsewhere, on JAMINDI, north of BRYAH, the Horseshoe Formation overlies the Ravelstone Formation and the contact is gradational and conformable. The Horseshoe Formation underlies the Labouchere Formation of the Padbury Group. The nature of this upper contact appears conformable; however, Martin (1994) suggested that there is a regional unconformity between these units.

Structurally, the Horseshoe Formation forms a broad syncline with its axis trending approximately easterly. The southern limb of this syncline is in sheared contact with rocks of the Narracoota Formation. In this area the Horseshoe Formation is complexly folded, with axes trending 070°, parallel to the shear zone.

In the Horseshoe Range, Gee (1987) recognized three units: 1) a lowermost part consisting of regularly bedded wacke and shale, similar to the underlying Ravelstone succession, but finer grained, more calcareous, and containing less chlorite and more feldspar and quartz, indicative of a granitic rather than mafic volcanic provenance; 2) a middle iron-formation member with several BIF (chert–magnetite–stilpnomelane; white chert) horizons intercalated with chloritic shale; and 3) an upper unit of calcareous manganese-bearing shale and wacke. The lowermost unit is exposed on MILGUN in the low hills east of Fortnum airstrip, where fine-grained, carbonate-cemented wacke and shale contain disharmonic-folded white-chert lenses (2–12 cm thick) and less common discontinuous quartz–magnetite layers (2–3 cm). The quartz wacke component of the Horseshoe Formation contains quartz, plagioclase, microcline, biotite, and muscovite, all as detrital minerals. Near the Peak Hill opencut, the iron formation is made up of biotite, amphibole, chlorite, quartz, magnetite, and garnet. This unusually high grade assemblage may be related to the metamorphism of the Peak Hill Schist (see **Metamorphism**).

About 1 km north of the Ravelstone manganese deposits, a reasonably good exposure of the Horseshoe Formation was examined in detail. A stratigraphic column for this locality is shown in Figure 17. This is a folded, upward-coarsening package, approximately 350 m thick, which from base to top consists of quartz–lithic wacke with banded chert interbeds displaying a well-developed axial planar cleavage, quartz wacke with iron formation and shale interbeds, massive beds of coarse-grained quartz–lithic wacke intercalated with thin granular iron-formation, amphibole- and garnet-bearing granular iron-formation layers, and massive quartz–lithic wacke intercalated with thin iron-formation bands. The quartz–lithic wacke contains chert clasts, detrital subangular quartz, fresh plagioclase crystals, and biotite in a matrix of sericite, green chlorite, and iron oxide grains. Banded cherty material is composed of granular quartz aggregates, brown biotite, actinolite, and very fine carbonate-rich laminae (this rock is best classified as a quartz–biotite–

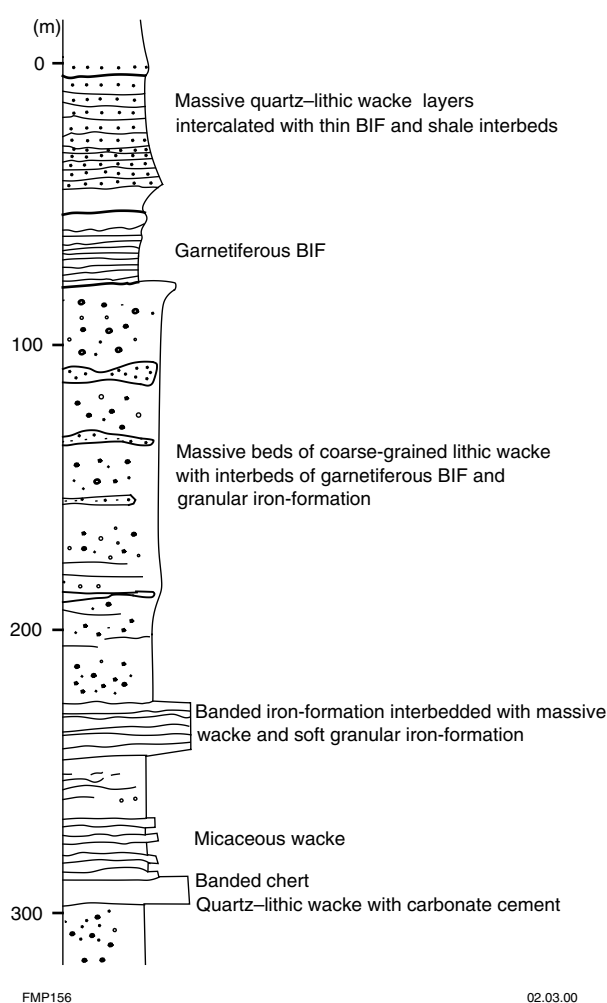


Figure 17. Schematic stratigraphy of the Horseshoe Formation, from an area of outcrops about 12 km west-northwest of the Peak Hill mine (after Pirajno and Occhipinti, 1998; width of column reflects relative resistance to weathering)

actinolite schist). The granular iron-formation consists of granular aggregates of quartz and iron oxides with interstitial biotite and chlorite. Syntectonic garnet porphyroblasts are replaced in part by quartz and carbonate. Massive lithic wacke consists of a packed aggregate of angular quartz, feldspar, and chert grains; the matrix is volumetrically small and made up of biotite, quartz, and sericite. Garnetiferous iron-formation has dark laminae of quartz granules with interstitial actinolite–chlorite, iron oxides, and light-coloured microbands (1 cm thick) of quartz with actinolite–chlorite, iron oxides, and disseminated syn–late-tectonic garnet porphyroblasts. Garnet is also present as porphyroblasts growing across microband boundaries.

Padbury Group

The Padbury Group locally unconformably overlies the Horseshoe Formation of the Bryah Group, but, in places, is in faulted contact with the Bryah Group and Yarlalweelor gneiss complex (Narryer Terrane, Yilgarn

Craton; Fig. 2). Considerable onlap of the Padbury succession onto the various formations of the Bryah Group can be inferred; these contacts were faulted, possibly in several stages, during basin closure. The age of the Padbury Group is poorly constrained. Nelson (1997) reported a maximum age of c. 2.0 Ga from the upper part of the Wilthorpe Formation, and Windh (1992) inferred a minimum age of c. 1.8 Ga from a leucogranite dyke.

Martin (1994, 1998) proposed a formal stratigraphy for the lower Padbury Group based on detailed sedimentological studies in the area covering the southeastern and central parts of MILGUN. This formal stratigraphy replaced previous stratigraphic divisions (Barnett, 1975; Gee, 1979, 1987; Windh, 1992), and has since been expanded to include two distinct lithostratigraphic units as members within the Wilthorpe Formation: the Heines and Beatty Park Members (Occhipinti *et al.*, 1997). Martin (1994, 1998) interpreted the Labouchere and Wilthorpe Formations as an upward-coarsening deep-water turbidite complex overlain by shales and iron formation of the Robinson Range Formation. The turbidites were derived by erosion from the granite–gneiss basement (Yilgarn Craton) and by reworking of underlying sedimentary and mafic volcanic rocks in the Bryah Basin.

The Padbury Group contains quartz wacke, siltstone, conglomerate, iron formations, hematitic shale, and minor clastic rocks and dolomite (Martin, 1994; Occhipinti *et al.*, 1997) and is subdivided into four formations: Labouchere, Wilthorpe, Robinson Range, and Millidie Creek Formations. Martin (1994) interpreted the Padbury Group to have been deposited in a retroarc foreland basin that developed on top of the Bryah Group.

Labouchere Formation

The Labouchere Formation occupies areas in the northwestern part of the Bryah Basin, where it is faulted against the Yarlalweelor gneiss complex. Martin (1994, 1998) suggested that the Labouchere Formation unconformably overlies the Horseshoe Formation (Bryah Group), based on the regional geometry in the Fortnum mine – Dandy Well area on MILGUN. The regional unconformity is inferred from the low-angle truncation of an iron-formation marker unit in the Horseshoe Formation against lowermost quartz arenite of the Labouchere Formation in the area south of Yarlalweelor Creek. North of the Fortnum Fault, iron formation within the Horseshoe Formation is nearly parallel to bedding in the Labouchere Formation. Elsewhere in the region, contacts between various formations of the Bryah and Padbury Groups are interpreted as unconformities (Windh, 1992) or, alternatively, as faults or shear zones (Pirajno and Occhipinti, 1998; Occhipinti *et al.*, 1998b). On BRYAH the Labouchere–Horseshoe Formation contact is marked by a conglomeratic unit. The Labouchere Formation is conformably overlain by and grades into the Wilthorpe Formation (Martin, 1994), although this contact was previously described as an unconformity (Gee, 1979). Gee (1979) estimated the Labouchere Formation (including the Wilthorpe Formation) to be 5000 m thick, extending from

Mount Labouchere on MILGUN (type area; Martin, 1994) to the Horseshoe Range, the southern continuation of which is in northwestern BRYAH. Martin's (1994, 1998) type section is a composite stratigraphy (up to 7000 m thick) based on four separate sections in southeastern MILGUN.

The Labouchere Formation consists of quartz arenite, medium- to coarse-grained sericitic quartz wacke and sericitic siltstone, minor conglomerate, and banded iron-formation in an upward-coarsening succession. Near the Horseshoe manganese mining area, the Labouchere Formation consists of a thick succession of upward-fining cycles up to 700 m thick. Each cycle consists of conglomerate or a coarse lithic–quartz–sericite wacke unit at the base, grading up through coarse- to fine-grained quartz–feldspar–lithic wacke and sericitic siltstone to iron-rich shale. These cycles, however, become increasingly coarser upwards, so that there is regional upward coarsening. The base of the topmost cycle begins with a quartz-pebble conglomerate. Minor and thin bands of iron-formation are locally present as intercalations within the sedimentary units.

Quartz arenite contains grain-supported, well-rounded quartz in a sericitic matrix and is extensively silicified. A prominent quartz arenite marker forms the ridge including Mount Labouchere north of Fortnum mine on MILGUN, and can be traced for many tens of kilometres to the southeast where, gradually, more quartz wacke is interbedded with the arenite. A second quartz arenite marker approximately halfway up the Labouchere Formation is present in the area north of the Fortnum Fault. In the same area, an iron formation – chert layer is present about 250 m above this second quartz arenite. Martin (1994) emphasized that the deep-water environment of this iron formation indicates a similar depositional environment for the clastic rocks. Quartz wacke has a matrix-supported framework of variably rounded quartz grains, minor lithic fragments, and feldspar in a sericite–chlorite matrix, whereas laminated shale consists of sericite–chlorite. Wacke and siltstone form numerous upward-fining cycles.

Muscovite–quartz schist or slate developed from quartz wacke and siltstone in zones of high strain and higher metamorphic grade adjacent to the Yarlalweelor gneiss complex. Strongly foliated quartz wacke and muscovite–quartz schist occupy a 4 km-wide zone near the Labouchere mine on MILGUN. Another belt of schist and slate is present between the Billara Fault and Despair Granite in southwestern MILGUN. These strongly foliated rocks can be traced northwards into recognizable, though strongly foliated, pebbly quartz wacke. The fine-grained schist consists of elongate, polygonal–granoblastic quartz with spaced trails of aligned muscovite flakes. Bedding–cleavage relationships are found in less-deformed areas, whereas in high-strain zones, differentiated layering developed from a pervasive crenulation cleavage.

Sericite is abundant throughout most of the rocks of the Labouchere Formation. The quartz–sericite wacke is composed of subangular quartz grains embedded in a sericitized matrix with occasional large muscovite 'books' and scattered small crystals of tourmaline and anatase.

Quartz–feldspar–lithic wacke is made up of subangular quartz grains, polycrystalline quartz, K-feldspar, and plagioclase in a matrix of quartz, sericite, biotite, and minor detrital zircons.

Wilthorpe Formation

The Wilthorpe Formation (formerly ‘Wilthorpe Conglomerate’; Gee, 1987), including the Beatty Park and Heines Members, comprises quartz- and chert-pebble conglomerate, quartz wacke, sericitic siltstone, chlorite–quartz shale, quartz–sericite–hematite schist, dolomitic sandstone, and finely laminated chert lenses. The Wilthorpe Formation is conformably overlain by the Robinson Range Formation.

Martin (1994) measured the type section of the Wilthorpe Formation (about 1300 m thick) along the Talbot Divide. In this area, the characteristic quartz-pebble conglomerate forms a prominent ridge to the east of hills underlain by the Robinson Range Formation. In the Fortnum–Labouchere area on MILGUN, the exact location of the Labouchere–Wilthorpe Formation transitional boundary is less well defined (Swager and Myers, 1999). Along the western wall of the Nathans Deep South opencut (labelled Nathan Deep on Plate 1), several upward-fining cycles of quartz-pebble conglomerate grading into quartz wacke and quartz–muscovite siltstone can be observed. These cycles are underlain by fine-grained chloritic shale interbedded with quartz wacke. This chloritic shale with detrital ilmenite is derived from a mafic precursor, probably the Narracoota Formation (Windh, 1992). Occhipinti et al. (1998a) recognized comparable ‘mafic’ clastic rocks as a mappable unit (Beatty Park Member — see below) at the top of the Wilthorpe Formation on PADBURY.

The conglomerate contains well-rounded, slightly elongate or faceted vein-quartz clasts and, less commonly, chert, quartzite, quartz wacke, and rare siltstone–mudstone clasts in a quartz wacke matrix. Clasts range in size from pebbles to boulders. Quartzite pebbles locally contain folded foliation fabrics. Bunting et al. (1977) suggested that large quartzite boulders in the southern part of the type area were derived from the basal Finlayson Member of the Juderina Formation (Yerrida Group). Martin (1994, 1998) recognized two polymictic conglomerate intervals in the type area, which included silicified dolomite clasts. These intervals are similar to the polymictic conglomerate and sandstone of the Heines Member defined on BRYAH (Pirajno and Occhipinti, 1998). Siltstone forms a distinct mappable upper unit along the gradational contact with the Robinson Range Formation.

Beatty Park and Heines Members

The Beatty Park Member outcrops in the Mount Padbury area on PADBURY and contains clastic rocks that were possibly sourced, at least in part, from the mafic volcanic rocks of the underlying Narracoota Formation (Bryah Group), with sedimentary chert lenses towards its top. A sensitive high-resolution ion microprobe (SHRIMP) U–Pb date obtained from detrital zircons in one of these

chert lenses suggests a maximum age of 1996 ± 35 Ma (Nelson, 1997). The clastic rocks of the Beatty Park Member are dominated by metamorphosed chlorite–quartz shale, siltstone, and wacke; several conglomeratic or breccia lenses; and finely laminated chert layers in places (Occhipinti et al., 1997). The contact between the Beatty Park Member and the overlying Robinson Range Formation is gradational, with chloritic siltstone and chert layers and lenses grading into sericite–quartz siltstone. The lower contact of the Beatty Park Member with the Wilthorpe Formation appears to be gradational in the area west of the Fraser Synclinorium (see **Structure**), where ferruginized kaolinitic siltstone and quartz wacke grade into chloritic siltstone. In this area, the minimum thickness of 470 m is implied because the upper part of the Beatty Park Member is not exposed.

The shale–siltstone layers are well bedded to finely laminated, and consist of quartz and chlorite, with minor sericite, epidote, feldspar, titanite, and detrital hornblende. These layers are accompanied by very fine grained, recrystallized, white chert beds in the upper part of the Beatty Park Member. West of the Fraser Synclinorium, sedimentary structures such as bedding-parallel laminations, flame structures, and contorted bedding can be observed within chloritic siltstone. Two types of wacke units are present: one containing quartz, dolomite, chlorite, feldspar, sericite, epidote, sphene, and opaque minerals (either magnetite or pyrite); and the other containing quartz, feldspar, muscovite, epidote, chlorite, carbonate, and opaque minerals. Lithic fragments in wacke layers include metabasalt and mafic schists in which leucoxene pseudomorphs of iron oxides can still be recognized. Lenses of coarse-grained lithic wacke and conglomerate comprise rock fragments of basalt, mafic schist, chert, chlorite–quartz wacke, and coarse detrital grains (quartz, feldspar) in a sericite–chlorite–quartz matrix. Coarse clastic rocks fill channels that cut into the fine-grained rocks and contain numerous rip-up clasts. This suggests that, at least in part, the Beatty Park Member was deposited distally from the source region. Locally, white chert lenses crosscut erosional contacts, indicating that the chert is diagenetic or epigenetic.

Within all rocks of the Beatty Park Member, sericite and muscovite are of metamorphic origin. They replace chlorite in the fine-grained chloritic shale–siltstone layers, and feldspar clasts in the wacke units. In several examples, fine-grained muscovite has grown along late cleavage planes.

A quartz–chloritoid–sericite–chlorite(–sulfide) unit previously interpreted to be a carbonate intrusion (Lewis, 1971; Elias and Williams, 1980) has been assigned to the Beatty Park Member. The chloritoid is crystallized in sprays and displays a ‘bow-tie’ texture. The presence of abundant chloritoid indicates that this rock has a high alumina content, implying either a pelitic precursor or that the protolith was extensively metasomatized.

The Heines Member consists of an upward-fining succession of sedimentary rocks, with a polymictic conglomerate at its base, followed by clastic sedimentary units (sandstone to shale). The type area is near Durack

Well, on BRYAH. At this locality the Heines Member is folded into a syncline, and its southern limb is in faulted contact with the underlying Narracoota Formation. The northern contact is obscured here by the Cainozoic cover. The Heines Member includes those outcrops south of the Robinson Syncline, at the Heines Find prospect, Randell Bore, and 3.5 km northwest of Durack Well, which were previously mapped as 'Wilthorpe Conglomerate' by Gee (1987). The succession is approximately 600 m thick, although basal units may have been sheared off along the faulted contact. The basal polymictic conglomerate contains clasts of mafic lithic wacke, limestone, quartz arenite, and hematitic shale supported by a carbonate matrix. This is followed upward by a series of sandstone–shale units, with the shale component becoming volumetrically greater with stratigraphic height. The basal conglomerate of the Heines Member contains no volcanic clasts of the underlying Narracoota Formation, and this is taken as evidence that the contact with the latter formation is tectonic. The provenance of the various clasts in the basal conglomerate is not known. In the Heines Find prospect area, the Heines Member is overlain by the Robinson Range Formation.

Robinson Range Formation

The Robinson Range Formation forms elongate outcrops that extend from east to west in the centre of the Bryah–Padbury Basin, and in a northerly direction on the eastern margin of the Yarlalweelor gneiss complex on MILGUN and PADBURY (Plate 1). The Robinson Range Formation is defined by the appearance of ferruginous or hematitic shale followed by two iron formations — a well-defined lower banded unit, separated by 100 m of ferruginous shale from an upper unit with clastic textures as mapped by Gee (1987), which is in turn overlain by hematite–chlorite siltstone. The Robinson Range Formation is conformably overlain by the Millidie Creek Formation.

The Robinson Range Formation consists of a succession of BIF, siltstone, and iron-rich shale. Granular iron formation is present as irregular lenses. The BIF consists of laminae up to 3 cm thick. These laminations comprise various amounts of quartz, iron oxides (hematite or magnetite), biotite, and, locally, ferro-actinolite. The shale and siltstone consist of fine-grained sericite, quartz, chlorite, iron oxides, and, in a few places, minor sphene. The mesostructure, microstructure, and petrology of the BIF are relatively simple. Microbands or laminae less than 1 to 2–3 mm thick are made up of alternating microcrystalline quartz(– iron oxides), green–brown biotite(– iron oxides), quartz grains(– acicular crystals – iron oxides), quartz grains(– iron oxides – biotite – acicular crystals). Commonly, the quartz grain(– acicular crystal) assemblage displays a polygonized texture suggestive of annealing due to metamorphism. The acicular crystals are weathered to iron oxides, but on the basis of their morphology, they could be either stilpnomelane crystals or amphiboles. The iron oxides are either hematite or magnetite. Incident light microscopy reveals that a primary titaniferous magnetite is replaced by hematite, which in turn is replaced by goethite in the supergene environment. The biotite is porphyroblastic and

mostly grown under conditions of peak metamorphism (see **Metamorphism**).

Granular iron-formation is characterized by a granular texture and the presence of elongate peloids 1 to 4 mm long. The peloids consist of microcrystalline chert outlined by rims of iron oxides (hematite with inclusions of ilmenite). The chert peloids are enclosed in fine microcrystalline cherty or chalcedonic material. The peloids and chert make up bands approximately 1 to 1.5 cm thick, with occasional laminae of fine chert(– iron oxides).

The ferruginous shale is composed of silt-sized quartz grains and iron oxides, with abundant interstitial biotite and minor disseminated euhedral tourmaline crystals. The tourmaline was formed either during metamorphism or a hydrothermal event.

The iron formations of the Robinson Range Formation have been correlated with the granular iron-formation of the Frere Formation (Earaheedy Basin), 150 to 450 km to the east-southeast, by Hall and Goode (1978), who compared them to those of the Lake Superior region in North America.

Millidie Creek Formation

The Millidie Creek Formation, defined by Barnett (1975) and modified by Gee (1979) and Occhipinti *et al.* (1997), forms comparatively small outcrops in the cores of the Robinson Syncline and Fraser Synclinorium (see **Structure**).

Ferruginous shale and siltstone, intercalated with irregularly banded manganiferous iron-formation, forms the basal unit of the formation. This unit is locally lateritized and hosts many manganese deposits, such as the Millidie (or Elsa) mine (see **Mineralization**). The banded manganiferous iron-formation commonly forms low ridges. On PADBURY the Millidie Creek Formation consists of iron-rich shale and siltstone, irregularly banded manganiferous iron-formation, dolomitic sandstone, ferruginous quartz wacke, and chloritic siltstone. On BRYAH the Millidie Creek Formation consists of ferruginous shales with a well-developed pencil cleavage, sandstone, and minor granular iron-formation.

Dolomitic sandstone and quartz wacke are locally present within this formation. The quartz wacke is well bedded, matrix supported, and commonly contains subangular to subrounded quartz grains. The matrix of this rock is composed of randomly oriented fine-grained biotite and includes late sphene and minor sericite. The dolomitic sandstone comprises carbonate, quartz, and muscovite.

In low hills 3 km north of 5 Mile Well (Plate 1), finely bedded micaceous siltstone–shale with interbedded quartz–dolomite siltstone layers, previously assigned to the Labouchere Formation (Elias *et al.*, 1982), have been assigned to the Millidie Creek Formation. These rocks are folded about northwesterly trending D₄ fold axes and contain S₄ foliation. They are unconformably overlain by

subhorizontal to shallowly dipping basal quartz arenite of the Bangemall Group.

Chloritic siltstone at the top of the Millidie Creek Formation is compositionally similar to the Beatty Park Member, and comprises quartz, feldspar, lithic fragments of sericite-quartz schist, and detrital cordierite grains in a foliated matrix of chlorite.

Unassigned units of the Padbury Group

Metasedimentary rocks and biotite-sericite schist, which outcrop within the Despair Granite near the Wilthorpe gold mine (Plate 1), were previously referred to as chlorite-muscovite-quartz schist and not assigned to any group (Elias et al., 1982). Occhipinti and Myers (1999) tentatively assigned these units to the Padbury Group. There are two main outcrops: one in the Wilthorpe mine and the other just outside the mine as a fault-bounded inclusion within the granite.

Sedimentary rock found within the Despair Granite is heterogeneously deformed and metamorphosed. Sedimentary structures such as cross-bedding and bedding-parallel laminations are present. This rock consists of alternating layers of very fine grained biotite, quartz, sericite, and feldspar. Accessory minerals include opaque minerals. In a few places this rock contains a foliation parallel to faults or fold-axial planes. Opaque minerals commonly crosscut the dominant (bedding) fabric. The preservation of the primary sedimentary textures suggests that strong deformation did not accompany low-grade greenschist-facies metamorphism of these rocks.

Within the Wilthorpe mine the metasedimentary rocks contain a slightly different mineralogy and are in faulted contact with the sericitized Despair Granite. For instance, in one sample there are two distinct layers composed of either sericite, quartz, biotite, and opaque minerals or biotite, sericite, quartz, and minor opaque minerals. This variation in bedding composition is consistent with that observed in the metasedimentary rocks outcropping outside the mine. The rocks within the mine are coarser grained and comprise quartz, biotite, sericite, and andalusite. Sericite and biotite overprint the foliation in the rock.

Structure

The Padbury and Bryah Basins are pervasively deformed. This deformation may have solely occurred during the c. 1.8 Ga Capricorn Orogeny, a period of oblique collision between the Archaean Pilbara and Yilgarn Cratons (Tyler and Thorne, 1990; Tyler et al., 1998; Fig. 2), or in part during the earlier c. 2.0 Ga Glenburgh Orogeny (Occhipinti et al., 1999). In addition to deforming the Bryah and Padbury Groups, this deformation also resulted in the reworking of parts of the Archaean Narryer Terrane, and the Marymia Inlier of the Yilgarn Craton (Fig. 2), to form the Yarlarweelor gneiss complex and Peak Hill Schist. The rocks of the Bryah

and Padbury Groups are locally interleaved with the Yarlarweelor gneiss complex in the western part of the region (Fig. 18). To the south, the Bryah and Padbury Groups are tectonically juxtaposed against autochthonous rocks of the Archaean Murchison Terrane of the Yilgarn Craton and the Palaeoproterozoic Yerrida Group (Fig. 2).

The Yarlarweelor gneiss complex dominantly consists of Archaean granitic gneisses that were intruded by felsic magmas at c. 1960 Ma (Sheppard and Swager, 1999) and 1820–1800 Ma (Occhipinti et al., 1998b; Sheppard and Swager, 1999). Granite sheets and veins intruded into the Archaean gneisses were pervasively deformed into open to tight folds, and metamorphosed at medium to high grades during the Capricorn Orogeny. Occhipinti and Myers (1999) suggested that these folds were originally northerly trending; however, they are probably more likely to have been northeasterly trending. Dextral strike-slip shear movement involved a transition from early ductile to later brittle deformation (Occhipinti et al., 1998b), coincident with uplift, which probably progressed from northeast to southwest in the region. This deformation produced regional-scale fault-bend folds in both the Yarlarweelor gneiss complex and overlying Palaeoproterozoic Bryah and Padbury Group rocks.

Deformation histories presented for the Yerrida, Bryah, and Padbury Groups by various authors (including Windh, 1992, and Gee, 1990) have many elements in common (Table 5). This includes major north-south compression that was responsible for the development of prominent regional, easterly trending upright folds, such as the Robinson Syncline (Fig. 18). Northerly striking folds and faults in the domain just east of the Yarlarweelor gneiss complex have been recognized as a later deformation stage (Windh, 1992; Martin, 1994). Gee (1990), Windh (1992), and Martin (1994) proposed that eastward movement of the Narryer Terrane (here referred to as the Yarlarweelor gneiss complex) was responsible for the development of these northerly trending folds. In their interpretation, the northerly striking folds formed in front of an advancing thrust sheet of Archaean gneiss and granite overriding the Bryah and Padbury Groups. Myers (1989, 1990) and Myers et al. (1996), on the other hand, regarded the Bryah and Padbury Groups as allochthonous sheets that were thrust over Archaean granite-gneiss.

Contacts of the Bryah and Padbury Groups with the Narryer Terrane, Yarlarweelor gneiss complex, Marymia Inlier, Murchison Terrane, and the Palaeoproterozoic Yerrida Group are zones of high strain, and therefore inferred to be faults. Unconformable contacts between the Bryah and Padbury Groups were reported by Martin (1994, 1998), whereas sheared and faulted contacts were reported by Pirajno and Occhipinti (1998), Occhipinti et al. (1998a,c), and Occhipinti and Myers (1999). For example, the Bryah Group is in faulted contact with the Yarlarweelor gneiss complex north of Livingstones Find, and the Murchison and Narryer Terranes are separated from the Bryah and Padbury Groups by the steep, easterly trending Murchison Fault, which has a sinistral strike-slip component (Plate 1, Fig. 2).

The Goodin Fault, a high-angle reverse fault (Pirajno and Occhipinti, 1998), is the boundary between the

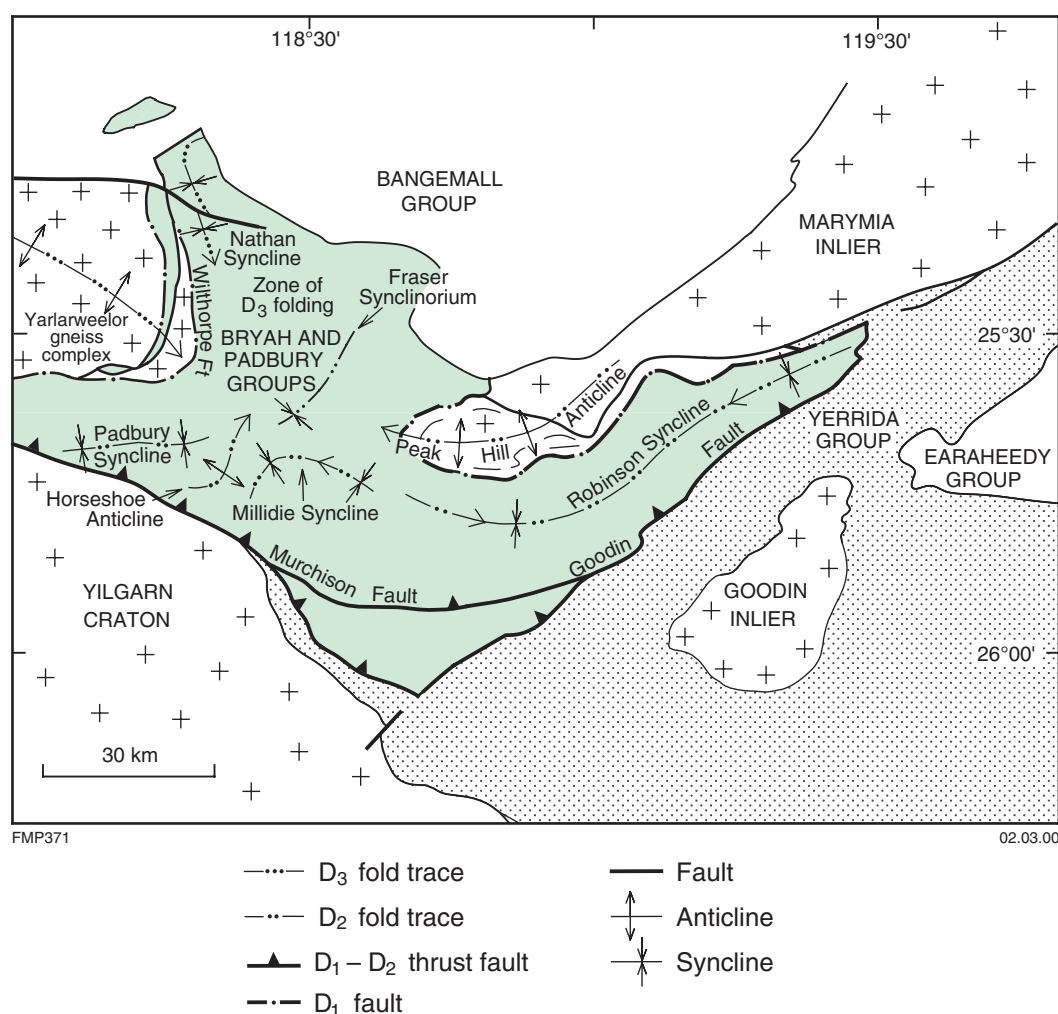


Figure 18. Major regional structures in the Bryah and Padbury Groups (after Occhipinti et al., 1998a)

Yerrida and Bryah Groups (Fig. 2, Plate 1). East of this fault, the Doolgunna Formation (Yerrida Group) is folded into isoclinal upright folds; however, much of the deformation in the Yerrida Group dies out rapidly to the east and southeast. To the west, the Goodin Fault merges with the Murchison Fault, which has juxtaposed the Bryah and Padbury Groups against the Yilgarn Craton. The Murchison Fault has a sinistral strike-slip component, which offsets Archaean structures in the Murchison and Narryer Terranes.

In this Report, four distinct groups of structures, D_1 – D_4 , representing progressive compressional deformation are recognized (Table 5). This deformation history, although in broad agreement with the previously published structural histories (e.g. Windh, 1992) recognizes separate early layer parallel structures. The structures resulting from the four deformation events are not developed everywhere, or with the same intensity everywhere.

The earliest deformation events are defined in the Peak Hill Anticline area as D_1 layer-parallel mylonitic thrust faults and originally subhorizontal folds, overprinted by D_2 upright east–west striking regional folds. Both D_1 and D_2 structures developed by north–south compression, and

can be interpreted as successive stages of progressive deformation. Northerly trending regional D_3 folds and upright foliations recording east–west compression are weakly developed in the Peak Hill Anticline, but better developed and largely restricted to a domain immediately east of the Yarlalweelor gneiss complex. However, these northerly trending structures do not always overprint older easterly trending structures and, in places, these two sets of structures (D_2 and D_3) tend to be mutually exclusive, suggesting that they probably developed during the same progressive deformation event. Late, medium-scale D_4 structures include west–northwesterly to northwesterly trending subvertical foliations, shear zones, zones of small-scale folding, and faults now outlined by quartz blows. These locally developed structures suggest late north–northeast to south–southwest compression.

Major fold structures in the Padbury and Bryah Basins are the Peak Hill Anticline, Robinson Syncline, Millidie Syncline, Fraser Synclinorium, Horseshoe Anticline, and Padbury Syncline (Plate 1 and Fig. 18). The Peak Hill Anticline, Robinson Syncline, Fraser Synclinorium, and Millidie Syncline all represent refolded folds. The easterly trending, doubly plunging Robinson Syncline and Peak Hill Anticline are D_2 folds, refolded during D_3 ; D_1

Table 5. Sequence of deformation events in the Bryah and Padbury Basins

<i>Deformation event</i>	<i>Compression</i>
D ₄	North-northeast–south-southwest compression; Small-scale folds, subvertical foliation; shear zones, faults, with quartz blows; all trending 280°–310°
D ₃	East–west compression; north–south trending folds; subvertical foliation; subvertical faults or shear zones localized east of Narryer Terrane; increasingly disharmonic east-northeasterly trending folds eastwards
D ₂	North–south compression; upright tight–isoclinal east–west folds and subvertical foliation; east–west shear zones, south-verging thrust faults
D ₁	North–south compression; subhorizontal mylonites, thrusts, and folds; mesoscale recumbent folds; tight–isoclinal, rootless

folds are also present within these structures (see **D₁ structures**). The Horseshoe Anticline appears to be a D₃ fold contained within the fault-bounded Horseshoe antichinal block. This fault-bounded block also appears to be cut by northwesterly trending (?D₄) faults.

D₁ structures

The first Palaeoproterozoic deformation event (D₁) produced layer-parallel folds, a locally pervasive S₁ schistosity, mylonites, and faults. However, because these structures were pervasively overprinted by D₂ structures, they are rarely observed. F₁ folds are locally observed in the Peak Hill Antiform, Robinson Syncline, Fraser Synclinorium, an area 5 km northeast of Mount Fraser, and the Millidie Syncline. These folds are also observed near the Peak Hill mine, in F₂ fold–hinge zones of quartz blastomylonites of the Peak Hill Schist (Fig. 6). Here, they are small-scale, rootless, isoclinal, plunge shallowly towards the east, and strike east–west. In the Fraser Synclinorium and Millidie Syncline, the F₁ folds are small-scale isoclinal folds that plunge gently towards the east-northeast or west-southwest, and strike east-northeasterly. F₁ folds are also inferred from aeromagnetic data to be present within the Fraser Synclinorium and Millidie Syncline (Figs 18 and 19).

The Goodin and Murchison Faults may be D₁ faults that were reactivated during D₂ (Occhipinti et al., 1998c). The Murchison Fault (Figs 18 and 19; Plate 1) separates largely undeformed basaltic hyaloclastite rocks in the south from foliated mafic schists to the north.

Mesoscale F₁ folds in the shale and banded iron-formation of the Robinson Range Formation are observed near Mount Padbury, north-northwest of Beatty Park Bore

(Plate 1), in the hinge zone of the Robinson Syncline, north of Tank Well, and northeast of Randell Bore. These F₁ folds are tight to isoclinal with shallow plunges that trend to the east or west. The F₁ folds in the area are interpreted as originally recumbent. D₁ zones of high strain and mylonite developed locally, mainly in the Peak Hill Schist (Pirajno and Occhipinti, 1998) and along contacts between the Yarlalweelor gneiss complex and Palaeoproterozoic cover rocks. These mylonite zones are not observed at higher stratigraphic levels within the basin, suggesting that they are restricted to a deeper crustal level, represented by the Peak Hill Schist, and basement–cover contacts. Quartz blastomylonites and the Crispin Mylonite (Pirajno and Occhipinti, 1998) form continuous units within the Peak Hill Schist (Plate 1). The internal structure of these units suggests that they may be D₁ shear zones, which were refolded during the later deformation events. The original nature and orientation of these shear zones is not known. The Crispin Mylonite consists of quartzite pebble- and boulder-sized clasts in a sericite–quartz-rich matrix, and has the appearance of a conglomerate. For that reason it was mapped by Gee (1987) as the ‘Crispin Conglomerate’. However, mesoscopic and microscopic structures indicate that it is a mylonite (Figs 4 and 7). Both the quartzite clasts and matrix contain a mylonitic fabric. The Crispin Mylonite is interpreted as a ‘pseudo-conglomerate’ (Raymond, 1984a,b) formed by shearing, probably along or close to a fault plane that separated an arkosic or granitic unit from a quartz-rich unit.

Like the Crispin Mylonite, the quartz blastomylonites form arcuate lenses within quartz–muscovite schist of the Peak Hill Schist, and are refolded by F₂ and F₃ folds. The quartz blastomylonites contain isoclinal and sometimes rootless F₁ folds, and are interpreted to have been deformed in a ductile high-strain zone (fault or shear zone) during D₁. It is not possible to determine the sense of movement during D₁ because no shear sense indicators were observed during mapping.

D₂ structures

The D₂ deformation produced large-scale, upright, regional F₂ folds with variably developed S₂ foliation, as well as faults and shear zones. These structures are easterly trending, recording north–south shortening. However, more complex patterns in the Mount Fraser area suggest complicated refolding patterns. Prominent D₂ folds include the doubly plunging Robinson Syncline and the Padbury Syncline, which has the hinge zone largely sheared out (Fig. 18, Plate 1). Mesoscale F₂ folds show steeper plunges and the S₂ foliation becomes more intense to the north. A pervasive S₂ foliation is developed over large areas in the mafic schists of the Narracoota Formation. The Goodin Fault is a high-angle reverse fault that forms the boundary between the Yerrida and Bryah Groups. This fault may have developed during D₂ because south of the fault, the Doolgunna Formation is folded into tight to isoclinal upright folds (with fold-axial surfaces subparallel to the Goodin Fault) that are similar to D₂ folds in the Bryah and Padbury Basins.

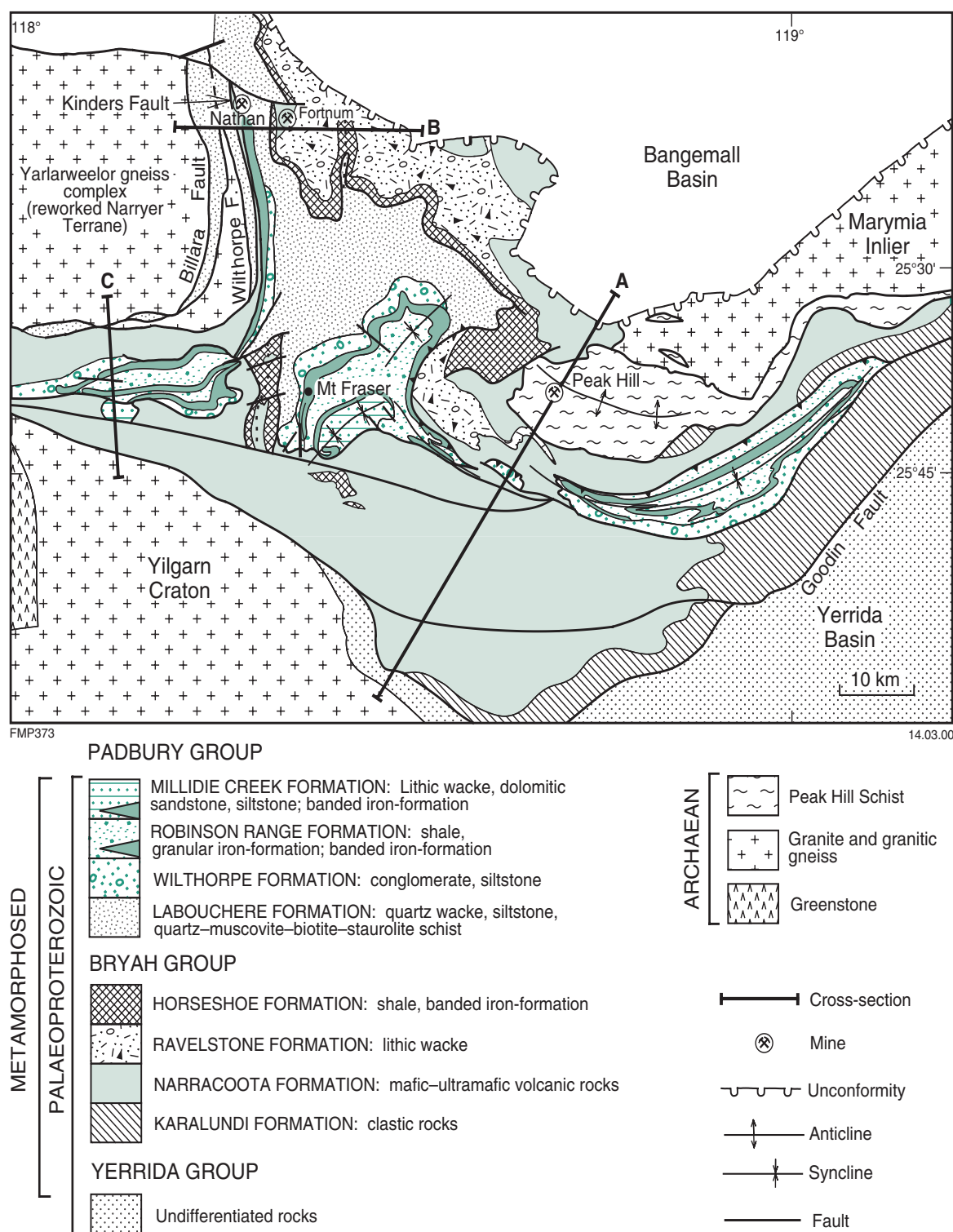


Figure 19. Simplified geological map of the Bryah and Padbury Groups (after Occhipinti et al., 1998a). See Figures 20, 22, and 23 for cross sections

The Livingstone Synform, a steep easterly plunging tight fold on MOORARIE, may be part of a larger scale D_2 fold structure that is confined between the Kerba Fault in the north and the Mount Seabrook Fault in the south (Occhipinti and Myers, 1999).

Within the Yarlalweelor gneiss complex, granitic gneisses form open to isoclinal, easterly to northeasterly and northerly trending, shallowly to steeply plunging folds. These folds plunge either to the east and northeast or to the west and west-southwest, indicating that on a

regional scale they are doubly plunging, possibly recording later refolding and east–west shortening (D_3). These folds deform both the Archaean gneiss and c. 1960 and c. 1820 Ma granite sheets that intruded the gneiss (Sheppard and Swager, 1999; Occhipinti et al., 1998c). They re-fold tight to isoclinal, subhorizontal to shallowly plunging folds in the Archaean granitic gneisses, which may have developed during the Archaean.

The sense of shear of the steeply dipping D_2 shear zones could not be determined. South of the Robinson and Fraser Synclines, regional anastomosing D_2 shear zones developed in the basaltic rocks of the Narracoota Formation. To the northeast this regional structure becomes the Jensen Fault (Pirajno and Adamides, 2000), which can be shown to have displaced the Mesoproterozoic Bangemall Group, suggesting that the fault was reactivated after this time. Along the southern limb of the Fraser Syncline, another fault extends into the D_2 shear zones mentioned above. A shear zone cuts the southern limb of the Heines Syncline, which lies between the Robinson and Fraser Synclines.

D_3 structures and their relationship to D_2 structures

Northerly trending D_3 folds, faults, and, locally, an upright S_3 foliation indicating an east–west compression are well developed in the area east of the Yarlarweelor gneiss complex. Further east, F_3 fold intensities decrease, and folds are locally more disharmonic. The D_3 event was responsible for the doubly plunging nature of the Robinson Syncline, and the Peak Hill Anticline.

The Kinders Fault (Fig. 20; Elias and Williams, 1980) is a northerly trending D_3 fault separating a wedge of mafic volcanic schists of the Narracoota Formation (Bryah Group) from the Robinson Range, Wilthorpe, and Labouchere Formation rocks (Padbury Group). This fault lies along the western limb of the sheared-out hinge of the F_3 Nathan Syncline (Plate 1 and Fig. 18). This syncline was previously correlated with the Padbury Syncline to the south (Elias and Williams, 1980; Martin, 1994, 1998). Part of the southerly plunging fold hinge of the Nathan Syncline is preserved in the Nathan mine area, and the closure of this syncline can be traced further north. The wedge of mafic–ultramafic schists of the Narracoota Formation was interpreted by Occhipinti et al. (1998c) and Martin (1994, 1998) to represent an F_3 anticlinal fold-thrust wedge overlying pervasively foliated and metamorphosed quartz wacke of the Labouchere Formation to the west (Figs 19 and 20).

West of the Kinders Fault, along the Billara Fault, sericite–quartz schist, locally with quartz-pebble conglomerate layers, contains a pervasive S_3 fabric. F_3 folds, however, are difficult to trace. East of the Kinders Fault, open to close and locally tight to isoclinal folds are outlined by marker beds in the Labouchere and Horseshoe Formations. S_3 foliations and moderate to steep, southerly plunging, small-scale F_3 folds are well developed in the area of the Horseshoe Syncline and further north.

Several observations suggest that D_2 and D_3 structures may not reflect two separate events, but may have developed contemporaneously in different domains. Intense D_3 folding is largely restricted to the area between two basement highs, represented by the Yarlarweelor gneiss complex in the west and the Peak Hill Schist in the east (Figs 18 and 19). In the domain just east of and adjacent to the Yarlarweelor gneiss complex, there is no evidence for D_3 refolding D_2 (i.e. upright northerly trending D_3 folds overprinting upright easterly trending D_2 folds), even though weak northerly trending D_3 folds deform easterly trending F_2 folds around and within the Peak Hill Anticline.

In the Mount Fraser area, complex fold and foliation patterns show orientations different from and transitional to both the regional D_2 and D_3 deformation. Large-scale, east-northeasterly trending F_2 folds, such as the Robinson Syncline and Peak Hill Anticline, die out in this area. The Millidie Syncline can be traced from a west-northwesterly strike (subparallel to and en echelon with the Robinson Syncline) to a west-southwesterly strike, and is then cut off to the south by D_3 faults (Figs 18 and 19).

These observations suggest that the intensity and trend of the D_2 and D_3 structures were influenced by their spatial relationship to the Yarlarweelor gneiss complex and Peak Hill Schist.

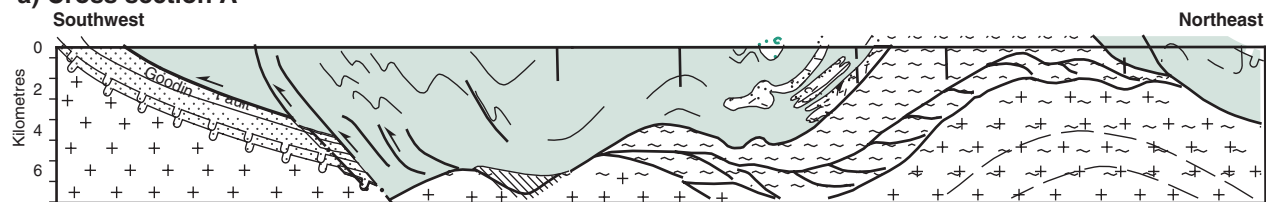
D_4 structures

D_4 structures include mesoscopic chevron folds, kinks, shear zones, and faults, and were locally accompanied by the development of a foliation. These D_4 structures developed locally throughout the Bryah and Padbury Basins, Yarlarweelor gneiss complex, and the northernmost part of the Murchison Terrane. In the Padbury–Bryah domain, most structures trend between west-northwest and northwest, although in the Yarlarweelor gneiss complex, a few late structures trend between north-northwest to north. Brittle faults cutting the Yarlarweelor gneiss complex often show dextral strike-slip shear movement.

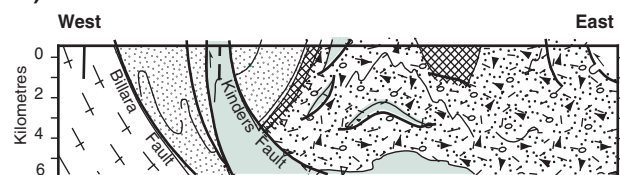
Metamorphism

Regional metamorphic zones within the volcano-sedimentary succession are related to the geometry of the Peak Hill Anticline and Yarlarweelor gneiss complex. The highest metamorphic grade assemblages are found in the contact zones between the Yarlarweelor gneiss complex and overlying metasedimentary rocks. Assemblages in the Peak Hill Schist and within quartz–mica schists (Labouchere Formation) along faulted contacts with the Yarlarweelor gneiss complex record upper greenschist- to lower amphibolite-facies conditions. Within the Yarlarweelor gneiss complex, upper amphibolite-facies conditions were reached as incipient (minimum) melt patches within granitic gneiss, and amoeboid textures in Palaeoproterozoic coarse-grained granite probably developed during D_2 (Sheppard and Swager, 1999). In the Bryah and Padbury Groups, however, metamorphism typically does not exceed greenschist facies, and east of

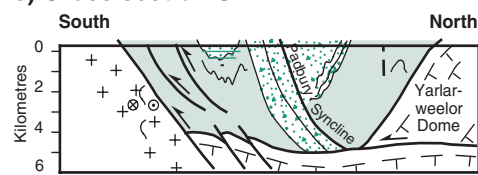
a) Cross section A



b) Cross section B



c) Cross section C



MIDDLE PROTEROZOIC

Bangemall Group

EARLY PROTEROZOIC

PADBURY GROUP

- Millidie Creek Formation: sandstone, shale, dolomitic siltstone
- Robinson Range Formation: ferruginous shale, banded iron-formation
- Wilthorpe Formation: quartz-pebble conglomerate
- Labouchere Formation: quartz wacke, siltstone, quartz arenite

BRYAH GROUP

- Horseshoe Formation: ferruginous shale, iron formation
- Ravelstone Formation: lithic wacke
- Narracoota Formation: metabasalt; subordinate dolerite, picrite, and peridotite
- Karalundi Formation: clastic rocks

YERRIDA GROUP

Undifferentiated rocks

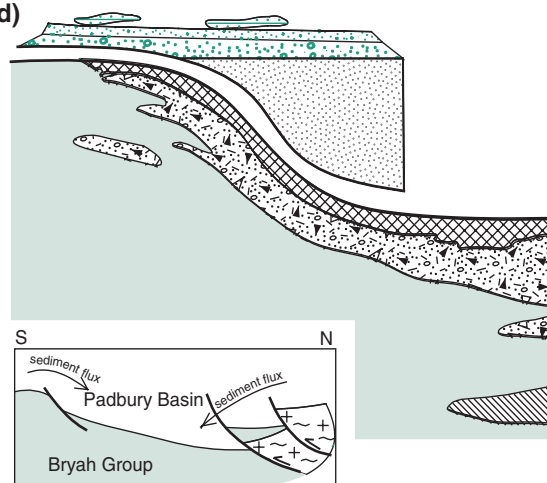
ARCHAEAN (reworked during Early Proterozoic)

- Peak Hill Schist: quartz-muscovite schist, quartz mylonite, phyllonite
- Granite-greenstone: Marymia Inlier – Murchison Terrane
- Granite gneiss and granite, with lenses of supracrustal rock: Narryer Terrane

ARCHAEAN (in situ)

Granite-greenstone: Murchison Terrane

d)



- Geological boundary
- Unconformity
- Bedding or layering trend
- Foliation
- High-strain zone
- Fault
- Normal fault reworked during D₂ thrusting
- Movement along fault
- Movement away and towards observer

the Goodin Fault in the Yerrida Group, metamorphic grade decreases to subgreenschist facies (prehnite–pumpellyite). The relationships between metamorphic mineral growth and deformation are summarized in Table 6.

M_1 was a prograde regional metamorphic event that typically reached greenschist facies (Pirajno and Occhipinti, 1998), and was probably coincident with D_1 in the Bryah and Padbury Groups and Peak Hill Schist. Thornett (1995) suggested that some parts of the Peak Hill Schist reached amphibolite-facies metamorphism, with temperatures between 500° and 620°C, and pressures of 6.5–7 kbar. Metamorphic mineral assemblages observed, however, commonly do not concur with these data. The second metamorphic episode, M_2 , was commonly one of retrogression throughout most of the Bryah and Padbury Basin, and probably associated with metasomatism in high-strain zones during D_2 – D_3 . During M_2 , in the western part of the Bryah and Padbury Basins adjacent to the Billara Fault (Fig. 18), staurolite–andalusite–biotite–muscovite–quartz schist developed from the metamorphism of Padbury Group sedimentary rocks. These rocks indicate metamorphism at amphibolite facies. Inclusion trails in staurolite and andalusite porphyroblasts suggest that the porphyroblastic growth occurred after D_1 , but before D_2 . The S_2 foliation is defined by the alignment of muscovite and biotite, which wraps around the porphyroblasts and probably developed in D_2 during M_2 . As staurolite is locally partially replaced by fine-grained muscovite, this foliation may have developed in the greenschist facies. This foliation is locally overprinted by chloritoid. Further west, at the contact between the Palaeoproterozoic Kerba Granite and the Narracoota Formation, a quartz–kyanite–tremolite–feldspar schist indicates upper greenschist-facies metamorphism, with the pressure of metamorphism estimated to have been between 3 and 4 kbar (Spear, 1993; Occhipinti and Myers, 1999).

For the most part, M_2 involved retrogression, metasomatism, and local hydrothermal alteration. Mineral assemblages formed during M_2 are commonly observed in high-strain zones where the S_2 schistosity is well developed. These include a domain of well-developed D_2 shear zones south of the Robinson Syncline, where pervasive retrogression of metabasalts to actinolite–chlorite schist is observed (Pirajno et al., 1995a). In

addition, in the Mount Pleasant opencut, growth of albite porphyroblasts and the development of chlorite at the expense of biotite and epidote also occurred during M_2 .

Banded iron-formation in the Robinson Range Formation shows a change in metamorphic mineral assemblage from east to west across the trend of the D_2 Robinson Syncline. To the west, randomly oriented biotite overprinted quartz, stilpnomelane, and iron oxides. The appearance of this late-stage biotite coincides with regional geochemical trends (elevated Sb, As, and W; Davy et al., 1999) along the same structure, suggesting a late- or post- D_2 , low-temperature, metasomatic event. Albite porphyroblasts in alteration zones associated with gold mineralization in the Peak Hill Schist also grew at a late stage because they overprint S_2 .

South of the Murchison Fault, little-deformed basaltic hyaloclastites contain mineral assemblages characteristic of prehnite–pumpellyite to lower greenschist facies. This suggests that rocks south of the Murchison Fault were not exposed to the regional greenschist-facies metamorphism or moderate- to high-grade metamorphism that occurred elsewhere in the region.

Structural synthesis

A number of models have previously been presented to explain the structural and metamorphic history of the Bryah–Padbury region. For these models the driving force was assumed to be collisional tectonics related to the Capricorn Orogeny (e.g. Tyler et al., 1998; Occhipinti et al., 1998c; Pirajno et al., 1998b).

Gee (1990, p. 207; Gee and Grey, 1993) interpreted the movement of the ‘Yarlarweelor Gneiss Belt’ and ‘Marymia Dome’ in terms of rising ‘solid-state, crystal-plastic’ domes. They suggested that the resulting rise and southward movement of the ‘Yarlarweelor Gneiss Belt’ and ‘Marymia Dome’ produced recumbent folds in the overlying sedimentary rocks of the Bryah Basin. Further rise and convergence of the domes following deposition of the Padbury Group caused complex refolding. The ‘Yarlarweelor Gneiss Belt’ was thrust to the east over the Bryah and Padbury Groups at this time. Martin (1994) interpreted the emplacement of the ‘Narryer

Figure 20. Selected idealized cross sections through the Bryah and Padbury Groups (after Occhipinti et al., 1998a). Locations of a) to c) are shown on Figure 19 (note difference in scale):

- Northeast–southwest section in the central-eastern part of the Bryah and Padbury Basins showing the fault-bend fold model for the Peak Hill Anticline, and inferred suture between the Yilgarn Craton (Murchison Terrane) and reworked Archaean Marymia Inlier. The extensional fault slice along the northern margin of the craton formed during early development of the Bryah Basin (‘passive margin’) and was preserved in this idealized section after basin closure;
- East–west section across the zone of D_3 fold and fault structures. The section highlights the intense deformation across the zone between the Billara and Kinders Faults, and shows an inferred major detachment (within underlying mafic volcanic rocks of the Narracoota Formation) zone of highly disharmonic F_3 folding mapped at the surface;
- North–south section in the central-western part of the Bryah and Padbury Basins showing the Yarlarweelor Dome, the sheared-out Padbury Syncline, and the Murchison Fault as the suture between in situ and reworked Archaean Narryer Terrane. Note the inferred detachment of the Bryah–Padbury succession along the contact with the Narryer Terrane;
- The development and onlap of the Padbury Basin onto the underlying Bryah Group

Table 6. Mineral paragenesis of the Bryah Group and relationships between diagnostic metamorphic minerals of the Bryah Group and deformation fabrics

Formation	Rock type	Mineralogy	Pre- S_1 M_1	S_1	Post- S_1	S_2 - S_3 M_2	Post-tectonic
Peak Hill Schist	pelite	quartz				
		biotite				
		muscovite				
		chlorite				
		albite				
		tourmaline				
	chemical sediment	quartz				
		spessartine				
		magnetite				
	calc-silicate	quartz				
		epidote				
		chlorite				
		actinolite				
		titanite				
		magnetite				
	psammite	quartz				
		muscovite				
		andesine				
		opaques				
Narracoota	metabasite	quartz				
		actinolite				
		epidote				
		chlorite				
		sericite				
		arfvedsonite				
		titanite				
		calcite				
	volcanic breccia	albite				
		pumpellyite				
Ravelstone	pelitic tourmalinite	quartz				
		muscovite				
		tourmaline				
		garnet				
		feldspar				
	subarkosic wacke	quartz				
		biotite				
		albite				
		sericite				
		tourmaline				
Horseshoe	banded iron-formation	quartz				
		biotite				
		grunerite				
		spessartine				
		chlorite				
Robinson Range	banded iron-formation	quartz				
		stilpnomelane				
		biotite				

NOTE: No data are available for the Labouchere and Wilthorpe Formations

Gneiss Complex' ('Yarlarweelor Gneiss Belt') as due to 'lateral escape tectonics' resulting from the 'transcurrent suturing' of the Yilgarn and Pilbara Cratons during the Capricorn Orogeny. Martin (1994) suggested that early north-south movements, which changed to localized east-west movements, indicate the onset of 'lateral escape tectonics', and the eastward expulsion of the northeastern part of the 'Yarlarweelor Gneiss Belt' along the Wilthorpe and Kinders Faults. In contrast, Myers (1989, 1990) regarded both the 'Yarlarweelor Gneiss Belt' and the volcano-sedimentary rocks of the Bryah and Padbury Groups as allochthonous sheets that were thrust over the

Yilgarn Craton basement, and subsequently folded about east-west axes.

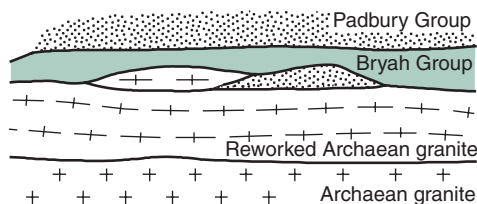
An alternative model was presented by Occhipinti et al. (1998c; Fig. 21), who suggested that the Bryah Basin developed initially as a rift and the Padbury Basin developed over the Bryah Basin in a retroarc foreland-basin setting (see also Martin, 1994). Formation of the Padbury Basin in a compressional regime was essentially concomitant with the closure of the Bryah Basin and the development of D_1 structures as subhorizontal shear zones between the Archaean Narryer Terrane basement and the

supracrustal rocks of the Bryah and Padbury Groups. The overall movement direction was interpreted as being from north to south, but, locally, because of the possible effect of later dextral shear movement, may actually have been

northwest to southeast. Substantial movement and high strains can be inferred from tectonic interleaving (e.g. between the Billara and Wilthorpe Faults; Fig. 19), and from the development of the mylonitic zones in possible thrust duplexes in the Peak Hill Schist. Other possible D_1 structures, in particular subhorizontal thrust faults, may have locally developed along the contacts between the Bryah and Padbury Groups. Small-scale, early, layer-parallel folds in chert and BIF layers, particularly from within the Padbury Group, suggest that subhorizontal D_1 structures locally formed within the volcano-sedimentary succession (Pirajno and Occhipinti, 1998; Swager and Myers, 1999). Deposition of the Padbury Group in a retroarc foreland basin (Martin, 1994) was probably contemporaneous with the early stages of D_1 .

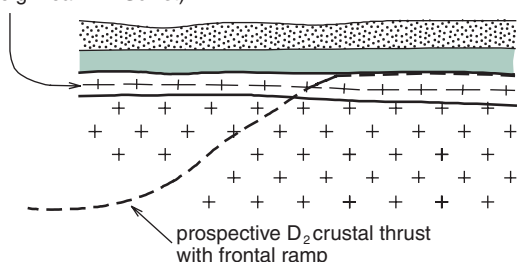
The Yarlalweelor gneiss complex and Peak Hill Schist were described by Occhipinti et al. (1998c) as 'basement-cored anticlines' that developed above frontal thrust ramps. The overlying supracrustal rocks and their high-strain D_1 contact zones were folded by north to south movement over these ramps during D_2 deformation. In the Peak Hill Schist, subhorizontal D_1 folds are refolded about an upright, apparently easterly trending, D_2 antiform. The hinge of this fold may be sheared out along the contact with the Marymia Inlier, which is marked by a quartz blastomylonite, previously mapped as deformed quartzite of the Juderina Formation (Adamides, 1998). The original orientation of the D_2 fold may have been east-northeasterly. The Peak Hill Schist outcrops around a domal structure produced by refolding of the D_2 fold about an approximately northerly trending D_3 fold-axial surface. It was argued by Occhipinti et al. (1998c) that the D_3 folds developed in a structural 'depression' between the two

a) D_1 tectonic interleaving between reworked Archaean crust (underplate) and Bryah–Padbury succession

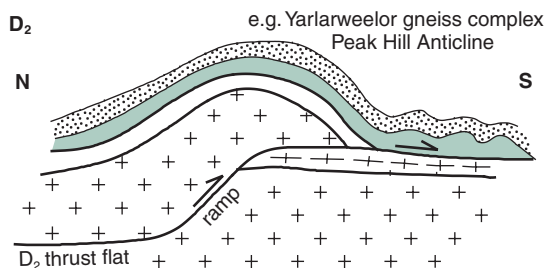


b) Post- D_1 and pre- D_2

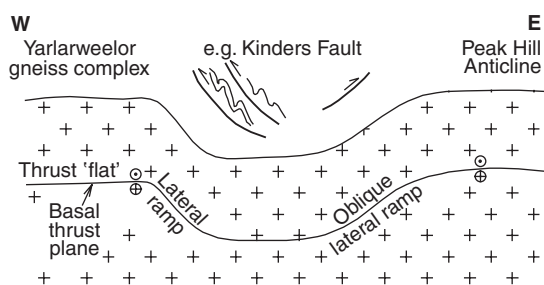
D_1 tectonic interleaving zone
(e.g. Peak Hill Schist)



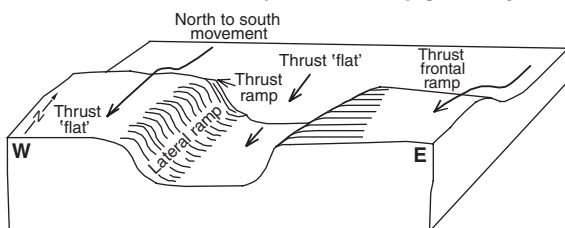
c) D_2



d) Post- D_2/D_3



e) D_2 thrust flat – frontal ramp – lateral ramp geometry



FMP374

01.11.99

Figure 21. Model of the structural development of the Bryah–Padbury Group succession (after Occhipinti et al., 1998a):

a) Zone of D_1 subhorizontal tectonic interleaving (by thrust duplexing) between reworked Archaean crust and overlying rocks of the Bryah–Padbury succession. This zone includes high-strain or mylonitic rocks formed by 'underplating' of the Archaean rocks beneath the volcano-sedimentary rocks during initial closure of the Bryah back-arc basin;

b) Post- D_1 geometry with trace of incipient D_2 crustal-scale thrust with frontal ramp;

c) D_2 geometry with fault-bend anticline developed above the crustal D_2 thrust ramp. Upright folds in the volcano-sedimentary succession (e.g. Padbury and Robinson Synclines) formed ahead of the main thrust;

d) Post- D_2/D_3 geometry along schematic east-west section; D_2 fault-bend anticlines are not shown. North-to-south movement, i.e. movement towards viewer, leads to east-west compression, and hence north-south folds and reverse or thrust faults in the depression between (oblique) lateral ramps at the same time as east-west D_2 folding occurred elsewhere;

e) Schematic view, looking north-northwest, of the basal thrust fault with frontal and lateral ramps, highlighting the north-to-south movement direction of the thrust sheet

basement-cored anticlines, which acted as lateral ramps in the thrust plane. Northerly trending structures developed during north–south compression as the lateral ramps were slightly oblique to the movement direction, leading to space problems between the basement-cored anticlines. This resulted in either lateral shortening or vertical expulsion (or both) of the Bryah and Padbury Groups.

Occhipinti et al. (1998c) assumed that the Yarlswheel gneiss complex (referred to by them as the Narryer Terrane) was an Archaean crustal fragment that influenced the structural deformation in the Palaeoproterozoic Bryah and Padbury Groups, but was not itself largely deformed during the Palaeoproterozoic. Subsequently, Sheppard and Swager (1999) and Occhipinti and Myers (1999) recognized Palaeoproterozoic deformation, metamorphism, and felsic magmatism within the Yarlswheel gneiss complex. This indicates that the Yarlswheel gneiss complex was extensively reworked during the Palaeoproterozoic, and underwent the same D_2 – M_2 metamorphic event that has been recognized in the Bryah and Padbury Groups and Peak Hill Schist.

Occhipinti et al. (1998b) found that Palaeoproterozoic coarse-grained granites and pegmatites, with ages between 1820 and 1780 Ma (Nelson, 1998), intruded as sheets synchronously with the D_2 deformation event. D. McB. Martin (1999, pers. comm.) interpreted granite exposed southwest of the Labouchere open-cut as intruding the Padbury Group sedimentary rocks, and suggested that this granite may also be of this age. Intrusion of granitoid dykes and sheet-like plutons accompanied uplift of the Yarlswheel gneiss complex, and is interpreted as being concomitant with dextral shearing in the region and possibly D_3 (Occhipinti et al., 1998a; Sheppard and Swager, 1999). This movement was attributed to an oblique north–south to northwest–southeast collision of the Pilbara and Yilgarn Cratons during the Capricorn Orogeny (Occhipinti et al., 1998b, 1999).

In the northwestern part of the Bryah and Padbury Basins the metamorphic grade increases from greenschist facies in the east to amphibolite facies in the west. Further west, in the Yarlswheel gneiss complex, the metamorphic grade reached at least upper amphibolite facies (Sheppard and Swager, 1999). Uplift of the Yarlswheel gneiss complex from 9–10 kbar to greenschist facies occurred between c. 1812 and c. 1800 Ma (Occhipinti et al., 1998b). The c. 1812 Ma granitoid sheets and dykes were metamorphosed at high grade (see below), whereas c. 1800 Ma granites were only metamorphosed to greenschist facies (Occhipinti et al., 1998b). Medium-grade metamorphism of the Padbury Group is solely preserved adjacent to the Yarlswheel gneiss complex, between the Billara and Wilthorpe Faults (see **Metamorphism**; Fig. 18; Plate 1). The drop in metamorphic grade to greenschist facies only 1.5–2.5 km east of the contact suggests either a rapid increase in temperature close to the Yarlswheel gneiss complex, or that amphibolite-facies or upper greenschist-facies (or both) Bryah and Padbury Group rocks have been faulted out. The latter explanation is preferred because the boundary between amphibolite-facies and lower to middle greenschist-facies rocks of the Labouchere Formation is sharp.

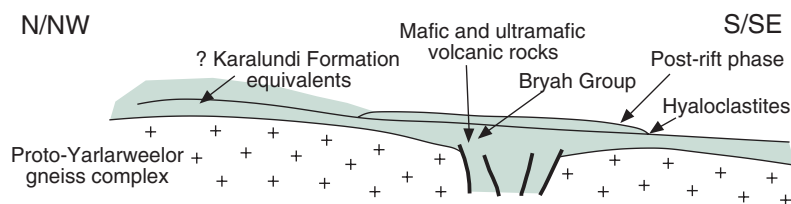
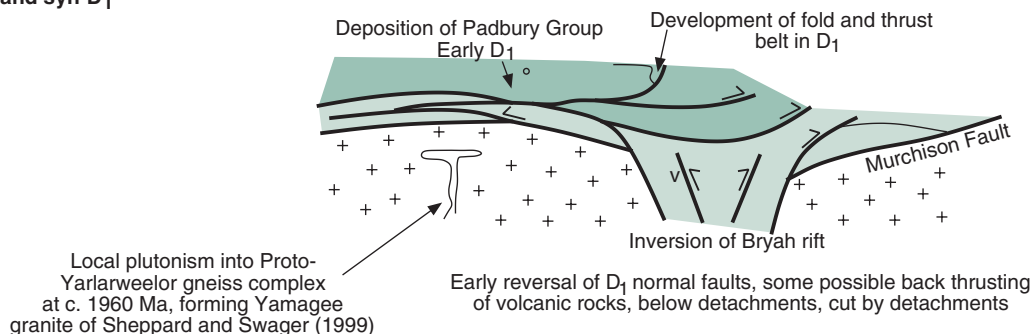
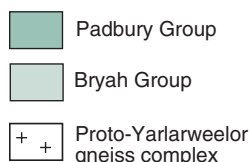
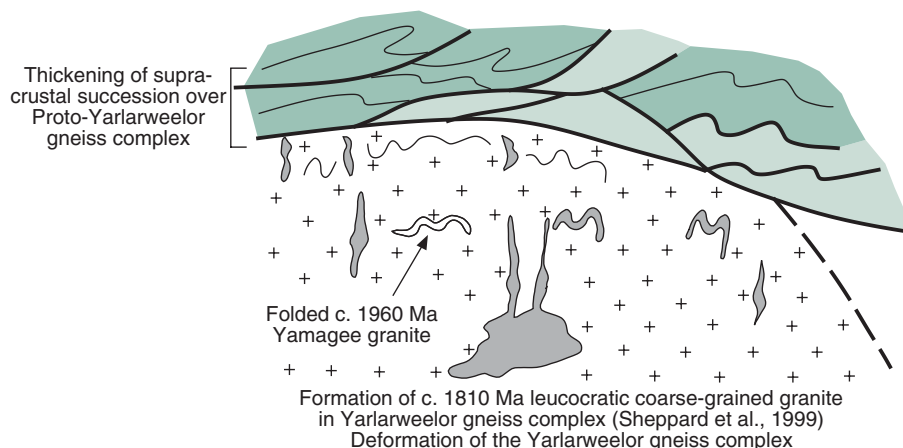
In the Bryah and Padbury Groups and Peak Hill Schist, metasomatism accompanied retrogression of D_1 – M_1 assemblages to greenschist facies during M_2 , particularly in D_2 shear zones. In the Yarlswheel gneiss complex, there is no evidence for D_1 – M_1 , and M_2 was initially a high-grade metamorphic event, with the formation of incipient minimum melt during the early stages of D_2 (Occhipinti et al., 1998b). Post- M_2 , the metamorphic grade dropped significantly to greenschist facies.

In the proposed model shown in Figure 22, the Bryah Group developed in a back-arc ‘rift-type setting’ (Pirajno et al., 1998b; see **Tectonic model and conclusions**). If the Bryah and Padbury Groups are c. 2.0 Ga or older, then D_1 structures could have developed during the c. 2.0 Ga Glenburgh Orogeny (Occhipinti et al., 1999; Tyler, 1999) as a result of west to east or northwest to southeast compression. Plutonism in the future Yarlswheel gneiss complex produced the 1960 Ma felsic granitoid rocks during the late stages of D_1 (Sheppard et al., 1999; Fig. 22c). Alternatively, if the Bryah and Padbury Groups were deposited sometime between c. 1945 and 1812 Ma, D_1 could have developed during the c. 1.8 Ga Capricorn Orogeny due to north–northwest to south–southeast compression (Figs 22 and 23). Further geochronological work is required to establish the age of D_1 and the depositional age of the Bryah and Padbury Groups.

In either case, closure of the Bryah Basin took place during D_1 , with deposition of the Padbury Group in a retroarc foreland basin overlying the Bryah Group and possibly the ‘future’ Yarlswheel gneiss complex (Fig. 22b). D_1 décollements would have developed between the Bryah and Padbury Groups, the future Yarlswheel gneiss complex, and the Peak Hill Schist (Figs 22b and 23a). Duplexes developed in the Peak Hill Schist during D_1 , and it was detached from the Marymia Inlier (Fig. 23b). In addition, early D_1 faults and folds formed between and within the Bryah and Padbury Groups.

The second deformation event, D_2 , occurred during the Capricorn Orogeny. Early in D_2 , approximately northwest to southeast compression caused further thickening of the Bryah and Padbury Groups over the Yarlswheel gneiss complex, destabilizing this piece of crust (Figs 22b and 22c). The resulting increased pressure and temperature may have caused the underlying Archaean crust to start to melt. This melt produced the c. 1820 to c. 1812 Ma felsic granitoid rocks (Occhipinti et al., 1998a; Sheppard and Swager, 1999; Sheppard et al., 1999) that intruded the upper parts of the Yarlswheel gneiss complex as veins and sheets (Sheppard and Swager, 1999; Fig. 22c). As these developed synchronously with the deformation (D_2), they were commonly folded into upright, steeply to shallowly plunging, isoclinal to open folds. These rocks were also metamorphosed at high grade during the D_2 deformation event. Regionally, this metamorphism corresponds to M_2 .

Padbury Group sedimentary rocks were metamorphosed to medium grade along contact zones with the Yarlswheel gneiss complex during M_2 . This high- and medium-grade metamorphism may have released fluid that moved through faults and shear zones and

a) Pre-D₁, extension–rift phase**b) Early- and syn-D₁****c) D₂–D₃**

SAO62

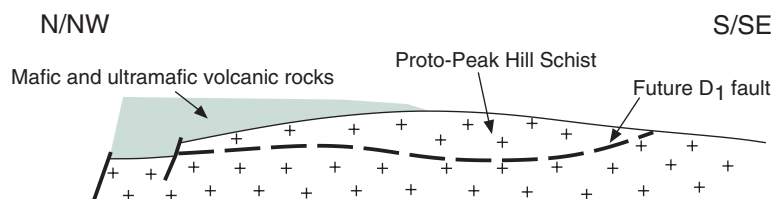
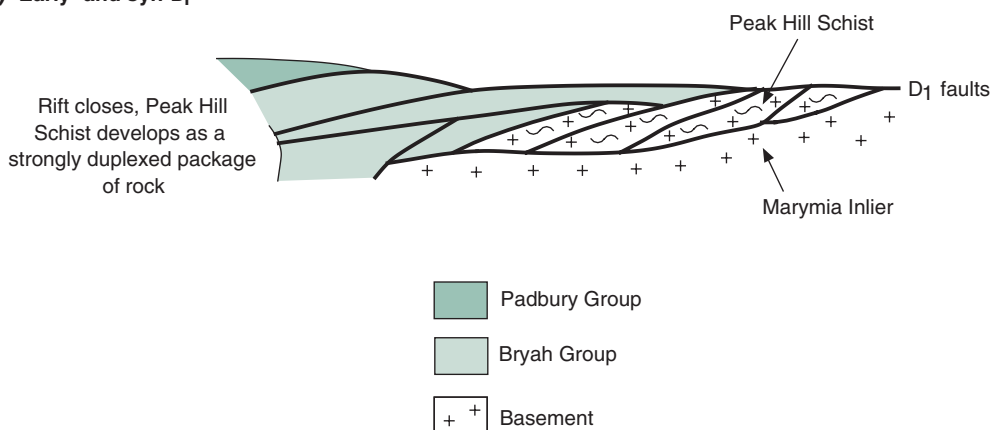
13.03.00

Figure 22. Schematic sections illustrating the proposed model of the structural development of the Bryah–Padbury Group succession in the west:

a) Development of the Bryah Group, pre-D₁, over the Proto-Yarlarweelor gneiss complex and the northern margin of the Yilgarn Craton in an extensional-rift setting;

b) Early- and syn-D₁ deposition of the Padbury Group in a fold-and-thrust belt, foreland-basin type setting over the Bryah Group. Inversion of the Bryah rift-basin, by possible reversal of D₁ normal faults. Development of D₁ faults between the Bryah Group, Padbury Group, Yarlarweelor gneiss complex, and Yilgarn Craton;

c) D₂ to D₃; local interleaving of the Bryah and Padbury Groups with the development of folds and faults. Deformation of the Bryah and Padbury Groups above basal detachments. Early D₁ faults refolded about D₂ or D₃ folds. Formation of c. 1810 Ma leucocratic granite locally associated with incipient minimum melt in the Archaean gneiss component of the Yarlarweelor gneiss complex. Later, at c. 1800 Ma, sheet-like plutons developed, particularly along the faulted boundaries between the Yarlarweelor gneiss complex and Bryah and Padbury Groups

a) Pre-D₁, extension–rift phase**b) Early- and syn-D₁**

SAO63

15.03.00

Figure 23. Schematic section illustrating the proposed model for the structural development of the Bryah–Padbury Group succession and the Peak Hill Schist: a) Development of the Bryah Group in a rift setting, pre-D₁, over the Marymia Inlier (Yilgarn Craton); b) D₁ closure of the Bryah ‘rift’, inversion of normal faults; deposition of the Padbury Group, and formation of the Peak Hill Schist

metasomatized M₁ assemblages in the Bryah Group and Peak Hill Schist rocks during M₂–D₂. Elsewhere in the region, during D₂, the Peak Hill Schist and Bryah and Padbury Group rocks were folded into tight to isoclinal upright folds with mainly easterly to northeasterly trends (Occhipinti et al., 1998c). Post-D₂, during D₃, the Yarlarweelor gneiss complex was uplifted and retrogressed to greenschist facies. This uplift, in a dextral strike-slip regime, may have been accommodated by steeply dipping normal faults between the Yarlarweelor gneiss complex and the Bryah and Padbury Groups (Figs 17 and 18) that have now been inverted (Fig. 24).

In the Peak Hill Schist, subhorizontal D₁ mylonite zones and rootless folds are refolded about an easterly or east-northeasterly trending upright D₂ antiform. The domal shape of the Peak Hill Schist is an artefact of a northerly trending, upright D₃ antiform refolding the D₂ antiform. The Yarlarweelor gneiss complex apparently does not contain D₁ folds, although shearing along basement–cover contacts between the Yarlarweelor gneiss complex and the Bryah and Padbury Groups may have developed during D₁ (Fig. 22b). The D₂ fold-axial surfaces within the

Yarlarweelor gneiss complex parallel the arcuate faulted boundary with the Bryah and Padbury Group rocks. This change in the trend of D₂ may be explained in terms of a fault-bend fold developed during dextral shearing (Occhipinti and Myers, 1999) that may have accompanied uplift during D₃.

Mineralization

The mineral resources of the Peak Hill Schist, Bryah Group, and Padbury Group are considerable, considering the relatively small total area of these basins (about 6000 km²). These resources include gold, manganese, iron ore, talc, and silver. Pirajno and Occhipinti (1995) discussed the mineral potential of the Bryah Basin, and Pirajno and Preston (1998) described the mineral deposits of the Bryah–Padbury region and Peak Hill Schist. Mineral production and defined resources within these tectonic units as at 30 June 1999 are presented in Tables 7 and 8. Known deposits and occurrences are listed in Table 9.

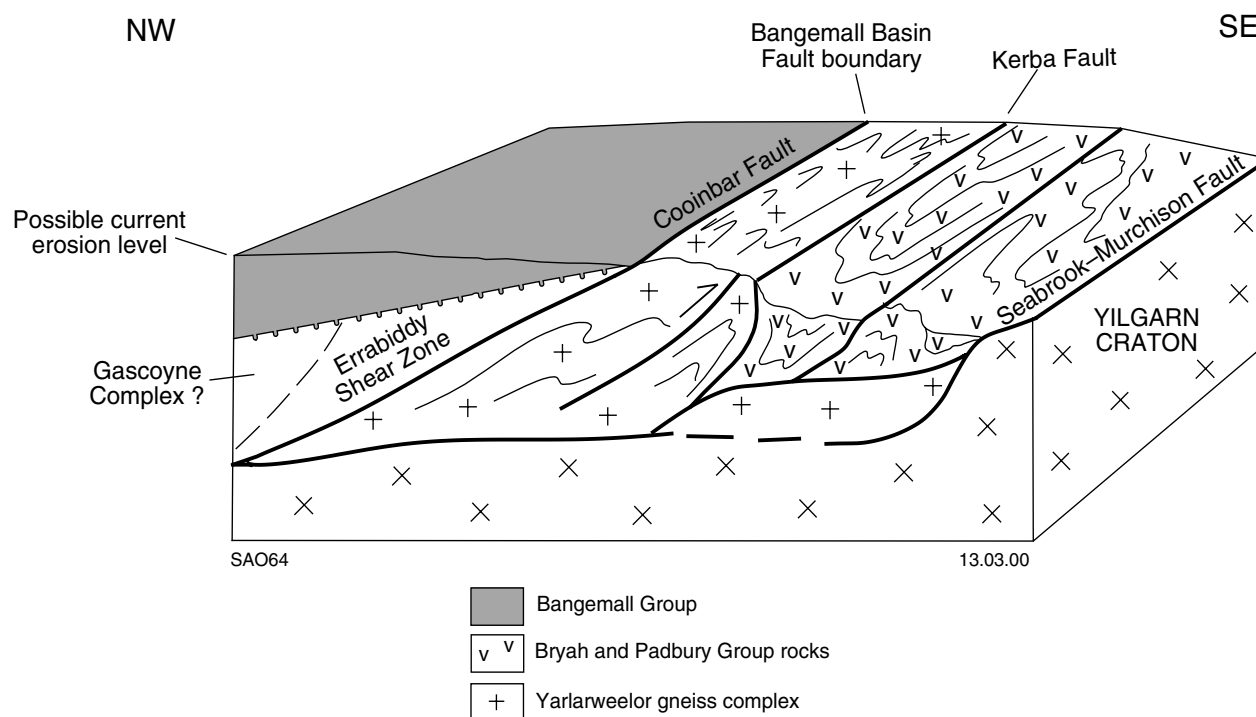


Figure 24. Schematic north-northwest to south-southeast cross section from the Bangemall Basin, into the Yarlarweelor gneiss complex, and then into the Bryah and Padbury Basins, showing the possible present-day configuration of these units.

The mineral deposits of the Peak Hill Schist, and Bryah and Padbury Groups include mesothermal-style gold-only lodes, volcanogenic massive sulfide (VMS) copper-gold, supergene-enriched manganese, banded iron-formation iron ore, and talc in metasomatized dolomitic rocks. The distribution of these mineral deposits is shown in Figures 25 and 26, and Plate 1.

Gold deposits

The most important mineral deposits exploited to date have been the mesothermal-style gold-only lodes, all of which are in the Peak Hill Schist, and the Bryah and Padbury Groups. If the area occupied by these groups alone is taken into account (about 6000 km²), then the identified contained gold per unit area is 12.5 kg gold/km². The mesothermal gold deposits, including past and present producers, include Peak Hill, Jubilee, and Mount Pleasant in the Peak Hill Schist; Harmony, Mikhaburra, Wembley, Cashman, and Ruby Well in the Bryah Group (Figs 25 and 26); and Horseshoe, Labouchere, Nathans Deep South, and Fortnum in the Padbury Group. The Wilthorpe deposit is hosted in Upper Archaean granitic rocks, which are tectonically interleaved with rocks of the Bryah and Padbury Groups.

The total gold produced is 59.5 t, with total (produced plus remaining inferred, indicated and measured) resources estimated at approximately 75 t of contained gold. The Labouchere and Fortnum areas contain the region's largest pre-mining resource estimated as 33.3 t of contained gold at a grade of about 2.4 g/t gold. Approximately two-thirds (22.5 t) has been exploited,

largely between 1989 and 1995, with the remaining resource (10.7 t) being in the Fortnum area. Details of the Labouchere and Fortnum deposits can be found in Hanna and Ivey (1990) and Hill and Cranney (1990) respectively. The area around the Peak Hill opencut (including Ravelstone) has produced approximately 20 t of fine gold at an average grade of 4 g/t gold, more than half of which has been extracted in the last 13 years. Remaining measured and indicated resources are estimated at about 4.7 t of contained gold. The Harmony deposit (New Baxters Find), which was recently exhausted, had total pre-mining resources estimated at about 9.2 t, with a grade of 3.5 g/t gold.

The lode deposits are hosted in mylonitic schist, metasedimentary rocks, metavolcanic rocks, or along their contact zones. They are spatially associated with high-strain zones and hydrothermal alteration dominated by pyrite, quartz, muscovite, biotite, and alkali feldspars. The mineralization is in ductile and brittle-ductile shears (e.g. Peak Hill) and in discrete brittle fractures (e.g. Cashman), indicating a relationship of structural style with the rheology of the host rocks. The development of ductile, brittle-ductile, and brittle structures (zones of high permeability) was accompanied by infiltration of hydrothermal fluids, which produced alteration and mineralization. The precise timing of the mineralization is difficult to ascertain. Windh (1992) suggested syn-D₃, but from field and petrological observations it is more likely that circulation of mineralizing fluids occurred during a continuum related to D₁-D₂ tectonism and metamorphism, under conditions of ductile or brittle-ductile regimes, with perhaps some remobilization into brittle structures occurring during D₃. Lead isotope data

Table 7. Gold production and remaining resources in the Bryah and Padbury Groups

Mining centre or mine	Production (P)					Remaining resources (R)			Total pre-mining resources (P+R) (kg)
	Ore	Contained metal	Alluvial	Dollied	Total contained metal	Resource type	Ore	Contained metal	
	(kt)	(kg)	(kg)	(kg)	(kg)		(kt)	(kg)	
Pre-1986									
Mount Fraser Mining Centre	0.9	24	2.7	1.3	28.8	—	—	—	28.8
Mount Seabrook Mining Centre	1.7	38.3	—	0.2	38.5	—	—	—	38.5
Ravelstone Mining Centre	4.9	105.8	—	3.2	109	—	—	—	109
Wilthorpe Mining Centre	0.1	1.5	—	—	1.5	—	—	—	1.5
Peak Hill sundry parcels	2.7	770.6	88.9	13.9	873.4	—	—	—	873.4
Peak Hill Mint deposits ^(a)	—	—	2.5	3.3	5.8	—	—	—	5.8
Ruby Well Mining Centre	8.5	146	32.5	14.2	192.7	—	—	—	192.7
Horseshoe Mining Centre	904.9	2 966.9	35.2	88.9	3 091	—	—	—	3 091
Peak Hill Mining Centre	621.7	8 200	36.7	62.8	8 299.5	—	—	—	8 299.5
1986 to 30 June 1999									
Horseshoe Lights ^(b) mine	905.9	3 737.3	21.7	—	3 759	—	—	—	3 759
Fortnum mine	5 832	15 602.5	37.7	—	15 640.2	MES + IND	2 221	7 542	23 182.2
						INF	991	3 194	3 194
Labouchere mine	2 910.8	6 905.2	—	—	6 905.2	—	—	—	6 905.2
Mount Pleasant mine	144.9	433	—	—	433	—	—	—	433
Peak Hill mine	6 573.8	20 126.6	90.8 ^(c)	—	20 217.4	MES + IND	2 200	4 760	24 977.4
Total	17 912.8	59 057.7	348.7	187.8	59 595		5 412	15 496	75 091

NOTES: (a) Gold from the Peak Hill Mining Centre deposited at the Perth Mint;
 (b) Horseshoe Lights also produced 261 675 t of copper concentrates containing 2580.3 kg of gold;
 (c) Includes 62.5 kg of gold produced from retreated tailings;
 MES: Measured resources; IND: Indicated resources; INF: Inferred resources

SOURCE: Data are from the Western Australia Department of Minerals and Energy's mines and mineral deposits information (MINEDEX) database

Table 8. Mineral production and remaining resources in the Bryah and Padbury Groups

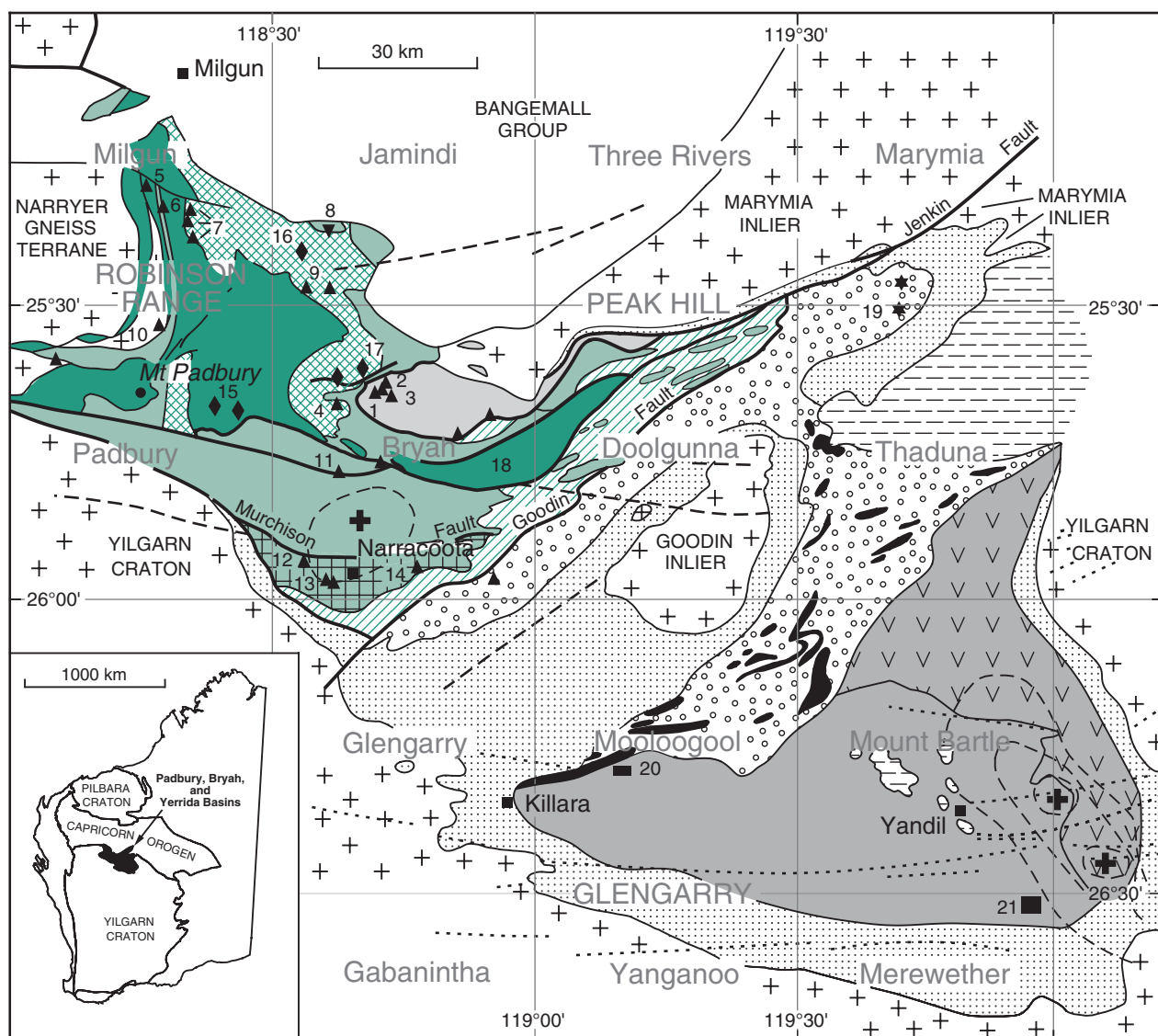
Commodity	Mine	Production (P) to 30.06.99		Resource type	Remaining resources (R)		Total resource (P+R) Contained metal (t)
		Ore or concentrate (t)	Contained metal (t)		Ore or concentrate (t)	Contained metal (t)	
Copper and cupreous ore	Cashman	7	1.1	–	–	–	1.1
	Peak Hill sundry	63	22.3				22.3
	Horseshoe Lights	261 675	49 159	Indicated	2 080 000	22 897	72 056
				Inferred	3 340 000	22 879	22 879
	Total	261 745	49 182.4		5 420 000	45776	94 958.4
Manganese	Horseshoe	489 895	203 899	Measured + Indicated	80 000	21 000	224 899
				Inferred	205 000	100 000	100 000
	Mount Fraser	228	108	Measured + Indicated	32 000	9 000	9 108
	Mount Padbury	7 319	3 498	Measured + Indicated	5 000	2 000	5 498
	Ravelstone (Peak Hill)	76 237	36 938	–	–	–	36 938
	Total	573 679	244 443	Measured + Indicated	117 000	32 000	276 443
				Inferred	205 000	100 000	100 000
Iron	Robinson Range	–	–	Inferred	10 000 000	6 000 000	6 000 000
Talc	Mount Seabrook – Livingstone	–	540 416	Indicated	–	1 470 000	2 010 416
				Inferred	–	250 000	250 000
	Total	–	540 416		–	1 720 000	2 260 416
Silver (by-product)	Horseshoe Lights (post-1982)	–	72 719.4 kg	–	–	–	72 719.4 kg
	Peak Hill general	–	118.2 kg	–	–	–	118.2 kg
	(including Horseshoe pre-1983)						
	Total	–	72 837.6 kg	–	–	–	72 837.6 kg

SOURCE: Data are from the Western Australia Department of Minerals and Energy's mines and mineral deposits information (MINEDEX) database

Table 9. Mineral deposits and occurrences in the Bryah and Padbury Basins

<i>Mine (M), prospect (P), or occurrence (O)</i>	<i>AMG coordinates Easting</i>	<i>AMG coordinates Northing</i>	<i>Principal commodity</i>	<i>Mineralization style</i>	<i>Expression</i>	<i>Ore minerals</i>	<i>Relationship to host</i>
Cashman (M)	662129	7126994	Gold	Regolith enrichment and mesothermal lode	Outcrop	Gold	Discordant
Durack (P)	670440	7150520	Gold	Mesothermal lode	Drill intersections	Gold, pyrite, magnetite	Discordant
Harmony (M)	664145	7161267	Gold	Regolith enrichment and primary mesothermal lode	Drill intersections	Gold, chalcopyrite, pyrrhotite, scheelite, pentlandite, pyrite	Discordant
Heines Find (P)	682759	7145164	Gold	Mesothermal lode	Outcrop	Gold	Discordant
Horseshoe (P)	656994	7183734	Gold	Eluvial		Gold	–
Horseshoe (P)	657579	7184413	Gold	Eluvial		Gold	–
Horseshoe (P)	661219	7182977	Gold	Eluvial		Gold	–
Horseshoe (P)			Copper–gold	Multiple veins	Outcrop	Gold	Discordant
Horseshoe Lights (M)	662648	7193894	Copper–gold of VHMS	Supergene enrichment	Gossan	Chalcocite, pyrite, chalcopyrite, native copper and gold	Discordant,
Jubilee (M)	671889	7165443	Gold	Mesothermal lode	Quartz vein	Gold, pyrite	Discordant
Labouchere (M)	627730	7204710	Gold	Mesothermal lode	Not known	Gold, pyrite	Discordant
Livingstone (M)	567540	7171032	Talc	Replacement	Outcrop	Talc	Discordant
Mikhaburra (P)	656252	7130396	Gold	Multiple veins	Outcrop	Gold	Discordant
Mount Pleasant (M)	674287	7162089	Gold	Mesothermal lode	Outcrop	Gold, pyrite	Discordant
Mount Seabrook (M)	572631	7168338	Talc	Replacement	Outcrop	Talc	Discordant
Nathans Deep South (M)	631713	7198812	Gold	Mesothermal lode	Not known	Gold, pyrite	Discordant
Peak Hill (M)	672190	7163003	Gold	Mesothermal lode	Quartz vein	Gold, pyrite, altaite, chalcopyrite, bismuthotelluride, molybdenite, magnetite	Discordant
Ravelstone (M)	665734	7166777	Manganese	Supergene enrichment	Outcrop	Mn oxides	Stratabound
Ravelstone (M)	669313	7166423	Manganese	Supergene enrichment	Outcrop	Mn oxides	Stratabound
Ruby Well area (M)	674665	7129915	Gold	Eluvial	–	Gold	–
Ruby Well area (P)	672600	7124378	Gold	Eluvial	–	Gold	–
Ruby Well area (P)	674142	7127027	Gold	Eluvial	–	Gold	–
Ruby Well area (P)	677928	7129727	Gold	Eluvial	–	Gold	–
Ruby Well area (P)	677408	7130112	Gold	Eluvial	–	Gold	–
St Crispin (P)	691358	7158940	Gold	Mesothermal lode	Outcrop	Gold	Discordant
Treves, Starlight (M)	636412	7198887	Gold	Mesothermal lode	Not known	Gold, pyrite	Discordant
Unnamed (O)	611598	7168985	?Variscite	Not known	Not known	?Variscite	Discordant
Unnamed (O)	611909	7167084	?Variscite	Not known	Not known	?Variscite	Discordant
Unnamed (P)	656664	7185310	Manganese	Supergene enrichment	Outcrop	Mn oxides	Stratabound
Wembley (P)	663983	7149044	Gold	Mesothermal lode	Outcrop	Gold	Discordant
Wilgeena (M)	685369	7155622	Gold	Mesothermal lode	Outcrop	Gold	Discordant
Wilthorpe (M)	630414	7176521	Gold	Mesothermal lode	Outcrop	Gold, pyrite, galena arsenopyrite	Discordant
Yarlarweelor (M)	636723	7196423	Gold	Mesothermal lode	Not known	Gold, pyrite	Discordant

Figure 25. Distribution of mineral deposits and occurrences in the Bryah–Padbury and Yerrida Basins (modified from Pirajno and Preston, 1998; see also Plate 1)



FMP100b

18.10.99

- BANGEMALL GROUP**
- Bangemall Group
 - Earacheedy Group
 - Padbury Group
- BRYAH GROUP**
- Horseshoe and Ravelstone Formations
 - Narracoota Formation: mafic and ultramafic schist/metabasaltic hyaloclastite
 - Karalundi Formation

- YERRIDA GROUP**
- Mooloogool Subgroup
 - Windplain Subgroup
- MINERALIZATION STYLE**
- ▲ Mesothermal Au, Au-Cu
 - ★ Shear zone-hosted Cu
 - Epigenetic Pb
 - ▼ Volcanogenic massive sulfide
 - ◆ Supergene Mn
 - Shale-hosted stratabound sulfides

- Peak Hill Schist
- Archaean basement

- Fault
- Aeromagnetic lineament
- Geological boundary
- Microgabbro dyke
- Bouguer gravity anomaly
- Homestead

Bryah 1:100 000 map sheet
PEAK HILL 1:250 000 map sheet

MINERAL DEPOSITS

- 2. Jubilee
- 3. Mount Pleasant
- 4. Harmony (New Baxters Find)
- 5. Labouchere
- 6. Nathans Deep South
- 7. Fortnum group
- 8. Horseshoe Lights
- 9. Horseshoe gold
- 10. Wilthorpe
- 11. Wembley
- 12. Mikhaburra
- 13. Cashman
- 14. Ruby Well
- 15. Mount Padbury – Mount Fraser group (including Elsa)
- 16. Horseshoe magnagense
- 17. Ravelstone
- 18. Robinson Range BIF (no specific locality)
- 19. Thaduna
- 20. PGE-bearing gossan
- 21. Magellan

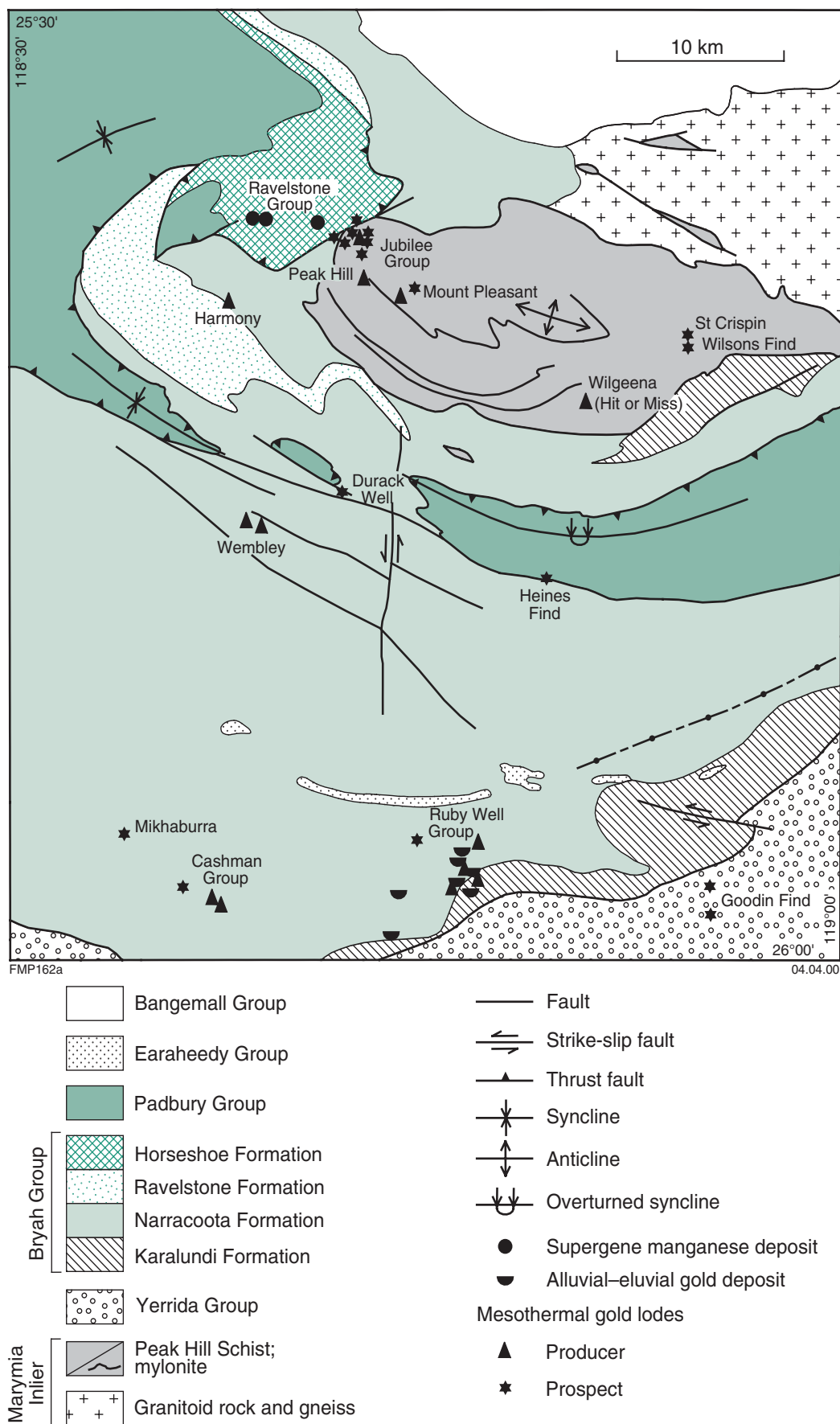


Figure 26. Distribution of mineral deposits and occurrences in the Bryah Group, within the BRYAH 1:100 000 map sheet (after Pirajno and Occhipinti, 1998)

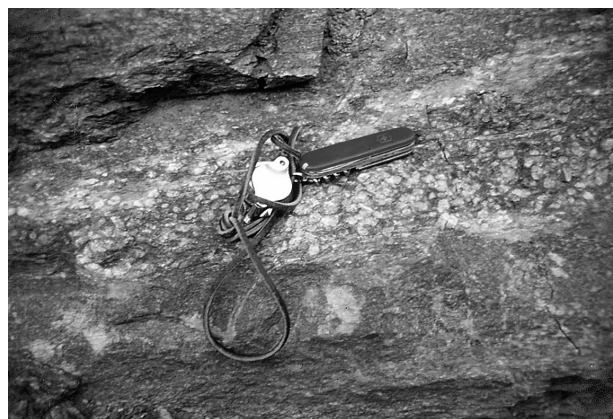
(palaeo-isochrons) suggest that in the Bryah and Padbury Basins, mineralization occurred between 1.92 and 1.7 Ga (Windh, 1992; Thornett, 1995). The results of lead isotopic studies also indicate that the lead was derived from Yilgarn Craton rocks (Dyer, 1991; Windh, 1992; Thornett, 1995), although there is a suggestion that the lead from the Peak Hill deposit is similar to that from a galena in the Marymia gold deposit in the Marymia Inlier (McMillan, 1993).

The nature of the mineralizing fluids is poorly constrained. Alteration assemblages at the Peak Hill and Mount Pleasant deposits indicate that the ore fluids were enriched in Fe, K, Na, S, B, CO₂, SiO₂, and H₂O (Thornett, 1995). Fluid inclusion studies of mineralized materials from the Fortnum and Labouchere gold deposits (Dyer, 1991; Windh, 1992) indicate that the ore fluids were rich in H₂O and H₂O–CO₂, with salinities of 7–12 wt% and 5–17 wt% NaCl equivalent respectively. Microthermometric measurements (Dyer, 1991; Windh, 1992) indicate temperatures ranging from approximately 170° to 320°C.

Peak Hill, Jubilee, and Mount Pleasant deposits

Mine geologists subdivided the Peak Hill, Jubilee, and Mount Pleasant lithologies into the Core sequence, Honey Quartzite, Intermediate sequence, Mine sequence, Marker Quartzite, and Hangingwall sequence.

The Core sequence is at the structural base and well exposed in the Mount Pleasant opencut, where it reaches a thickness of 55 m. The contact with the Intermediate sequence is marked by the Honey Quartzite, which is a mylonite consisting of laminated or ribbon quartz. The Core sequence rocks have a mylonitic fabric and are made up of quartz–biotite–carbonate–muscovite(–epidote–hornblende–garnet–magnetite–pyrite), locally with abundant very fine zircons and monazite in the biotite-rich varieties (Barrett, 1989). At Mount Pleasant, as mentioned above, graphitic schist is present near the top and associated with a zone of chlorite–biotite(–garnet) schist with albite porphyroblasts (Fig. 27), containing inclusions of monazite and zircon. Geochemical discriminant plots using immobile elements suggest either a granitic (Nb, Sr, La, and Ce) or mafic–intermediate (Ni, Cr, and Ti) protolith (Thornett, 1995). Barrett (1989), on the other hand, proposed that much of the Core sequence could be derived from a sedimentary protolith. The origin of the albite porphyroblasts is uncertain. Based on geochemistry, petrology, and textural features, Thornett (1995) advocated a combined hydrothermal – retrograde metamorphic origin, and compared the Peak Hill – Mount Pleasant albites to those studied by Watkins (1983) in the Dalradian schists of Scotland. Another possibility that could account for the presence of the albite porphyroblasts is ‘reaction softening’ as proposed by Dixon and Williams (1983). These authors advanced the hypothesis, supported by geochemical and mineralogical data, that mylonitization of a quartzofeldspathic parent may be accompanied by mineralogical changes involving the breakdown of plagioclase, with release of Na₂O and, to a lesser extent,



FMP 178

20.10.99

Figure 27. Albite porphyroblasts in mylonitic schist at the Mount Pleasant deposit

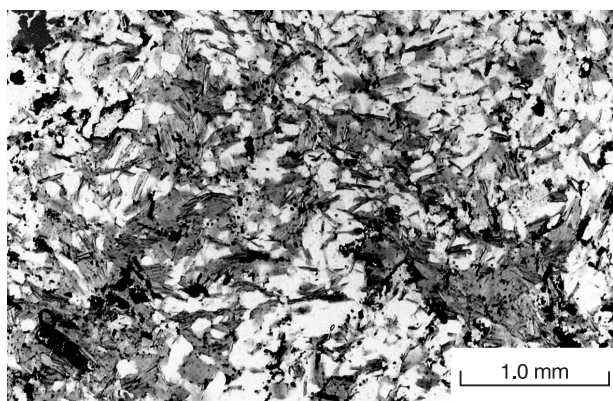
CaO, and formation of muscovite. This would result in the production of quartz–muscovite mylonites and sodium-rich fluids.

The Intermediate sequence is discontinuous, with layers up to 2 m thick, and is composed of a quartz–mylonite-bearing white mica. The Intermediate sequence lies above the Honey Quartzite, has an estimated thickness of between 200 and 400 m, and forms the footwall to the Mine sequence at Peak Hill and the hangingwall to the ore zones at Mount Pleasant. The Intermediate sequence is dominantly quartz–muscovite schist, with minor plagioclase, biotite, microcline, carbonate, and chlorite. Barrett (1989) interpreted this rock as either a felsic porphyry or an arkose. The lower part of the Intermediate sequence consists of mainly biotite schist with garnet and epidote. Rocks of the Intermediate sequence exhibit millimetre-scale metamorphic differentiation layering, which define a dominant S₂ schistosity (Thornett, 1995). This is interpreted by the present authors as a typical mylonitic structure.

The Mine sequence, mostly found in drillholes, is characterized by biotite – white mica(–chlorite–carbonate–amphibole–garnet–albite) schist and graphite schist (Fig. 28), and may be 40 to 50 m thick. Drillcore samples of a hornblende–plagioclase–quartz rock (with garnet porphyroblasts) have been interpreted as an unaltered amphibolite (Barrett, 1989; Thornett, 1995).

The Marker Quartzite is a recrystallized quartz mylonite (‘Marker Chert’ of mine geologists), 1 to 3 m thick, at the top of the Mine sequence. Outcrops of Marker Quartzite exhibit radiating iron-oxide pseudomorphs after acicular crystals and iron-oxide pseudomorphs after porphyroblasts. Windh (1992) identified these acicular crystals using the scanning electron microscope as grunerite. The porphyroblast pseudomorphs are possibly after garnet.

The Hangingwall sequence can be up to 700 m thick and is made up of white mica – magnetite(–garnet–chlorite), mafic schist, and metabasite. The latter is locally



FMP 179

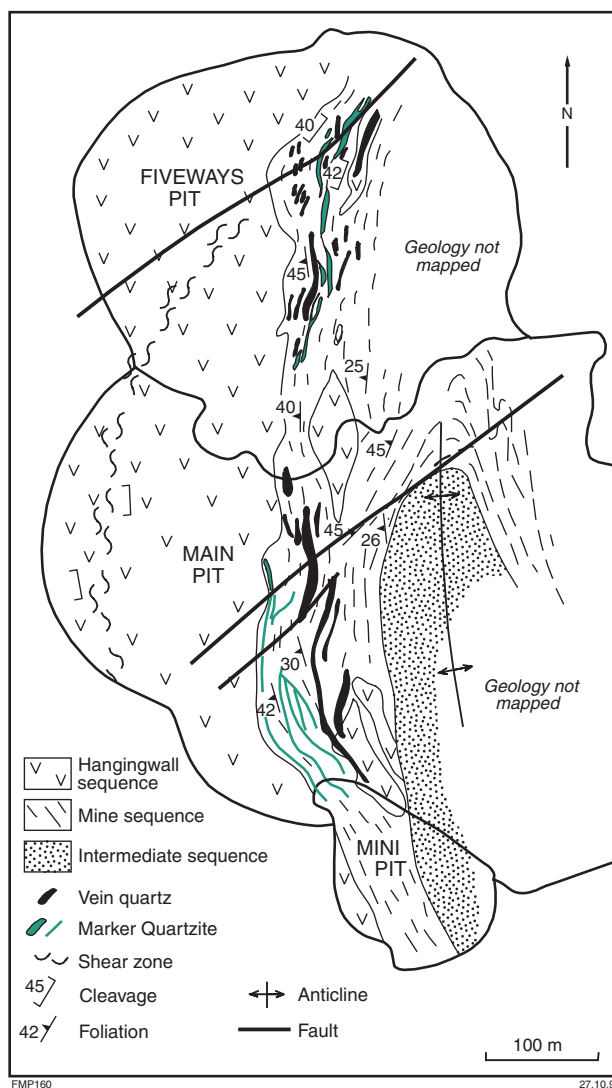
20.10.99

Figure 28. The Mine Sequence schist at the Peak Hill deposit, showing biotite alteration; the biotite is partly retrogressed to chlorite; plane polarized light

garnetiferous, and characterized by a metamorphic (and ?hydrothermal) assemblage containing variable amounts of hornblende, plagioclase, quartz, garnet, epidote, and titanite. The metabasite is overlain by mylonitic schist containing mainly quartz–plagioclase–biotite, and locally associated with zones of albite–muscovite and garnet–epidote (calc-silicate).

The Peak Hill, Jubilee, and Mount Pleasant deposits were studied by Barrett (1989), who based most of his work on drillcore samples, and Thornett (1995). These authors provided much of the information summarized below, augmented by data from this study. The Peak Hill, Jubilee, and Mount Pleasant gold deposits are situated in the west-northwestern portion of the Peak Hill Anticline and hosted in the Peak Hill Schist (Figs 4–7 and 26). In the mine areas the rocks are intensely weathered to depths locally exceeding 200 m. Weathering products are predominantly kaolinitic clays and iron oxyhydroxides. This weathering is particularly well developed in zones of hydrothermal alteration, which in turn are related to high-strain zones, the latter having facilitated percolation of meteoric waters. Hydrothermal alteration is dominated by sulfidation (pyrite) and alkali metasomatism (biotite and albite), and contained within late-stage quartz–carbonate veins hosted in highly strained metabasites and quartz mylonites. Other important alteration minerals include iron-rich chlorite, sericite, garnet, tourmaline, dolomite, and calcite. In all, about 20 t of gold has been produced.

The Peak Hill mineralization was exploited in three adjoining pits, which from north to south are: Fiveways, Peak Hill Main, and Mini. In plan view (Fig. 29) the entire Peak Hill mineralized system is contained within a package of mylonitic schist (Mine sequence) at the footwall of northerly trending and westerly dipping shear zones. The mylonitic schist contains quartz pods, veins, lenses, and stringers, and locally graphitic quartz mylonite units (Marker Quartzite, see below and Fig. 30). The Mine sequence contains lenses of mafic rocks (e.g., metadolerite). The overall picture is one of a complex zone of shearing and tectonic interleaving between rocks of the



FMP160

27.10.99

Figure 29. Schematic geological map of the Fiveways, Main, and Mini opencuts, Peak Hill deposit, (after Thornett, 1995)



FMP 417

19.11.97

Figure 30. Peak Hill Mini opencut, showing the ore-bearing mylonitic schist, graphitic schist (dark bands), and Marker quartzite unit (above the upper graphitic schist)

Narracoota Formation and Peak Hill Schist. Kinematic indicators (C–S surfaces) indicate a thrust movement from west to east (Thornett, 1995).

The main orebody has a westerly dip ranging from 20° to 50° (averaging 35°), and is hosted in rocks of the Mine sequence. High-grade zones can contain up to 30–40 g/t gold. The ore zones are characterized by pervasive alteration consisting of chlorite–biotite–quartz–carbonate–graphite. The principal ore minerals are pyrite, chalcopyrite, and gold. Other ore minerals include altaite, tetrahedrite, bismuthotelluride, molybdenite, and various bismuth–lead–tellurium compounds. The gold mineralization is thought to have been emplaced in at least two stages. In the first stage, gold mineralization was emplaced along the contact between the Marker Quartzite and the Mine sequence (see below). During the second stage, cross-faults were formed, with the gold being redistributed or rearranged along these cross-faults.

The Jubilee deposit was at first mined underground in 1892 from a number of workings, but the production is unknown. In 1992 a small pit was excavated, based on probable reserves of approximately 50 000 t at 4 g/t gold. In this pit, gold mineralization is hosted in rocks of the Hangingwall sequence and is in a complex quartz stockwork system emplaced along the margins of a 250 m-thick undeformed metabasite. The gold is on both the hangingwall and footwall sides of the metabasite body. Tourmaline is present in the ore-bearing material. Near the Jubilee pit, a northerly striking, westerly dipping quartz vein almost perpendicular to the dominant foliation trend extends for about 200 m. This vein was mined in the past and contained maximum grades of approximately 30 g/t gold.

Mining at Mount Pleasant began at the turn of the century, with the production of 8000 t of ore with an average grade of 9 g/t gold. Mining resumed in the 1980s when about 145 000 t of ore was extracted, with an average grade of 3 g/t gold, and 0.4 t of gold was produced. The ore zones are nearly flat lying, and were emplaced in subparallel fashion, one above the other. The deeper northern zone is hosted by the Core sequence. Gold is in quartz–carbonate veins, associated with zones of albite (Fig. 27), iron-rich chlorite, sericite, carbonate, and pyrite alteration, as well as zones of nearly flat lying graphitic schist (dip is 10° to the south). The veins are either vertical or of saddle-reef type lodged in anticlinal folds.

Harmony deposit

The Harmony (also known as New Baxters Find or Contact) gold deposit is located approximately 10 km west of Peak Hill in a featureless area of no outcrops, and covered by colluvium, lateritic duricrust, and hardpan material. Details of the geology of the Harmony deposit can be found in Harper et al. (1998), from whom the brief review that follows is taken.

The Harmony gold deposit consists of a subhorizontal supergene zone hosted in ferruginous lateritic materials

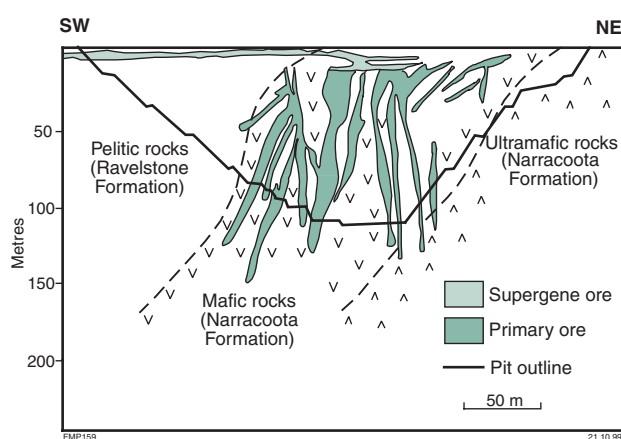


Figure 31. Diagrammatic cross section of the Harmony ore zones (modified from Harper et al., 1998)

(transported and residual regolith), a northeasterly trending, subvertical, primary vein system, and carbonate-bearing breccias. Most of the ore is contained within the vein system, which is hosted in rocks of the Narracoota Formation, and at the contact between the Narracoota and Ravelstone Formation (Fig. 31), with lesser low-grade mineralization in laterite. The Harmony mineralization is hosted in a northwesterly plunging antiform (Enigma structural zone) of a southwesterly dipping succession of altered mafic rocks at the top of the Narracoota Formation, and within a shear zone along the contact with overlying metasedimentary rocks of the Ravelstone Formation. The mineralized array of quartz veins become locally closely spaced, forming a stockwork that is commonly associated with high-grade ore. Primary ore minerals include pyrite with gold inclusions, pyrrhotite, pentlandite, chalcopyrite, and scheelite. The primary mineralization was enriched by supergene processes.

Hydrothermal alteration is characterized mainly by silicification, carbonitization, and, locally, chloritization. Harper et al. (1998) reported that mafic rocks show a paragenetic sequence of early albite and quartz, followed by muscovite and chlorite. Alteration in the metasedimentary rocks in the hangingwall is characterized mainly by sericite and chlorite. This primary alteration grades into zones of supergene alteration containing limonite, kaolinite, smectite group minerals, and hematite. The weathered bedrock extends to approximately 60 m depth. Regolith studies from drillholes have revealed anomalous Au, W, As, Sb, and Se in the ferruginous materials.

Labouchere, Nathans, and Fortnum deposits

In the northwestern part of the Bryah–Padbury Basin (on MILGUN), three distinct zones of gold mineralization have been recognized in high-strain zones associated with the margin of the Yarlalweelor gneiss complex (Fig. 25 and Plate 1). The Labouchere group (Labouchere and Central Valley deposits) and Nathans group (Labouchere–Nathans, Nathan Bitter, and Nathans Deep South deposits) had early

mining activity recorded from 1939 to the early 1940s, with additional discoveries in the mid-1980s (Hanna and Ivey, 1990). The Fortnum deposits (Trevs, Starlight, Twilight, Ricks, Toms Hill, Alton, Eldorado, Callies, D39, and Yarlalweelor) were discovered in the early 1980s (Hill and Cranney, 1990).

Gold mineralization is structurally controlled in host rocks of both the Bryah and Padbury Groups (Hill and Cranney, 1990). Windh (1992) concluded from detailed studies at the Labouchere, Nathans Deep South, and Fortnum mines that aqueous fluids of high temperature and moderate salinity were responsible for mineralization. Constraints on temperature are derived from the lower to middle greenschist-facies alteration assemblages (muscovite–chlorite–albite(–biotite)) and fluid inclusion trapping temperatures of up to 320°C. Based on lead isotope work (galena from Nathans Deep South), Windh (1992) suggested that the syn-D₄ gold mineralization occurred between 1.9 and 1.8 Ga. The main features of the ore deposits are described below from the available literature.

At the Labouchere-Nathans mine, gold mineralization is hosted in pyritic chert lenses or pods that lie within mafic–ultramafic schist and along the contact with overlying quartz wacke of the Labouchere Formation. Windh (1992) described volcanic breccia (with high Ni and Cr) with fuchsitic ultramafic and chert clasts, similar to the reworked clastic rocks immediately overlying the mafic–ultramafic volcanic rocks in the Narracoota Formation at the Fortnum mine. The mafic–ultramafic schist lies in the core of a southerly plunging anticline, and is here interpreted as part of the Narracoota Formation. The Narracoota Formation – Labouchere Formation contact is interpreted as an early (D₁–D₂) fault or shear zone that was tightly folded during D₃. The structure is crosscut and slightly offset by D₄ faults trending 270°–290°, including a shear that forms the southern limit to the mineralization (Hanna and Ivey, 1990). Gold is associated with quartz veining and pyrite in the altered chert, with siderite–muscovite–pyrite alteration around the veins (Windh, 1992). Production figures are only known for the combined output of the Labouchere-Nathans and Nathans Deep South opencuts (nearly 7 t of gold over five years; Table 7).

At the Nathans group of workings, the Nathan Bitter shafts within the upper Labouchere Formation or lower Wilthorpe Formation have a recorded production of about 8 kg over the period 1943–1950 (Swager and Myers, 1999). About 500 m to the north-northwest, shallow shafts lie along the Kinders Fault between coarse and pebbly quartz wacke to the east and ultramafic schist of the Narracoota Formation to the west. The Nathans Deep South mineralization lies approximately 1 km south-southeast of Nathan Bitter and was discovered in 1986 (Hanna and Ivey, 1990). The mineralization is hosted by finely laminated, chloritic shale interbedded with coarse quartz wacke and overlain by coarse units grading from quartz-pebble conglomerate to quartz–sericite shale. The entire succession is here described as part of the Wilthorpe Formation, including the chloritic shale, which is most likely derived from mafic volcanic precursors (Hanna and

Ivey, 1990; Windh, 1992). Occhipinti et al. (1998a) mapped similar units in the Wilthorpe Formation as a separate member, the Beatty Park Member. The westerly younging succession contains a north–south S₃ foliation, axial planar to a few small-scale, parasitic D₃ folds plunging steeply south, and is overprinted by F₄ microfolds and kinks trending 290°. Gold mineralization is within pyrite, which has replaced finely bedded chlorite shale, near crosscutting D₄ quartz–ankerite veins. Highest grades are found adjacent to D₄ faults. These and other structural observations led Windh (1992) to infer a syn-D₄ timing of mineralization. However, small quartz-vein networks, possibly related to low-grade mineralization, in the overlying coarsely graded units are deformed by D₄ microfolding.

The Fortnum gold mineralization is hosted by the Narracoota Formation, which is truncated to the north against the Fortnum Fault and wedges out to the south. The package contains mafic–ultramafic schist with overlying reworked fragmental and volcanoclastic rocks, including rocks with a supposed felsic volcanic derivation, overlain by the Ravelstone Formation (Hill and Cranney, 1990).

Mineralization at Trevs (and closely associated orebodies, including a recent discovery named Starlight) is hosted by quartz-vein systems in a westerly dipping succession of graded sericitic siltstone and coarse wacke with medium- to coarse-grained feldspar, quartz, and lithic fragments, at least partly derived from the underlying mafic–ultramafic volcanic rocks. The Yarlalweelor mineralization is hosted by ovoid lenses of jasperoidal chert within variably schistose mafic–ultramafic volcanic rocks, including interleaved fine ?tuffaceous and coarse fragmental layers (Hill and Cranney, 1990). The chert lenses are within a westerly dipping, reverse D₃ shear zone characterized by quartz–chlorite–sericite alteration. Gold-bearing quartz(–pyrite) veins within the chert pods and within magnetite-bearing chlorite schist trend at 120°, dip steeply north, and are parallel to small sinistral D₄ faults (D₃ in Windh, 1992). Windh (1992) also reported a minor set of (dextral) faults trending 070° and crosscutting the D₃ shear zones. This may suggest a conjugate fault set recording east–west compression, possibly late during D₃ rather than during north-northeast–west-southwest D₄ compression.

Mining at the Fortnum group of workings from 1990 to 1998 yielded 11 928 kg of gold from 4.685 Mt of ore, with an average recovered grade of 2.54 g/t gold (Swager and Myers, 1999). Remaining measured and indicated resources at Fortnum, including Trevs and Starlight, contain an additional 17 970 kg of gold, with a further 4340 kg of gold estimated within inferred resources (Perilya Mines NL, 1998).

Wembley deposit

The Wembley deposit is located approximately 18 km southwest of Peak Hill and 2.5 km southeast of Murphy Well (from the Peak Hill road). Although rewarding (average grade of 17.5 g/t gold), ore production was very small (less than 1800 t).

The Wembley mineralization is hosted in altered metabasite rocks within a major shear zone trending 120° . The mineralized zone strikes at 075° and dips 63° to the northwest. A quartz vein near the old workings strikes at 060° and dips 54° to the northwest. Sedimentary units are intercalated with the volcanic rocks and consist of turbiditic rocks (greywacke–shale). As at the Durack prospect (see below), quartz mylonite units, trending 120° – 140° , are within the metabasites.

Wilgeena deposit

The Wilgeena (or Hit or Miss) gold mine area is located 15 km southeast of the Peak Hill mine. Production was less than 15 000 t at an average grade of 2.6 g/t gold.

The deposit is within rocks of the Peak Hill Schist and, more specifically, along the contact between the mylonites and quartz–sericite schist. A northerly trending, easterly dipping, stoped-out ore lens was approximately 2 m thick. The mineralization is hosted in quartz–muscovite–magnetite schist. Grab samples from the old excavations returned values ranging from 3 to 14 g/t gold (Mountford, 1984). Whitfield (1987) estimated inferred resources as approximately 600 000 t at 2.44 g/t gold.

Durack, St Crispin, and Heines Find prospects

The Durack prospect lies about 12 km south of Peak Hill, along and immediately west of the Old Peak Hill telegraph road. This gold deposit is blind, being covered by soil and lateritic material, and consists of primary mineralization and a supergene mineralized zone. The prospect was identified by a soil anomaly containing up to 100 ppb gold (Sabminco Annual Report, 1994).

The prospect area is underlain by rocks of the Narracoota Formation, which include metabasite (medium- to coarse-grained metabasalts) and mafic pyroclastic rocks. Thin, magnetite-bearing chert bands (possibly chemical sediments) intercalated within the metabasites define a broad synclinal structure. A number of mylonite zones, trending 120° – 125° , cut across the Narracoota Formation rocks and contain most of the primary mineralization. Grades intersected during drilling are in the order of 1.5 g/t gold over widths of 4 to 6 m.

The primary mineralization is contained within quartz–sulfide veins and stockworks hosted by altered metabasite rocks. The mineralized area is about 1.4 km long and 200 m wide. Hydrothermal alteration is pervasive and consists of quartz, chlorite, biotite, and iron-rich carbonate (ankerite). Pyrite is present as fine disseminations and veinlets. Selvages of silica–pyrite–carbonate surround the mineralized zones.

The supergene mineralization at the Durack prospect is controlled by subhorizontal redox fronts within the regolith material. Supergene enrichment shows grades of up to 12 g/t gold over an interval of about 5 m. In some cases the redox-front-related mineralization developed up to 45 m on each side of the primary zone.

The St Crispin prospect is situated 20 km east-southeast of Peak Hill. The mineralization is along a north-northwesterly trending structure and hosted in sericite(–graphite) schist of the Peak Hill Schist. Quartz veins are present in the schists and may host the mineralization.

The Heines Find prospect is located 20 km south-southeast of Peak Hill. Mineralization can be traced for about 6 km along the easterly trending contact between rocks of the Narracoota Formation and the Heines Member of the Wilthorpe Formation. This contact has a dip of 80° to the north, and is sheared. In this area, the Narracoota Formation consists of strongly deformed pillow lavas and chlorite schist. The sedimentary rocks of the overlying Heines Member include a basal polymictic conglomerate.

Ruby Well group

The Ruby Well area includes a number of mineral leases from which gold has been produced either from surface materials or from hard rock (0.2 t; Table 7). The Ruby Well leases lie on the northern side of the Great Northern Highway, about 80 km from Meekatharra and 4–5 km east of the Peak Hill turn-off.

The area is underlain by the Narracoota, Doolgunna, and Karalundi Formations. The Hard To Find, Ruby Anne, and Lucky Call deposits, within mafic schist of the Narracoota Formation, were exploited between 1912 and 1917. Most of the current production (figures not available) is from a number of dry-blowing workings surrounding these old mines.

Mikhaburra deposit

The old Mikhaburra gold mine (also known as Holdens Find) is in Narracoota Formation volcanic rocks in the southwestern part of BRYAH (Fig. 25). The recorded production of the Mikhaburra mine is about 226 kg of gold (MacLeod, 1970). The mineralization is associated with a system of auriferous quartz veins emplaced along a shear zone trending about 130° to 150° and dipping 68° to the southwest. The volcanic rocks include mainly chlorite schist. A quartz vein with a strike of 120° and dip of 58° southwest lies to the west of the old workings. This vein is about 1 m wide and locally displays a laminated structure.

Wilthorpe deposit

The Wilthorpe deposit is hosted by granitic rocks of the Despair Granite (Fig. 32), which contains xenoliths of mafic material. Gold mineralization is confined to a zone containing quartz veins, and flanked by bleached and silicified wallrocks. The ore zone is hydrothermally altered, with assemblages of chlorite–sericite–biotite and quartz–muscovite–biotite–tourmaline flanked by near-pervasive silicification. In addition to gold, the mineralized veins also contain pyrite, galena, arsenopyrite, and chalcopyrite. The wallrock granite has a cataclastic texture and consists of quartz and feldspar ‘eyes’ surrounded by a network of granulated quartz and sericite.

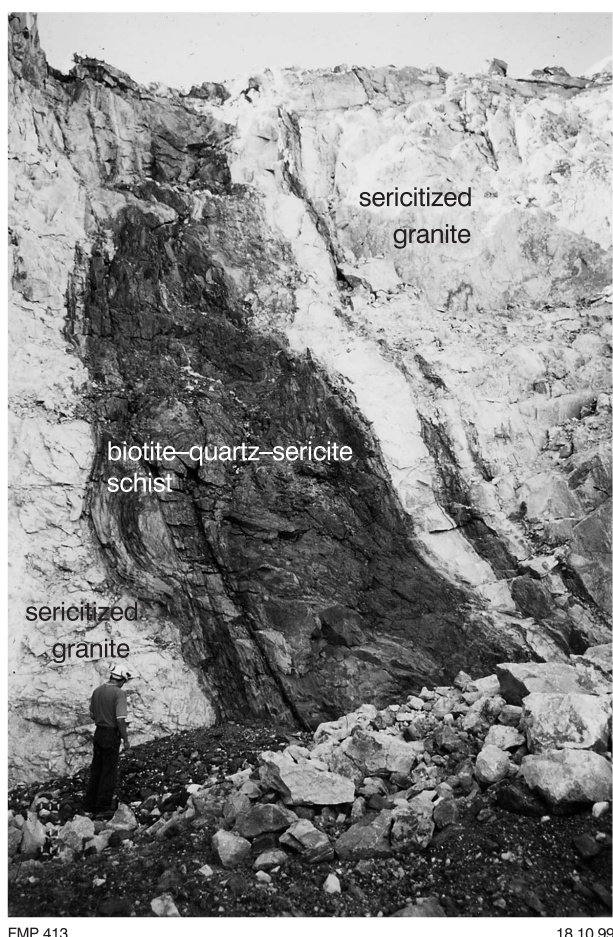


Figure 32. The west wall of the Wilthorpe opencut, showing the contact between biotite-sericite-quartz schist and deformed Despair Granite

Cashman deposit

The Cashman area on BRYAH includes a number of small mineral occurrences and deposits containing copper and copper-gold. The old Cashman copper mine is approximately 250 m from the gold workings. In 1917 this mine produced about 7 t of copper ore, grading 16.5% copper (Marston, 1979). The copper mineralization consists of a metre-wide cupriferous limonite vein with a strike of 042° and a shallow dip to the northwest. Ore minerals are chrysocolla and malachite as disseminations and veinlets (Marston, 1979).

In 1937 there was a small production of gold ore from quartz veins. In 1986–87 the gold potential of the Cashman area was reassessed, and on the basis of this work, a small opencut was excavated, from which 8000 t of ore material was produced and stockpiled (Whitfield, 1987). Gold mineralization is hosted in quartz veins within metabasaltic hyaloclastite. A 0.1 m-thick quartz vein in the pit has a strike of 115° and dips 35° to the northeast. At and near the surface, supergene enrichment is present in a horizon about 30 m wide and dipping about 20° to the north (Whitfield, 1987).

Volcanogenic copper-gold deposits

The Horseshoe Lights copper-gold deposit on JAMINDI has produced nearly 9 t of gold, of which almost 2.6 t was recovered from the copper concentrate operation between 1988 and 1993 (Table 7). The Horseshoe Lights deposit is hosted in felsic schist of the Narracoota Formation (Bryah Group). The mineralization consists of massive sulfides overlying and flanked by disseminated and stringer sulfides. Ore minerals are mainly chalcocite, pyrite, and chalcopyrite. Native copper is also present (Parker and Brown, 1990). The host rocks are mylonitized chlorite schist, kaolinite-sericite schist, and quartz-sericite schist. The geometry of the ore zones (massive sulfides and stringer zone), alteration patterns (silicification, sericitic, and chloritic alteration), predominantly felsic composition of the host rocks, and metal association (Cu–Au–Ag–Pb–Zn) suggest that the deposit was originally of the volcanogenic massive sulfide type, but subsequently enriched by supergene processes. Average grades have been about 8 g/t gold, about 10% copper, and 300 ppm silver. The stringer mineralization is of low grade, averaging between 0.2 and 0.3 g/t gold. Production ceased in 1994. Remaining resources (Table 8) are of low-grade mineralization.

Supergene manganese deposits

Manganese mineralization is part of a historically important manganese field, first recognized in 1905, with deposits in the Mount Fraser, Mount Padbury, Ravelstone (Peak Hill), and Horseshoe areas. The manganese mineralization is of supergene origin and related to manganese-rich and hematitic shale units and BIF of the Horseshoe Formation (Bryah Group), as well as units of the Padbury Group. The chief ore minerals are pyrolusite and cryptomelane. The ore is lateritic, locally pisolitic in nature, and, in places, forms caps overlying the primary manganese-rich sedimentary material. In places, notably at Horseshoe, there is evidence to suggest that some enrichment may have taken place in a palaeodrainage channel, lake, or swamp environment (MacLeod, 1970). In the Ravelstone area, just north of the Peak Hill gold deposit, the manganese supergene enrichment appears to have a structural control.

The Horseshoe area has been the main producing region, with production from two deposits, 2 and 3 km north and northwest of the Horseshoe townsite (Plate 1). The main production period was from 1948 to 1971, when 490 000 t was mined (Table 8), all but 5000 t of which was classified as metallurgical-grade ore. The enriched zone was 3 to 4.5 m thick and typically extended over lengths of 400 to 500 m. The North deposit averaged 30 m in width, whereas the South deposit was fan shaped, opening from 20 to 300 m wide at its maximum extent. Ore consisted of mixed manganese and iron oxides, with highly variable manganese and iron contents. Grades progressively decreased from 42 to 35–38% after 1966.

There are several small deposits in the Mount Fraser – Mount Padbury area, about 30 km west of Peak Hill.

They contain patches of high-grade ore within large deposits of ferruginous manganese material. Production of high-grade ore occurred sporadically since 1949 and amounted to 7547 t at grades in excess of 46% manganese. A third mining operation commenced at the Millidie (or Elsa) deposit in the early 1990s, but this has not progressed to a full-scale commercial operation. High-grade mineralization in the area is estimated to contain measured plus indicated resources of approximately 11 000 t of manganese (Table 8).

In the Ravelstone area, immediately north-northwest of Peak Hill, mining occurred between 1956 and 1964, producing 76 237 t of ore at 70–90% manganese oxide (Table 8). Remaining measured and indicated resources are estimated as 132 000 t of contained metal (Table 8). Manganese production at Ravelstone was from easterly striking orebodies reaching lengths of up to 100 m and widths of 30 m, but commonly small and narrow. Detailed examination of one specimen of ore revealed that it was composed mainly of cryptomelane and accessory pyrolusite. A partial geochemical analysis of the same sample provided the following results: 0.64 wt% SiO₂, 4.65 wt% Al₂O₃, 0.011 wt% P, 0.33 wt% MgO, 2.68 wt% K₂O, 70.38 wt% MnO, 1.19 wt% Fe, 0.05 ppm Au, 650 ppm Co, 31 ppm Cu, 53 ppm Ni, 20 ppm Pb, and 98 ppm Zn.

The manganese ore is characterized by high barium abundances (3000 ppm to 3.0% at Mount Fraser, 3000 ppm to 1% at Horseshoe, and 3943 to 9000 ppm at Ravelstone).

Iron ore

The Robinson Range Formation (Padbury Group) contains units of banded iron-formation (Fig. 2), within which are areas of supergene enrichment of hematite and goethite. These constitute demonstrated (pre-JORC code) iron-ore resources estimated at approximately 10 Mt, with grades in excess of 60% iron (Table 8). Enrichment is above two BIF units, approximately 100 m thick, separated by a hematitic shale horizon. Iron grades of the primary BIF vary between 20 and 50%. Hematite and hematite-goethite surficial enrichment contains grades in excess of 50% iron, as determined from the sampling of one of about 200 small pods of potentially ore grade material (Sofoulis, 1970).

Talc

Talc in the Mount Seabrook – Livingstone – Trillbar region is present within metasedimentary and meta-volcanic rocks and minor mafic and ultramafic rocks. Talc is hosted in metasomatized dolomite orebodies (Plate 1), as a series of steeply plunging lenses (Lipple, 1990). The Mount Seabrook deposit was discovered in 1965 and has produced over 540 000 t of talc, mostly of cosmetic grade, between 1973 and 1995. Indicated and inferred resources redefined at Mount Seabrook and Livingstone amount to 1.72 Mt of ore, with a significantly greater potential because the orebodies are open along strike.

Discussion

The Horseshoe Lights VMS-type copper–gold deposit is syn-volcanic and pre-orogenic. All other deposits are of epigenetic origin, and syn- to post-orogenic.

Figure 33 schematically depicts a simple regional model of ore genesis for the epigenetic mineral deposits in the Bryah–Padbury – Peak Hill Schist (BPPS) tectono-metamorphic domain and the adjacent Yerrida Basin. The Yerrida Basin and BPPS domain were tectonically juxtaposed along the northeasterly trending Goodin Fault. Deformation, which affected the BPPS domain, was transmitted across the Goodin Fault for a few kilometres into the Yerrida Basin. This deformation becomes weaker from the Goodin Fault eastward. The BPPS domain was subjected to metamorphism (upper to lower greenschist facies). At least two phases of metamorphism are recognized: a prograde phase, overprinted by a retrograde phase. Geothermometry and geobarometry studies in the area around Peak Hill by Thornett (1995) indicated temperatures of around 500–620°C for peak prograde metamorphism and 6.5 to 7 kbar for minimum pressure of the prograde assemblages. The timing of this metamorphism is probably linked to the collision between the Pilbara and Yilgarn Cratons (see **Tectonic model and conclusions**), which is postulated to have occurred between 1820 and 1800 Ma (Occhipinti et al., 1999).

A genetic model proposed by Pirajno and Preston (1998) envisages that fluids were generated during phases of dynamic and thermal metamorphism in the BPPS domain and that these fluids were largely responsible for the deposition of mesothermal gold-only and shear-zone-hosted deposits. The paragenesis of the alteration assemblages associated with the mesothermal deposits and textural relationships suggest that metamorphism

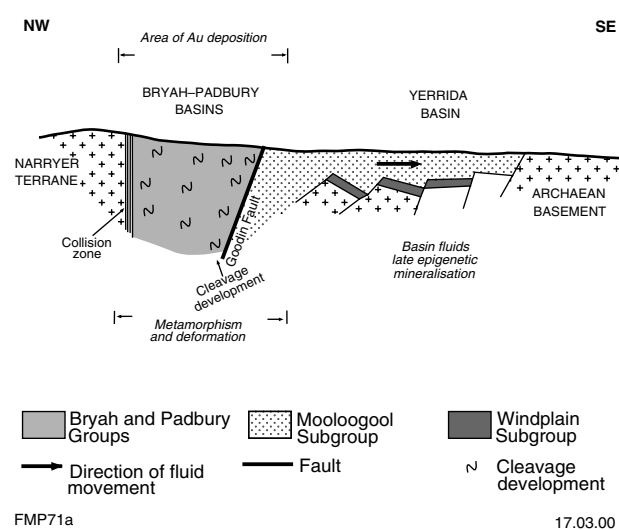


Figure 33. Sketch illustrating a conceptual model for the origin of precious and base metal epigenetic deposits in the Bryah–Padbury and Yerrida Basins (after Pirajno and Preston, 1998)

and mineralization were broadly contemporaneous, although alteration was, in most cases, from peak to retrograde metamorphism. Exceptions to this are localized zones of sodium metasomatism (albite and arfvedsonite), which overprint the retrograde assemblages. This sodium metasomatism may be related to central zones of higher temperatures within the mineralized structures. One possible explanation for the widespread sodium metasomatism is granite magmatism; however, there is no evidence in either the Bryah or the Padbury Basin of granitic plutons intruding the volcano-sedimentary successions. Therefore, a possible role of granitic magmatism as one of the heat and metal sources for the hydrothermal solutions, based on our present knowledge, is excluded.

Hydrothermal solutions responsible for the emplacement of mesothermal lodes are considered to be generated in tectonically active regions and are associated with compressional and extensional tectonics (Kerrick and Cassidy, 1994). The mesothermal-style gold-only lodes of the BPPS domain were formed in a compressional setting characterized by thin-skinned thrusting associated with prograde and retrograde mineral assemblages (Pirajno, 1996). Dyer (1991) concluded that the hydrothermal mineralization in the Labouchere–Fortnum area was generated by the mixing of two fluids of different density and salinity. Deeply sourced, hot, saline, CO₂-bearing fluids were mixed with cooler, less saline, near-surface aqueous fluids. The available evidence points to the conclusion that the mineralizing fluids were at first generated during compression and dehydration, and moved along ductile to brittle structures. During subsequent phases, meteoric fluids would have infiltrated along the same structures and mixed with the hotter metamorphic solutions. The whole mechanism could have been repeated again in the next phase of compression and extension, leading to multiphase ore genesis processes in which the latest phase leaves the most detectable imprint. There is no obvious link with magmatic activity.

Other metal deposits in the Bryah–Padbury Basin are supergene manganese and iron ore (Pirajno and Preston, 1998). The timing of the weathering event that led to the supergene enrichment of the manganese and iron ores is not known, although it may be possible that the warm and humid climate during the middle Tertiary (Cockbain and Hocking, 1990) played a major role in the genesis of this supergene mineralization.

Tectonic model and conclusions

Gee (1979), Hynes and Gee (1986), Windh (1992), and Gee and Grey (1993) interpreted the geodynamic evolution of the ‘Glengarry Basin’, as defined by Gee and Grey (1993), in terms of an ensialic or intracontinental basin. Tyler and Thorne (1990), Myers (1993), Martin (1994), and Myers *et al.* (1996) proposed models in which the former ‘Glengarry Basin’ would have formed in a back-arc setting, during the convergence of the Pilbara and Yilgarn Cratons, between 2000 and 1800 Ma.

In the light of the re-interpretation of the former ‘Glengarry Basin’ into the Bryah, Padbury, and Yerrida Basins, some modification of the above tectonic schemes is necessary. Lack of sufficient geochronological data, however, poses the problem of the precise timing of events. This lack of information must be taken into account when modelling basin tectonics. Pirajno (1996) and Pirajno *et al.* (1998b) suggested two models for the geodynamic evolution of the Bryah–Padbury and Yerrida Basins: 1) the basins were formed during convergence and subsequent collision in a back-arc–foreland basin setting, in which these basins were opened and infilled during southward subduction of oceanic crust (extensional back arc) and subsequently overlain by sediments in a newly developed foreland basin (syn-collisional); and 2) the basins were formed at the time of the oblique collision between the Pilbara and Yilgarn Cratons, as pull-apart structures in a strike-slip setting with transitions from extensional (transtension) to compressional (transpression) regimes.

In this study we propose a model whereby the Bryah Basin was formed as a back-arc rift, with a component of rifting along the Yilgarn continental margin, a kind of proto-oceanic rift comparable to that of the present-day Guayamas Basin in the Gulf of California (Lonsdale and Becker, 1985). The Padbury Basin developed as a foreland basin on top of the Bryah Basin during the oblique collision of the Pilbara and Yilgarn Cratons. Our model is shown in Figure 34, in which two stages are schematically depicted and briefly discussed below.

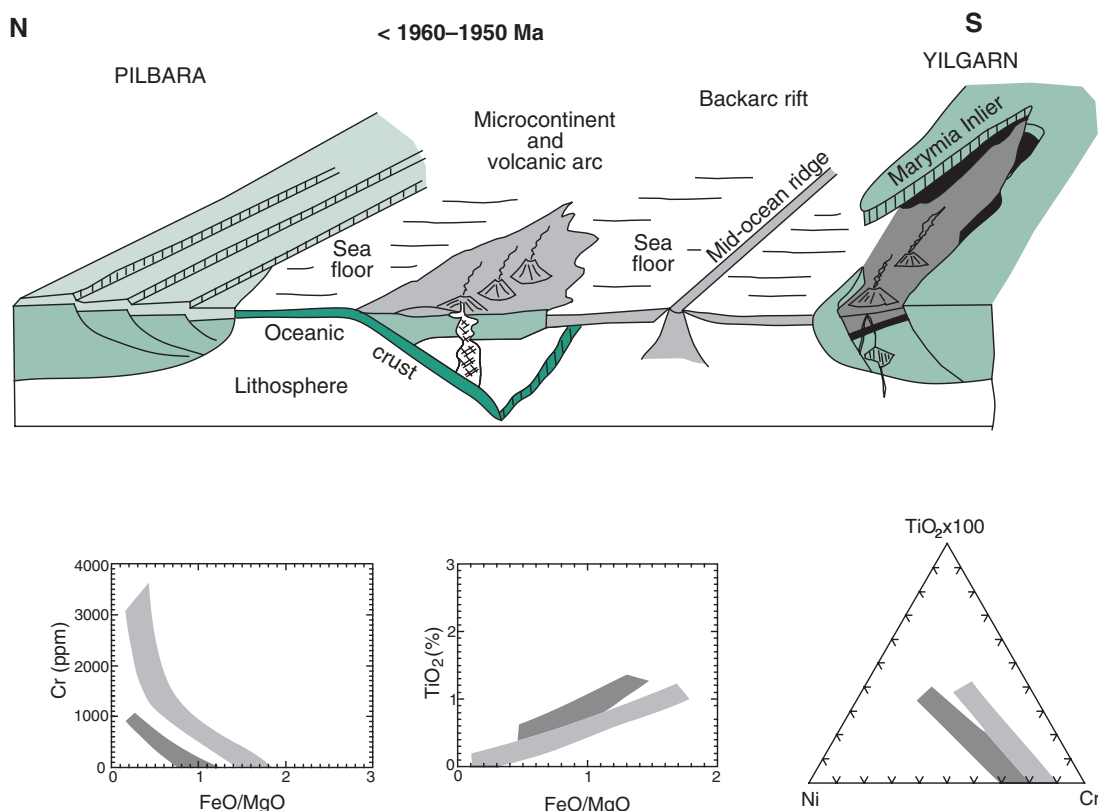
The Bryah Basin was formed by processes of back-arc opening during subduction of oceanic crust beneath the northern margin of the Yilgarn Craton, approximately

Figure 34. Schematic illustration showing the preferred model of the tectonic evolution of the Bryah and Padbury Basins, within the context of the Capricorn Orogen (modified from Myers, 1990, 1993; and Myers *et al.*, 1996):

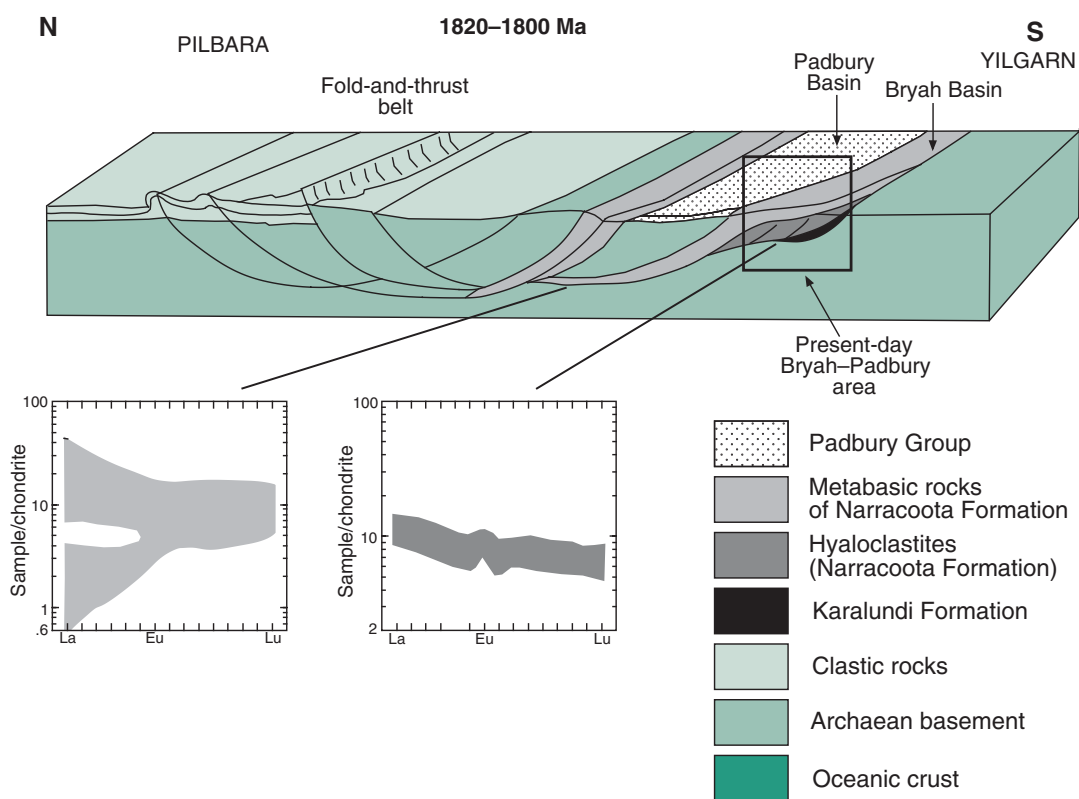
a) At about 1960–1950 Ma: development of Andean-type magmatic arc on a microcontinental active margin; back-arc rifting and spreading with creation of oceanic crust (dominantly high-Mg and high-Fe tholeiite associated with subvolcanic peridotitic cumulates representing future mafic–ultramafic schist of the Narracoota Formation); and eruption of basaltic hyaloclastites, probably from the same source as the mafic–ultramafic material, occurs on passive margin of Yilgarn Craton. Insets schematically show geochemical signatures of these volcanic rocks (see text for details);

b) Capricorn Orogeny involved collision between the Pilbara and Yilgarn Cratons, with formation of fold-and-thrust belts on both northern and southern sides of orogen, and thrusting of oceanic crust over hyaloclastite and margin of Yilgarn Craton. The thrust separating oceanic crust material from hyaloclastite is represented by the Murchison Fault (see Plate 1). Chondrite-normalized REE patterns for metabasites and hyaloclastites of the Narracoota Formation are shown in the insets

a)



b)



FMP376

17.03.00

between 1960 and 1950 Ma (Occhipinti *et al.*, 1999; Fig. 34a). Myers (1993) speculated that a southward oceanic subduction system with a south-facing Andean-type magmatic arc had developed off the northern passive margin of the Yilgarn Craton. Remnants of arc magmatic suites have not been found, but may be buried under the Mesoproterozoic Bangemall Basin. Back-arc rifting also affected the northern margin of the Yilgarn Craton, where rift propagation is postulated to have progressively advanced from west to east through a succession of crustal–lithospheric thinning, rupture, and graben formation. In this model, the Marymia Inlier is a remnant of a rift shoulder (Fig. 34a).

The closing of the ocean between the Pilbara and Yilgarn Cratons was followed by the oblique collision between the rifted passive margin on the Pilbara side, an inferred active magmatic arc and the passive northern margin of the Yilgarn Craton. Closure of the intervening ocean (1820–?1800 Ma) resulted in inversion of the Bryah back-arc rift, and thrusting of oceanic crust (now Narracoota Formation), over the Yilgarn Craton's northern margin (Fig. 34b). During and following this collision event, the southern side of the Pilbara was tectonically sliced by major thrusts, whereas most of the tectonic transport of the inferred magmatic and oceanic crust rocks was towards the south (Myers, 1993).

High-Mg tholeiitic rocks with pillow structures, sheeted dykes, the Trillbar layered complex, sea-floor metasomatism, and trace and rare-earth element geochemistry support the oceanic crust model for the origin of the mafic and ultramafic schist of the Narracoota Formation. The hyaloclastites, on the other hand, were erupted in shallow waters and locally characterized by explosive activity, and have mixed and overlapping geochemical signatures with the mafic schist. This feature can be interpreted as suggesting a more continental environment of emplacement and therefore were emplaced on Yilgarn crust (Fig. 34a). In contrast to the mafic–ultramafic schist, the hyaloclastites are relatively tectonically undeformed. Their contact with the mafic–ultramafic schist is along the Murchison Fault (Plate 1). We conclude that the Murchison Fault represents a tectonic boundary between these two components of the Narracoota Formation, and that oceanic crust material (precursors of the mafic–ultramafic schist) were thrust over the continental hyaloclastites during the Capricorn Orogeny, as shown in Figure 34b. The suggested Gulf of California-type palaeoenvironmental setting, with the future Marymia Inlier as one of the rift shoulders (analogous to the California peninsula), is shown in Figure 34a.

The absence of volcanic rocks of intermediate (andesitic) compositions suggests that the Narracoota Formation metabasites were not formed in a subduction-related volcanic-arc setting, as proposed by Myers *et al.* (1996). However, we concur with Sun (1997) that the boninitic component in the chemistry of the metabasites (see inset of Fig. 34 and Figs 12–15) needs explanation. We suggest that these boninitic characteristics of the Narracoota Formation can be compared to the boninites of the Koh Ophiolite in New Caledonia (Meffre *et al.*,

1996), which are considered to have formed in a back-arc spreading centre.

The overall high MgO and low TiO₂ abundances, depleted REE, and low La/Yb ratios of the Narracoota Formation are also consistent with the origin of the Narracoota Formation metabasites from a mantle plume (Pirajno *et al.*, 1998a).

The Padbury Basin was interpreted by Martin (1994) as a retroarc foreland basin, recording the collision of the Yilgarn and Pilbara Cratons. During and following collision, between 1820 and 1800 Ma (Occhipinti *et al.*, 1999), back-arc volcanism ceased and a foreland basin developed on top of the back-arc succession (Bryah Group). This basin was filled by siliciclastic rocks only (Padbury Group). During continued regional compression, the Bryah–Padbury Basin developed into a fold-and-thrust belt, and was partly thrust over the Yerrida Basin along the Goodin Fault.

In summary, the convergence between the Archaean Pilbara and Yilgarn Cratons resulted in progressive compressional deformation that affected the Bryah and Padbury Groups as a coherent package. At least four groups of structures are recognized in the regional deformation of the volcano-sedimentary succession and their reworked basement (*i.e.* Yarlarweelor Gneiss Complex). This same deformation and associated metamorphism was responsible for the mesothermal gold-only lodes of the Bryah and Padbury Basins.

Acknowledgements

We acknowledge the contribution of colleagues who participated in the Glengarry mapping program: John Myers, N. G. Adamides, and P. G. Le Blanc Smith. Richard Davy first introduced the senior author to the area. We are also grateful to the local pastoral community for their hospitality. The geological staff of Labouchere, Fortnum, Peak Hill, and Harmony gold mines are thanked for sharing their knowledge with us.

References

- ADAMIDES, N. G., 1998, Geology of the Doolgunna 1:100 000 sheet: Western Australia Geological Survey, 1:100 000 Geological Series Explanatory Notes, 23p.
- BAGAS, L. B., 1998, Geology of the Marymia 1:100 000 sheet: Western Australia Geological Survey, 1:100 000 Geological Series Explanatory Notes, 23p.
- BARNETT, J. C., 1975, Some probable Lower Proterozoic sediments in the Mount Padbury area: Western Australia Geological Survey, Annual Report 1974, p. 52–54.
- BARRETT, F., 1989, A study of wallrock alteration associated with gold mineralization — Peak Hill and Mt Pleasant area: Western Australia Geological Survey, M-series, Item 7706, A41555 (unpublished).
- BRADLEY, J. J., FAULKNER, J. A., and SANDERS, A. J., 1997, Geochemical mapping of the Robinson Range 1:250 000 sheet: Western Australia Geological Survey, 1:250 000 Regolith Geochemistry Series Explanatory Notes, 57p.
- BREITKOPF, J. H., and MAIDEN, K. J., 1988, Tectonic setting of the Matchless Belt pyritic copper deposits, Namibia: *Economic Geology*, v. 83, p. 710–723.
- BUNTING, J. A., COMMANDER, D. P., and GEE, R. D., 1977, Preliminary synthesis of Lower Proterozoic stratigraphy and structure adjacent to the northern margin of the Yilgarn Block: Western Australia Geological Survey, Annual Report 1976, p. 43–48.
- BURKE, K. C., KIDD, W. S. F., TURCOTTE, L., DEWEY, J. F., MOUGINIS-MARK, P. J., PARMENTIER, E. M., SENGOR, A. M., and TAPPONIER, P. E., 1981, Tectonics of basaltic volcanism, in *Basaltic volcanism on the terrestrial planets*: Houston, Lunar and Planetary Institute, p. 803–898.
- COCKBAIN, A. E., and HOCKING, R. M., 1990, Regolith, in *Geology and mineral resources of Western Australia*: Western Australia Geological Survey, Memoir 3, p. 591–602.
- CRAWFORD, R. A., FAULKNER, J. A., SANDERS, A. J., LEWIS, J. D., and GOZZARD, J. R., 1996, Geochemical mapping of the Glengarry 1:250 000 sheet: Western Australia Geological Survey, 1:250 000 Regolith Geochemistry Series Explanatory Notes, 57p.
- DAVY, R., PIRAJNO, F., SANDERS, A. J., and MORRIS, P. A., 1999, Regolith geochemical mapping as an adjunct to geological mapping and exploration; examples from three contiguous Proterozoic basins in Western Australia: *Journal of Geochemical Exploration*, v. 66, p. 37–53.
- DIXON, J., and WILLIAMS, G., 1983, Reaction softening in mylonites from the Arnaboll thrust, Sutherland: *Scottish Journal of Geology*, v. 19, p. 157–168.
- DUNCAN, A. R., 1987, The Karoo igneous province — a problem area for inferring tectonic setting from basalt geochemistry: *Journal of Volcanology and Geothermal Research*, v. 32, p. 13–34.
- DYER, F. L., 1991, The nature and origin of gold mineralization at the Fortnum, Nathans, and Labouchere deposits, Glengarry Basin, Western Australia: University of Western Australia, BSc Honours thesis (unpublished).
- ELIAS, M., 1982, Belele, W.A.: Western Australia Geological Survey, 1:250 000 Geological Series Explanatory Notes, 21p.
- ELIAS, M., BUNTING, J. A., and WHARTON, P. H., 1982, Glengarry, W.A.: Western Australia Geological Survey, 1:250 000 Geological Series Explanatory Notes, 27p.
- ELIAS, M., and WILLIAMS, S. J., 1980, Robinson Range, W.A.: Western Australia Geological Survey, 1:250 000 Geological Series Explanatory Notes, 32p.
- FISHER, R. V., and SCHMINCKE, H.-U., 1984, *Pyroclastic rocks*: Berlin, Springer-Verlag, 472p.
- GEE, R. D., 1979, The geology of the Peak Hill area: Western Australia Geological Survey, Annual Report 1978, p. 55–62.
- GEE, R. D., 1987, Peak Hill, W.A. (2nd edition): Western Australia Geological Survey, 1:250 000 Geological Series Explanatory Notes, 24p.
- GEE, R. D., 1990, Nabberu Basin, in *Geology and mineral resources of Western Australia*: Western Australia Geological Survey, Memoir 3, p. 202–210.
- GEE, R. D., and GREY, K., 1993, Proterozoic rocks on the Glengarry 1:250 000 sheet — stratigraphy, structure, and stromatolite biostratigraphy: Western Australia Geological Survey, Report 41, 30p.
- HALL, W. D. M., and GOODE, A. D. T., 1978, The Early Proterozoic Nabberu Basin and associated iron formations of Western Australia: *Precambrian Research*, v. 7, p. 129–184.
- HANNA, J. P., and IVEY, M. E., 1990, Labouchere and Deep South gold deposits, in *Geology of the mineral deposits of Australia and Papua New Guinea, Volume 1 edited by F. E. HUGHES*: Australasian Institute of Mining and Metallurgy, Monograph 14, p. 667–670.
- HARPER, M., HILL, M. G., RENTON, J. I., and THORNETT, S. E., 1998, Gold deposits of the Peak Hill area, Western Australia, in *Geology of the mineral deposits of Australia and Papua New Guinea, Volume 1 edited by F. E. HUGHES*: Australasian Institute of Mining and Metallurgy, Monograph 14, p. 81–87.
- HILL, A. D., and CRANNEY, P. J., 1990, Fortnum gold deposit, in *Geology of the mineral deposits of Australia and Papua New Guinea, Volume 1 edited by F. E. HUGHES*: Australasian Institute of Mining and Metallurgy, Monograph 14, p. 665–666.
- HYNES, A., and GEE, R. D., 1986, Geological setting and petrochemistry of the Narracoota Volcanics, Capricorn Orogen, Western Australia: *Precambrian Research*, v. 31, p. 107–132.
- JENSEN, L. S., 1976, A new cation plot for classifying subalkalic volcanic rocks: Canada, Ontario Division of Mines, MP 66, 22p.
- KERRICH, R., and CASSIDY, K. F., 1994, Temporal relationships of lode gold mineralization to accretion, magmatism, metamorphism and deformation — Archaean to present: a review: *Ore Geology Reviews*, v. 9, p. 263–310.
- LE MAITRE, R. W., 1989, *A classification of igneous rocks and glossary of terms*: Oxford, Blackwell Scientific Publications, 193p.

- LEWIS, J. D., 1971, The geology of some carbonate intrusions in the Mount Fraser area, Peak Hill Goldfield, Western Australia: Western Australia Geological Survey, Annual Report 1970, p. 50–56.
- LIPPLE, S. L., 1990, Talc, in *Geology and mineral resources of Western Australia*: Western Australia Geological Survey, Memoir 3, p. 678–679.
- LISTER, G. S., and SNOKE, A. W., 1984, S–C mylonites: *Journal of Structural Geology*, v. 6, p. 617–638.
- LONSDALE, P., and BECKER, K., 1985, Hydrothermal plumes, hot springs and conductive heat flow in the southern trough of Guayamas Basin: *Earth and Planetary Science Letters*, v. 73, p. 211–225.
- LUCAS, S. B., STERN, R. A., SYME, E. C., REILLY, B. A., and THOMAS, D. J., 1996, Intraoceanic tectonics and the development of continental crust: 1.92 – 1.84 Ga evolution of the Flin Flon belt, Canada: *Geological Society of America, Bulletin* 108, p. 602–629.
- MacLEOD, W. N., 1970, Peak Hill, W.A. (1st edition): Western Australia Geological Survey, 1:250 000 Geological Series Explanatory Notes, 21p.
- MARSHAK, S., TINKHAM, D., ALKMIN, F., BRUECKNER, H., and BORNHORST, T., 1997, Dome-and-keel provinces formed during Palaeoproterozoic orogenic collapse — core complexes, diapirs, or neither?: examples from the Quadrilatero Ferrifero and the Penkean orogen: *Geology*, v. 25, p. 415–418.
- MARSTON, R. J., 1979, Copper mineralization in Western Australia: Western Australia Geological Survey, Bulletin 13, 208p.
- MARTIN, D. McB., 1992, Turbidite facies and depositional environment of the Precambrian Labouchere Formation, Padbury Group, Western Australia: *Geological Society of Australia, Abstracts* 32, p. 168–170.
- MARTIN, D. McB., 1994, Sedimentology, sequence stratigraphy, and tectonic setting of a Palaeoproterozoic turbidite complex, Lower Padbury Group, Western Australia: University of Western Australia, PhD thesis (unpublished).
- MARTIN, D. McB., 1998, Lithostratigraphy and structure of the Palaeoproterozoic Padbury Group, Milgun 1:100 000 sheet, Western Australia: Western Australia Geological Survey, Report 62, 57p.
- MCDONALD, I. R., 1994, Final Report on the Glengarry nickel project ES/502 and E51/384: Western Australia Geological Survey, M-series, Item 7706, A41555 (unpublished).
- McMILLAN, N. M., 1993, Structure, metamorphism, alteration and timing of gold mineralisation at Marymia Gold Project in the Marymia Dome, in *An international conference on crustal evolution, metallogeny and exploration of the Eastern Goldfields*, Extended Abstracts compiled by P. R. WILLIAMS and J. A. HALDANE: Australian Geological Survey Organisation, Record 1993/54, p. 243–244.
- McPHIE, J., DOYLE, M., and ALLEN, R., 1993, Volcanic textures: Hobart, Tasmanian Government Printing Office, 198p.
- MEFFRE, S., AITCHISON, J. C., and CRAWFORD, A. J., 1996, Geochemical and tectonic significance of boninites and tholeiites from the Koh Ophiolite, New Caledonia: *Tectonics*, v. 15, p. 67–83.
- MOUNTFORD, B. R., 1984, Preliminary geological report on Prospecting Licences 52/104 and 52/105, Mt Padbury area, Western Australia: Western Australia Geological Survey, M-series, Item 3688, A16393 (unpublished).
- MYERS, J. S., 1989, Thrust sheets on the southern foreland of the Capricorn Orogen, Robinson Range, Western Australia: Western Australia Geological Survey, Report 26, Professional Papers, p. 127–130.
- MYERS, J. S., 1990, Capricorn Orogen, in *Geology and mineral resources of Western Australia*: Western Australia Geological Survey, Memoir 3, p. 197–198.
- MYERS, J. S., 1993, Precambrian history of the West Australian craton and adjacent orogens: *Annual Reviews of Earth and Planetary Science*, v. 21, p. 453–485.
- MYERS, J. S., SHAW, R. D., and TYLER, I. M., 1996, Tectonic evolution of Proterozoic Australia: *Tectonics*, v. 15, p. 1431–1446.
- NELSON, D. R., 1997, Compilation of SHRIMP U–Pb zircon geochronology data, 1996: Western Australia Geological Survey, Record 1997/2, 189p.
- NELSON, D. R., 1998, Compilation of SHRIMP U–Pb zircon geochronology data, 1997: Western Australia Geological Survey, Record 1998/2, 242p.
- O’NIONS, R. K., PANKHURST, R. J., and GRONVOLD, K., 1976, Nature and development of basalt magma sources beneath Iceland and the Reykjanes ridge. *Journal of Petrology*, v. 17, p. 315–338.
- OCCHIPINTI, S. A., GREY, K., PIRAJNO, F., ADAMIDES, N. G., BAGAS, L., DAWES, P., and LE BLANC SMITH, G., 1997, Stratigraphic revision of Palaeoproterozoic rocks of the Yerrida, Bryah and Padbury Basins (former Glengarry Basin): Western Australia Geological Survey, Record 1997/3, 57p.
- OCCHIPINTI, S. A., and MYERS, J. S., 1999, Geology of the Moorarie 1:100 000 sheet: Western Australia Geological Survey, 1:100 000 Geological Series Explanatory Notes, 20p.
- OCCHIPINTI, S. A., MYERS, J. S., and SWAGER, C. P., 1998a, Geology of the Padbury 1:100 000 sheet: Western Australia Geological Survey, 1:100 000 Geological Series Explanatory Notes, 29p.
- OCCHIPINTI, S. A., SHEPPARD, S., NELSON, D. R., MYERS, J. S., and TYLER, I. M., 1998b, Syntectonic granite in the southern margin of the Palaeoproterozoic Capricorn Orogen, Western Australia: *Australian Journal of Earth Sciences*, v. 45, p. 509–512.
- OCCHIPINTI, S. A., SHEPPARD, S., and TYLER, I. M., 1999, Palaeoproterozoic tectonic evolution of the southern margin of the Capricorn Orogen, Western Australia: Last Conference of the Millennium, Halls Gap, W.A., Abstract volume, p. 173–174.
- OCCHIPINTI, S. A., SWAGER, C. P., and PIRAJNO, F., 1998c, Structural–metamorphic evolution of the Palaeoproterozoic Bryah and Padbury Groups during the Capricorn Orogeny, Western Australia: *Precambrian Research*, v. 90, p. 141–158.
- PARKER, T. W. H., and BROWN, T., 1990, Horseshoe gold–copper–silver deposit, in *Geology of the mineral deposits of Australia and Papua New Guinea, Volume 1 edited by F. E. HUGHES*: Australasian Institute of Mining and Metallurgy, Monograph 14, p. 671–675.
- PEARCE, J. A., ERNEWEIN, M., BLOOMER, S. H., PARSON, L. M., MURTON, B. J., and JOHNSON, L. E., 1995, Geochemistry of Lau Basin volcanic rocks: influence of ridge segmentation and arc proximity: *Geological Society, Special Publication*, v. 81, p. 53–75.
- PEARCE, T. H., GORMAN, B. E., and BIRKETT, T. C., 1977, The relationship between major element chemistry and tectonic environment of basic and intermediate volcanic rocks: *Earth and Planetary Science Letters*, v. 36, p. 121–132.
- PERILYA MINES NL, 1998, Annual report for the year ending 30 June 1998, 60p.
- PETERS, S. G., 1993, Polygenetic mélange in the Hodgkinson goldfield, Northern Tasman Orogenic Zone: *Australian Journal of Earth Sciences*, v. 40, p. 115–129.
- PIRAJNO, F., 1996, Models for the geodynamic evolution of the Palaeoproterozoic Glengarry Basin, Western Australia: Western Australia Geological Survey, Annual Review 1995–96, p. 96–103.
- PIRAJNO, F., and ADAMIDES, N. G., 2000, Geology and mineralization of the Palaeoproterozoic Yerrida Basin, Western Australia: Western Australia Geological Survey, Report 60, 43p.

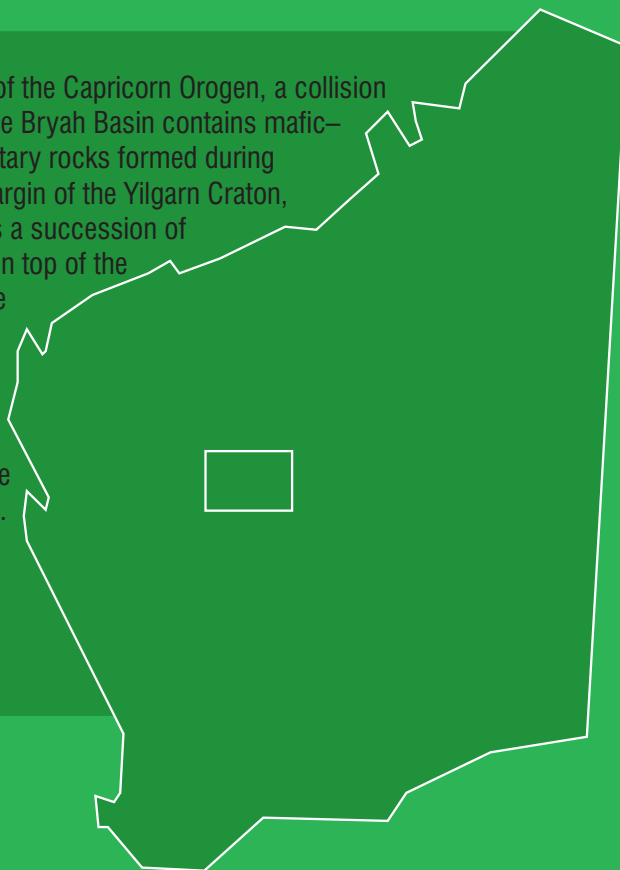
- PIRAJNO, F., and ADAMIDES, N. G., 1998, Geology of the Thaduna 1:100 000 sheet: Western Australia Geological Survey, 1:100 000 Geological Series Explanatory Notes, 24p.
- PIRAJNO, F., ADAMIDES, N. G., and FERDINANDO, D. D., 1998a, Geology of the Glengarry 1:100 000 sheet: Western Australia Geological Survey, 1:100 000 Geological Series Explanatory Notes, 16p.
- PIRAJNO, F., ADAMIDES, N. G., OCCHIPINTI, S. A., SWAGER, C. P., and BAGAS, L., 1995a, Geology and tectonic evolution of the early Proterozoic Glengarry Basin, Western Australia: Western Australia Geological Survey, Annual Review 1994–95, p. 71–80.
- PIRAJNO, F., BAGAS, L., SWAGER, C. P., OCCHIPINTI, S. A., and ADAMIDES, N. G., 1996, A reappraisal of the stratigraphy of the Glengarry Basin, Western Australia: Western Australia Geological Survey, Annual Review 1995–96, p. 81–87.
- PIRAJNO, F., and DAVY, R., 1996, Mafic volcanism in the Palaeoproterozoic Glengarry Basin, Western Australia, and implications for its tectonic evolution: Geological Society of Australia, Abstracts no. 41, p. 343.
- PIRAJNO, F., and OCCHIPINTI, S. A., 1995, Base metal potential of the Palaeoproterozoic Glengarry and Bryah Basins, Western Australia: Recent developments in base metal geology and exploration: Australian Institute of Geoscientists, Bulletin 16, p. 51–56.
- PIRAJNO, F., and OCCHIPINTI, S. A., 1998, Geology of the Bryah 1:100 000 sheet: Western Australia Geological Survey, 1:100 000 Geological Series Explanatory Notes, 41p.
- PIRAJNO, F., OCCHIPINTI, S., LE BLANC SMITH, G., and ADAMIDES, N. G., 1995b, Pillow lavas in the Peak Hill terranes: Western Australia Geological Survey, Annual Review 1993–94, p. 63–66.
- PIRAJNO, F., OCCHIPINTI, S. A., and SWAGER, C. P., 1998b, Geology and tectonic evolution of the Palaeoproterozoic Bryah, Padbury and Yerrida Basins (formerly Glengarry Basin), Western Australia: Precambrian Research, v. 90, p. 119–140.
- PIRAJNO, F., and PRESTON, W. A., 1998, Mineral deposits of the Padbury, Bryah and Yerrida Basins, in *Geology of Australian and Papua New Guinean mineral deposits* edited by D. A. BERKMAN and D. H. MACKENZIE: Australasian Institute of Mining and Metallurgy, Monograph 22, p. 63–69.
- RAYMOND, L. A., 1984a, Classification of mélanges: Geological Society of America, Special Paper 198, p. 7–20.
- RAYMOND, L. A., 1984b, Mélanges, their nature, origin and significance: Geological Society of America, Special Paper 198, 170p.
- ROLLINSON, H. R., 1993, Using geochemical data: evaluation, presentation, interpretation: Singapore, Longman, 352p.
- SABMINCO ANNUAL REPORT, 1994, Annual report on mining leases M52/202–203, vol. 1, 2 and 3: Western Australia Geological Survey, M-series, Item 8967, A42856 (unpublished).
- SCHILLING, J.-G., 1982, Galapagos hot spot – spreading center system 1. Spatial petrological and geochemical variations (83°W–101°W): *Journal of Geophysical Research*, v. 87, p. 5593–5610.
- SCHILLING, J.-G., MEYER, P. S., and KINGSLEY, R. H., 1982, Evolution of the Iceland hot spot: *Nature*, v. 296, p. 313–320.
- SHEPPARD, S., and SWAGER, C. P., 1999, Geology of the Marquis 1:100 000 sheet: Western Australia Geological Survey, 1:100 000 Geological Series Explanatory Notes, 21p.
- SHEPPARD, S., OCCHIPINTI, S. A., NELSON, D., and TYLER, I. M., 1999, Granites of the southern Capricorn Orogen, Western Australia: Geological Society of Australia, Abstracts no. 56, p. 44–46.
- SOFLOULIS, J., 1970, Iron deposits of the Robinson Range, Peak Hill Goldfield, W.A.: Western Australia Geological Survey, Record 1970/6, 10p.
- SPEAR, F. S., 1993, Metamorphic phase equilibria and pressure–temperature–time paths: Mineralogical Society of America Monograph, p. 799.
- STERN, R. A., SYME, E. C., and LUCAS, S. B., 1995, Geochemistry of 1.9 Ga MORB and OIB-like basalts from the Amisk collage, Flin Flon belt, Canada: evidence for an intra-oceanic origin: *Geochimica et Cosmochimica Acta*, v. 59, p. 3131–3154.
- SUBRAMANYA, A. G., FAULKNER, J. A., SANDERS, A. J., and GOZZARD, J. R., 1995, Geochemical mapping of the Peak Hill 1:250 000 sheet: Western Australia Geological Survey, 1:250 000 Regolith Geochemistry Series Explanatory Notes, 59p.
- SUN, S.-S., 1982, Chemical composition and origin of the Earth's primitive mantle: *Geochimica et Cosmochimica Acta*, v. 46, p. 179–192.
- SUN, S.-S., 1997, Chemical and isotopic features of Palaeoproterozoic mafic igneous rocks of Australia: implications for tectonic processes: Australian Geological Survey Organisation, Record 1997/4, p. 119–122.
- SWAGER, C. P., and MYERS, J. S., 1999, Geology of the Milgun 1:100 000 sheet: Western Australia Geological Survey, 1:100 000 Geological Series Explanatory Notes, 27p.
- THORNETT, S. E., 1995, The nature, origin and timing of gold mineralization in Proterozoic rocks of the Peak Hill District, W.A.: University of Western Australia, MSc thesis (unpublished).
- TYLER, I. M., 1999, Palaeoproterozoic orogeny in Western Australia: Geological Society of Australia, Abstracts no. 56, p. 47–49.
- TYLER, I. M., PIRAJNO, F., BAGAS, L., MYERS, J. S., and PRESTON, W. A., 1998, The geology and mineral deposits of the Proterozoic in Western Australia: Australian Geological Survey Organisation, *Journal of Geology and Geophysics*, v. 17, p. 223–244.
- TYLER, I. M., and THORNE, A. M., 1990, The northern margin of the Capricorn Orogen, Western Australia — an example of an Early Proterozoic collision zone: *Journal of Structural Geology*, v. 12, p. 685–701.
- WANG, P., and GLOVER, L., 1992, A tectonic test of the most commonly used geochemical discriminant diagrams and patterns: *Earth Science Reviews*, v. 33, p. 111–131.
- WATKINS, K. P., 1983, Petrogenesis of Dalradian albite porphyroblast schists: *Journal of the Geological Society of London*, v. 140, p. 601–618.
- WHITFIELD, G. B., 1987, Wilgeena gold mine. Progress report MS 52/111 and 112: Western Australia Geological Survey, M-series, Item 5862, A28194 (unpublished).
- WINDH, J., 1992, Tectonic evolution and metallogenesis of the Early Proterozoic Glengarry Basin, Western Australia: University of Western Australia, PhD thesis (unpublished).

Appendix

Gazetteer of localities

<i>Locality</i>	<i>AMG coordinate</i>	
	<i>Easting</i>	<i>Northing</i>
5 Mile Well	616500	7158100
Beatty Park Bore	632200	7163500
Cashman opencut	662129	7126994
Dandy Well	646400	7188740
Despair Bore	625300	7169600
Durack prospect	670440	7150520
Durack Well	671600	7143000
Fortnum mine	636372	7197627
Friday Pool	558620	7178625
Harmony (New Baxters Find) opencut	664145	7161267
Heines Find prospect	682759	7145164
Horseshoe Lights opencut	662648	7193894
Horseshoe Mn mine	656990	7186510
Horseshoe Au prospect	661219	7182977
Jubilee mine	671889	7165443
Labouchere mine	627730	7204710
Livingstone mine	567540	7171032
Lucky Call prospect (Ruby Well group)	676747	7127188
Mikhaburra (Holdens Find) opencut	656252	7130396
Millidie (Elsa) deposit	643000	7160000
Mount Fraser	639200	7163300
Mount Labouchere	630360	7212620
Mount Padbury	627400	7164100
Mount Padbury mine	635100	7165100
Mount Pleasant opencut	674287	7161900
Mount Seabrook mine	572631	7168338
Nathan Bitter mine	631100	7199820
Nathans Deep South mine	631713	7198812
Peak Hill opencut	672190	7163003
Peak Hill townsite	673000	7163150
Randell Bore	688000	7145200
Ravelstone Group	669000	7167500
Ravelstone opencut (Mn)	665734	7166777
Ravelstone opencut (Mn)	669313	7166423
Ruby Duffer Well	675290	7136000
Ruby Well group	677900	7129700
St Crispin prospect	691358	7158940
Tank Well	675400	7147000
Top Dimble Well	616600	7167600
Treys (and Starlight) opencut	636412	7198887
Trillbar Homestead	576023	7170846
Wembley mine	663983	7149044
Wilgeena (Hit or Miss) mine	685369	7155622
Wilthorpe mine	630414	7176521
Yarlarweelor opencut	636723	7196423

The Palaeoproterozoic Bryah and Padbury Basins are part of the Capricorn Orogen, a collision zone between the Archaean Pilbara and Yilgarn Cratons. The Bryah Basin contains mafic–ultramafic igneous rocks, turbidites, and chemical sedimentary rocks formed during back-arc sea-floor spreading and rifting on the northern margin of the Yilgarn Craton, at or near a mid-oceanic ridge. The Padbury Basin contains a succession of clastic and chemical sedimentary rocks, and was formed on top of the Bryah Basin as a foreland structure resulting from either the c. 1800 Ma oblique collision of the Pilbara and Yilgarn Cratons (Capricorn Orogeny) or the c. 2000 Ma collision of the Glenburgh Terrane and the Yilgarn Craton (Glenburgh Orogeny). Important mineral deposits include orogenic gold-only lode deposits, copper–gold volcanogenic massive sulfides, sedimentary and lateritic manganese, and iron ore. The origin of the gold mineralization is related to metamorphism and deformation linked to the Capricorn Orogeny at c. 1.8 Ga. The formation of other deposits is related to pre-orogenic syngenetic processes.



Further details of geological publications and maps produced by the Geological Survey of Western Australia can be obtained by contacting:

**Information Centre
Department of Minerals and Energy
100 Plain Street
East Perth WA 6004
Phone: (08) 9222 3459 Fax: (08) 9222 3444
www.dme.wa.gov.au**

